Università degli Studi di Trento
Dottorato di Ricerca in Ingegneria dei
Sistemi Strutturali Civili e Meccanici
XXIV ciclo

INSTABILITY OF DIELECTRIC ELASTOMER ACTUATORS

di
STEFANIA COLONNELLI

Relatore: Prof. Massimiliano Gei

Trento, Febbraio 2012

Università degli Studi di Trento

Dottorato di Ricerca in
Ingegneria dei Sistemi Strutturali Civili e Meccanici

XXIV ciclo
Settore Scientifico Disciplinare ICAR/08

Commissione esaminatrice:

Prof. R. Zandonini, Università degli Studi di Trento

Prof. E. Radi, Università degli Studi di Modena e Reggio Emilia

Prof. G. Magenes, Università degli Studi di Pavia

Membri esperti aggiunti:

Prof. J.W.G. van de Kuilen, Technische Universität München

Acknowledgements

First and foremost, I offer my gratitude to my advisor, Prof. Massimiliano Gei, who has supported me with his knowledge and patience: working with him meant for me a continuous growth in the field of Mechanics, and I will never cease to be deeply grateful to him for believing in me.

I am deeply indebted to Prof. Giuseppe Saccomandi, prof. Maria Cesarina Salvatori and prof. Dimitri Mugnai for their valuable knowledge and their uninterrupted support following my Master thesis.

I would like to thank Prof. Davide Bigoni, head of the Ph.D. course, and all the members of the Mechanical and Structural Engineering Department at University of Trento: Dr. Roberta Springhetti, Dr. Andrea Piccolroaz, Dr. Francesco Dal Corso, Prof. Luca Deseri.

I would also like to thank Prof. Salvatore Marzano of Politecnico di Bari for his hospitality, and give a special thank to Dr. Giuseppe Zurlo for the valuable suggestions about the "old topic" of the thesis and his friendly words of advice.

In addition, I would like to express my gratitude to Prof. Alberto Valli for giving me the opportunity to improve my teaching skills during this arduous studying period.

I would like to mention the Administration office (Rosanna, Cesarina and Elena) for being very accommodating throughout these three years.

For his unfailing support and steadfast encouragement, I would also like to thank my love Francesco: every page of this thesis has brought me closer to you.

Last but not least, I would like to thank Ilaria, Enrico, Lorenzo, Silvano, Nicola, Valentina, Mum, Dad, Romeo and Lella, who is part of my family, for their continuing encouragement and unconditioned love.

Trento, February 21, 2012

Stefania Colonnelli

Contents

Chapter 1

Introduction

Dielectric elastomers (DEs) are an important class of materials, currently employed in the design and realization of electrically-driven, highly deformable actuators and devices, which find application in several fields of technology and engineering, including aerospace, biomedical and mechanical engineering [8]. Subject to a voltage, a membrane of a soft dielectric elastomer coated by compliant electrodes reduces its thickness and expands its area, possibly deforming in-plane well beyond 100%: this principle, pointed out by Pelrine et al. [36], extending to silicones experimental observations made earlier on electrostrictive polyurethanes (Zhenyi et al. [56]), is exploited to conceive transducers for a broad range of applications, including soft robots, adaptive optics, Braille displays and energy harvesters.

Soft dielectrics undergo finite strains, and their modelling requires a formulation based on the Mechanics of Solids at large deformations. For conservative materials, the first theory of non-linear electroelasticity was developed by Toupin [47]; recently, it has been revisited, among others, by McMeeking and Landis [31], Dorfmann and Ogden [12], and Suo et al. [45], who have clarified the notion of Maxwell stress and discussed the different choices in terms of primary variables for the constitutive description.

A major problem that limits the widespread diffusion of such devices in everyday technology is the high voltage (high electric field) required to

(a) (b)

Figure 1.1: In (a) Mediterraneos Elastomer buoys, example of a generator transducer, installed by Mediterraneo Señales Maritimas (Valencia, Spain). In (b) electronic Braille cell, example of an actuator transducer, realized in the Research Center "E. Piaggio" (Pisa, Italy).

activate large strains, because of the low dielectric permittivity of typical materials (acrylic elastomers or silicones), in the order of few unities, which governs the electromechanical coupling. On the other hand, for the same reason, typical actuators are membrane-like, as the electric field is inversely proportional to the thickness at constant voltage.

Composite materials provide a way to overcome these limitations, as suggested by some experiments (Zhang et al. [55], Huang et al. [26]) and theoretical works, performed mainly with reference to layered geometries (deBotton et al. [11], Tian et al. [46]). The key principle is to enhance the coupling, reinforcing a soft matrix with stiff and high-permittivity particles, for the overall actuation performance to be improved despite the expected increase of stiffness. Therefore, a careful design and optimization of the composite is required in order to improve its effective behaviour.

To increase strains by enhancing the dielectric constant ϵ of such matrices and keeping low elastic modulus Y to control the ratio ϵ/Y, several attempts have been made: it is possible to improve the electromechanical

performance of DE actuators by electrically charging and polarizing soft elastomeric polyurethane matrices with a foamy structure, via the Corona process. Such matrices enhance the electromechanical strains, possibly due to the presence of macro-dipoles induced both at the matrix/pore surfaces and inside the bulk [9].

In addition, composites can display failure modes and instabilities not displayed by homogeneous specimens that must be thoroughly investigated. Commonly, instability phenomena are seen as a serious drawback, that should be predicted and avoided. However, in some cases they can be used to activate snap-through actuation, as in the case of buckling-like or highly-deformable balloon-like actuators. Electromechanical instabilities in homogeneous soft DEs have been investigated in detail [45], while methods to address incremental bifurcation and stability have been provided by Dorfmann and Ogden [13] and by Bertoldi and Gei [2], who classified the different unstable mechanisms within an extension of Hill's theory for nonlinear elastic solids [23]. In the latter paper, a first stability analysis on layered composites was performed, being the applied electric field perpendicular to the layer direction (see also Rudykh and deBotton [41]).

After having recalled in Chap. 2 the elements of physics of dielectric elastomer transducers, in Chap. 4 the non-linear theory of electroelasticity is introduced, preceded by a Chapter devoted uniquely to the basic notion of Solid Mechanics at finite strain. In particular, in Chap. 4 the modelling of soft DEs is described in terms both of dielectric displacement and electric field as independent electric variable. Well-known phenomena depending on electric interactions occurring for other types of material, such as piezoelectricity and electrostriction, are illustrated and fit within the general theory of electroelasticity in Chap. 5.

Performance and stability of both homogeneous and composite DE actuators are analyzed in this thesis.

In particular, as far as homogeneous systems are concerned (Chap. 7), the research goals are the following:

- investigate diffuse modes bifurcations of prestretched actuators and quantify electrostriction effects;

- formulate the criterion for the onset of the band-localization instability in electroelastic solids and analyze when critical modes for the actuated specimens are reached.

Regarding DE composites (Chap. 8), the goal is to evaluate in detail the behaviour of two-phase rank-1 laminates in terms of different types of actuation, geometric and mechanical properties of phases, applied boundary conditions, and instabilities phenomena, in order to establish precise ranges in which the performance enhancement is effective with respect to the homogeneous counterpart.

The results will be given adopting mainly extended Mooney-Rivlin and Gent strain energies (Chap. 3).

The conclusions are finally drawn in Chap. 9.

The content of the thesis has been summarised in the following papers:

- Gei, M., Colonnelli, S., Springhetti, R., "The role of electrostriction on the stability of dielectric elastomer actuators", submitted,
- Gei, M., Colonnelli, S., "Instability of soft dielectric elastomers: the role of electrostriction", EuroEAP 2011: I International Conference on EAP Transducers and Artificial Muscles, Pisa, June 8-9, 2011,
- Gei, M., Colonnelli, S., Springhetti, R., "Instability of soft dielectric composite actuators", XX AIMETA National Conference, Bologna, September 12-15, 2011,
- Gei, M., Colonnelli, S., Springhetti, R., "A framework to investigate instabilities of homogeneous composite dielectric elastomer actuators", Proc. Smart Structures/NDE 2012, paper No. 8340-34, San Diego (USA) March 11-15, 2012,
- Gei, M., Springhetti, R., Colonnelli, S., "Electrostrictive effects on the stability of dielectric elastomer actuators", VIII European Solid Mechanic Conference, ESMC2012, Graz, Austria, July 9-13, 2012.

Chapter 2

The Physics behind Dielectric Elastomer Transducers

A short treatise of the basic physics of the transducer is presented below. For further details see [45].

2.1 Dielectric Elastomer Transducers

A dielectric transducer is a device consisting of a soft solid that separates two electrodes, possibly subject to a force P, which can represent the effect of the weight or that of an external action (Fig. 2.1). The two electrodes are connected through a conducting wire to a battery, which gives the voltage $\Delta\phi$ and pumps surface charge (whose density is denoted by ω) to flow through the conducting wire from one electrode to the other, set at a distance equal to h. Because of the presence of the force P and the voltage $\Delta\phi$, the transducer is capable of two independent movements: deformation due to the applied force, and deformation due to the charge flowing. Consequently, the states of the transducer can be represented graphically on a plane. The two coordinates on the plane may be chosen from variables such as $P, \Delta\phi, h$ and ω.

Many uses of transducers involve cyclic changes of states. As an illus-

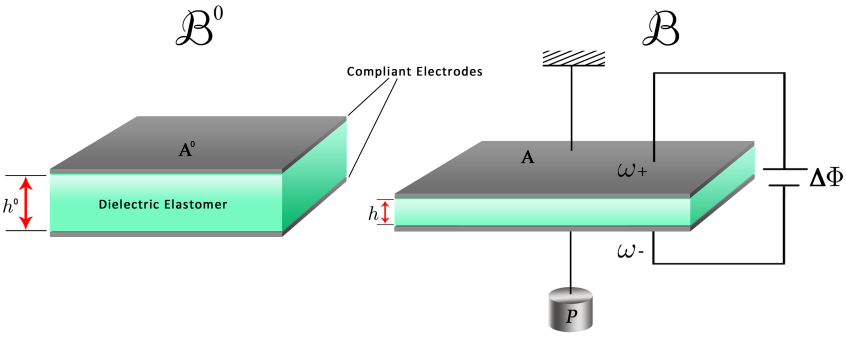

Figure 2.1: A dielectric elastomer transducer.

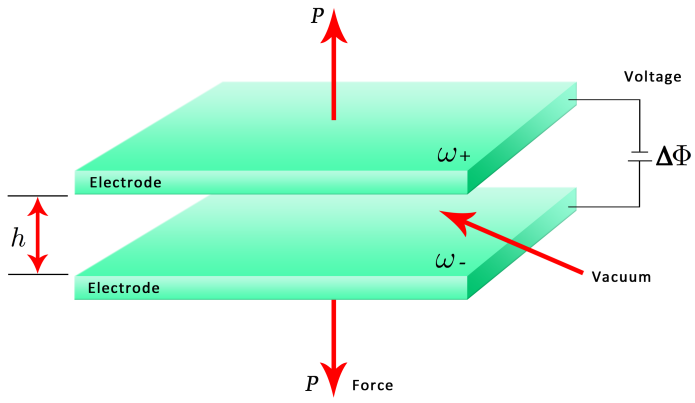

Figure 2.2: A capacitor under external forces.

tration, consider a simple system composed of a parallel-plate capacitor (two plates of electrodes separated by a thin layer of vacuum, see Fig. 2.2). The separation h between the two electrodes may vary, but the area A of

each electrode remains fixed, so that the charge Q can be introduced,

$$Q = \omega A.$$

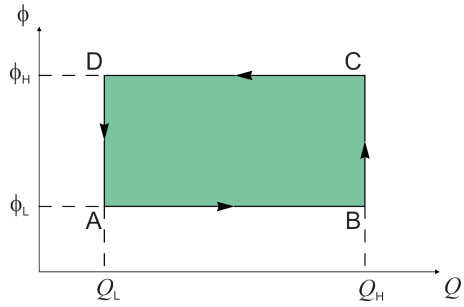

Figure 2.3: In (Q, ϕ)-plane, a point represents a state of a generator transducer. A use of the transducer typically involves a cyclic change of state. The rectangle represents a cycle involving two levels of voltage and two values of charge.

A particular cycle of state is presented in Fig. 2.3 on the $Q - \phi$ plane. To operate with a transducer in this cycle, we will need two batteries: one at a low voltage ϕ_L, and the other at a high voltage ϕ_H. The four sides of the rectangular cycle shown in Fig. 2.3 represent the following processes:

1. In changing from state A to state B, the simplified transducer is connected to the battery at a low voltage ϕ_L. The two electrodes attract each other, reducing the spacing between them, causing the charge on the electrodes to increase, and the applied force increases in order to avoid the overcharge.

2. Moving from state B to state C, the system is under an open-circuit condition and the electrodes maintain the constant charge Q_H. The applied force (constant) increases the spacing between the two electrodes, raising the voltage ϕ_H.

3. In changing from state C to state D, the simplified transducer is connected at a high voltage ϕ_H. A decreasing force is applied, increasing the spacing between the two electrodes and lowering the charge Q_L.

4. From state D to state A, the setup is under an open-circuit condition, maintaining a constant charge Q_L. The applied force (constant) decreases the spacing between the two electrodes, causing a lowering of the voltage, which reaches the ϕ_L level.

This cycle operation of an electromechanical parallel capacitor is analogous to the Carnot cycle, provided that we replace voltage with temperature and charge with entropy. During the cycle, the transducer receives mechanical work from the environment, draws an amount of charge from the low–voltage battery, and deposits the same amount of charge to the high–voltage battery. Thus, the transducer is a generator, producing electric energy by receiving mechanical work. Indeed, a closed curve of any shape on the (Q, ϕ)-plane represents a cyclic operation of the transducer. To operate such a cycle would require a variable-voltage source. The amount of energy converted per cycle is given by the area enclosed by the cycle on the (Q, ϕ)-plane. When the cycle runs counterclockwise, the transducer is a generator, converting mechanical energy into electrical energy; on the contrary, when the cycle runs clockwise, the transducer is an actuator, converting electrical energy into mechanical energy. In this work of thesis we focus on the latter.

2.2 Work-Conjugate Measures

When the scalar product between two quantities gives the work, they are said to be work-conjugate. A classic example in Physics is provided by forces and displacements, in Mechanics the second Piola-Kirchhoff stress and the Green-Langrange strain tensor are also qualified as work-conjugate measures [22]. More in general, we can define the Lagrangian and Eulerian work-conjugate measures, depending on the (deformed or undeformed) state considered. Our goal is to do the same analysis for the system taken into account. We introduce the fundamental quantities for the descrip-

tion of dielectric systems: the nominal electric field, denoted by $\mathbf{e}^0$, the corresponding true electric field (in the current configuration) $\mathbf{e}$, the electric displacement vectors $\mathbf{d}^0$ and $\mathbf{d}$, in the reference and in the current configuration, respectively. An Euclidean orthogonal reference system is considered, with the origin O and orthonormal basis $\mathbf{i}_k$, $k = 1, 2, 3$, so, in the case of a planar capacitor (with arms parallel to the plane $\mathbf{i}_1$-$\mathbf{i}_2$), we have that $\mathbf{e}^0 = e^0\mathbf{i}_2$ and $\mathbf{d}^0 = d^0\mathbf{i}_2$.

The voltage is equal to $\Delta\phi = e^0h^0$, the charge $Q = A^0d^0$ as $d^0_{ext} - d^0_{int} = -\omega^0$, where "*ext*" and "*int*" indicate external to the arms and within to the arms, respectively. As known from classical physics, the differential work δL, in terms of nominal quantities, is given by

$$\delta L = \Delta\phi\delta(\omega^0 A^0) = e^0h^0A^0\delta d^0 = (h^0A^0)e^0\delta d^0,$$

which means that e^0 and d^0 are work-conjugate physical quantities. In the current configuration, $\mathbf{e} = e\mathbf{i}_2$, so that $\Delta\phi = eh$ and $\mathbf{d} = d\mathbf{i}_2$, so that we have analogously $Q = Ad$ as $d_{ext} - d_{int} = -\omega$. Then the differential work, in terms of the actual quantities, is given by

$$\delta L = \Delta\phi\delta(\omega A) = ehA\delta d + ehd\delta A,$$

which means that e and d are not work-conjugate physical quantities.

2.3 Equations of State of an Actuator

The main component of the actuator is an elastomer, a three-dimensional network of long and flexible polymer chains. Its thermodynamic behaviour is highly entropic, characterized by the Helmholtz free energy W. By dropping by a small distance δh, the weight does the work $P\delta h$. By pumping a small amount of charge δQ, the battery does the work $\Delta\phi\delta Q$. The force is work-conjugated to the displacement, and the voltage is work-conjugated to the charge. When the system finds equilibrium with the applied force and the applied voltage, the change in the free energy of the transducer equals the sum of the work done by the weight and the work done by the

battery:

$$\delta W = P\delta h + \Delta\phi\delta Q. \tag{2.1}$$

This condition of equilibrium holds for arbitrary and independent small variations δh and δQ. The two independent variables (h, Q) characterize the state of the actuator, therefore

$$W = W(h, Q).$$

Associated with small variations δh and δQ, the free energy varies by the amount

$$\delta W = \frac{\partial W(h,Q)}{\partial h}\delta h + \frac{\partial W(h,Q)}{\partial Q}\delta Q. \tag{2.2}$$

A comparison of equations (2.1) and (2.2) gives

$$\left[\frac{\partial W(h,Q)}{\partial h} - P\right]\delta h + \left[\frac{\partial W(h,Q)}{\partial Q} - \Delta\phi\right]\delta Q = 0. \tag{2.3}$$

When the transducer equilibrates with the weight and the battery, the condition of equilibrium (2.3) holds for independent and arbitrary variations ∂h and ∂Q. Consequently, in equilibrium, the coefficients of the two variations in eq. (2.3) both vanish, giving

$$P = \frac{\partial W(h,Q)}{\partial h}, \tag{2.4}$$

$$\Delta\phi = \frac{\partial W(h,Q)}{\partial Q}. \tag{2.5}$$

Once the free-energy function $W(h, Q)$ is known, eqs. (2.4) and (2.5) express P and $\Delta\phi$ as functions of h and Q. That is, the two equations give the force and voltage needed to cause a certain displacement and a certain charge. The two equations (2.4) and (2.5) constitute the equations of state of the transducer. The equations represent the transformations that map the states of the transducer from one thermodynamic plane to another. Equation (2.4) can be used to determine the free-energy function from

the force-displacement curves of the transducer measured under the open-circuit conditions, when the electrodes maintain constant charges. For each value of Q, the free energy is the area under the force-displacement curve. Similarly, eq. (2.5) can be used to determine the free-energy function from the voltage-charge curves of the transducer. As mentioned before, (h, P) and (Q, ϕ) are convenient planes to represent the states of the transducer when we wish to highlight work and energy. As an illustration, consider the parallel-plate capacitor previously introduced in Fig. 2.2. The separation h between the two electrodes may vary, but the area A of either electrode remains fixed. Recall the elementary fact that the amount of charge on either electrode is linear in the voltage:

$$\Delta\phi = \frac{hQ}{\epsilon_0 A}, \tag{2.6}$$

where ϵ_0 is the permittivity of vacuum ($\epsilon_0 = 8.85412$ pF/m). Inserting eq. (2.6) into eq. (2.5), and integrating eq. (2.5) with respect to Q while holding h fixed, we obtain that

$$W(h, Q) = \frac{hQ^2}{2\epsilon_0 A}. \tag{2.7}$$

Inserting eq. (2.7) into eq. (2.4), we obtain that

$$P = \frac{Q^2}{2A\epsilon_0}. \tag{2.8}$$

Eqs. (2.6) and (2.8) constitute the equations of state of the parallel-plate capacitor. They are readily interpreted. The applied voltage causes charge to flow from one electrode to the other, so that one electrode is positively charged, and the other negatively charged. Equation (2.6) relates the charge to the applied voltage. The oppositely charged electrodes attract each other. To maintain equilibrium, a force needs to be applied to each electrode. Equation (2.8) relates the applied force to the charge. Define the electric field by $e = \Delta\phi/h$ and the stress by $T = P/A$. Rewrite eq. (2.8) as

$$T = \frac{1}{2}\epsilon_0 e^2. \tag{2.9}$$

This equation gives the stress needed to be applied to the electrodes to counteract the electrostatic attraction. This stress is known as the Maxwell stress.

2.4 Global Stability of Soft Dielectric Actuators

For a given system, the free energy $W(h, Q)$ may take a complicated functional form. The equations of state, eqs. (2.4) and (2.5), are in general nonlinear. If the transducer operates in the neighborhood of a particular state (h, Q), the equations of state can be linearized in this neighborhood, written in an incremental form:

$$\delta P = \frac{\partial^2 W(h,Q)}{\partial h^2}\delta h + \frac{\partial^2 W(h,Q)}{\partial Q \partial h}\delta Q, \tag{2.10}$$

$$\delta \phi = \frac{\partial^2 W(h,Q)}{\partial h \partial Q}\delta h + \frac{\partial^2 W(h,Q)}{\partial Q^2}\delta Q. \tag{2.11}$$

The increments δP and $\delta \phi$ are linear in the increments of the variables δh and δQ. This procedure is known as a linear perturbation. We call $\partial^2 W(h,Q)/\partial h^2$ the mechanical tangent stiffness of the transducer, and $\partial^2 W(h,Q)/\partial Q^2$ the electrical tangent stiffness of the transducer. The two electromechanical coupling effects are both characterized by the same cross derivative, $\partial^2 W(h,Q)/(\partial h \partial Q) = \partial^2 W(h,Q)/(\partial Q \partial h)$. The matrix

$$\mathbf{H}(h,Q) = \begin{bmatrix} \frac{\partial^2 W(h,Q)}{\partial h^2} & \frac{\partial^2 W(h,Q)}{\partial Q \partial h} \\ \frac{\partial^2 W(h,Q)}{\partial h \partial Q} & \frac{\partial^2 W(h,Q)}{\partial Q^2} \end{bmatrix}$$

is known as the Hessian of the free-energy function $W(h, Q)$. As mentioned above, a state of the transducer can be represented by a point in the (h, Q) plane, as well as by a point in the (P, ϕ) plane. For the same state of the transducer, the point in the (h, Q) plane is mapped to the point in the (P, ϕ) plane by the equations of state, (2.4) and (2.5). The mapping may not always be invertible. That is, given a pair of "loads" (P, ϕ), the equations of state may not be invertible to determine a state (h, Q). For

example, eqs. (2.10) and (2.11) are not invertible when the Hessian is a singular matrix, det$\mathbf{H} = 0$. This singularity may be understood in terms of thermodynamics. The transducer and the loading mechanisms (i.e., the weight and the battery) together constitute a thermodynamic system. The free energy of the system is the sum of the free energies of the individual parts – the transducer, the weight, and the battery. The free energy (i.e., the potential energy) of a constant weight is $-Ph$. The free energy of a battery of a constant voltage is $-\Delta\phi Q$. Consequently, the free energy of the thermodynamic system combining the transducer and the loading mechanisms is

$$G(h, Q) = W(h, Q) - Ph - \Delta\phi Q.$$

So the system has still two independent variables, h and Q. Thermodynamics requires that the system should reach a stable state of equilibrium when the free energy function $G(h, Q)$ is a minimum against small changes in h and Q. When the weight moves by δh and the battery pumps charges δQ, the free energy of the system varies by

$$\delta G = \left[\frac{\partial W(h,Q)}{\partial h} - P\right]\delta h + \left[\frac{\partial W(h,Q)}{\partial Q} - \phi\right]\delta Q + \frac{1}{2}\frac{\partial^2 W(h,Q)}{\partial h^2}(\delta h)^2 + \frac{\partial^2 W(h,Q)}{\partial h \partial Q}(\delta h)(\delta Q) + \frac{1}{2}\frac{\partial^2 W(h,Q)}{\partial Q^2}(\delta Q)^2.$$

We have expanded the Taylor series of the function $W(h, Q)$ up to terms quadratic in δh and δQ. In a state of equilibrium, the coefficients of the first-order variations vanish, recovering the equations of state (2.4) and (2.5). To ensure that this state of equilibrium minimizes G, the sum of the second-order variations must be positive for arbitrary combinations of δh and δQ. That is, a state of equilibrium is stable against small perturbations if the Hessian of the free energy of the transducer, $\mathbf{H}(h, Q)$, is positive-definite. The two-by-two (symmetric) matrix is positive-definite if and only if (Sylvester criterion)

$$\frac{\partial^2 W(h,Q)}{\partial h^2} > 0, \quad \left[\frac{\partial^2 W(h,Q)}{\partial h^2}\right]\left[\frac{\partial^2 W(h,Q)}{\partial Q^2}\right] > \left[\frac{\partial^2 W(h,Q)}{\partial h \partial Q}\right]^2.$$

When the Hessian of the free energy function is positive-definite, the function $W(h,Q)$ is convex at this state (h,Q). As an illustration, consider the parallel-plate capacitor again. Given the free-energy function (2.7), the second derivatives are

$$\frac{\partial^2 W(h,Q)}{\partial h^2}=0,\quad \frac{\partial^2 W(h,Q)}{\partial Q^2}=\frac{h}{\epsilon_0 A},\quad \left[\frac{\partial^2 W(h,Q)}{\partial h\partial Q}\right]=\frac{Q}{\epsilon_0 A}.$$

Consequently, the Hessian is not positive-definite in any state of equilibrium. That is, the parallel-plate capacitor subject to a constant force and a constant voltage cannot reach a stable state of equilibrium. The conclusion is readily understood. The weight is independent of the separation between the plates, but the electrostatic attractive force increases as the separation decreases. Subject to a fixed weight, the two plates will be pulled apart if the voltage is low, and will be pulled together if the voltage is high. The capacitor can be stabilized by a modification of the loading mechanisms. For example, we could replace the weight with a spring that restrains the relative movement of the plates. Let K be the stiffness of the spring, and h_0 be the separation between the electrodes when the spring is unstretched, so that the force in the spring is $P=K(h-h_0)$. The free energy of the system is the sum of the free energies of the capacitor, the spring and the battery:

$$G(h,Q)=\frac{hQ^2}{2\epsilon_0 A}+\frac{1}{2}K(h-h_0)^2-\Delta\phi Q.$$

In a state of equilibrium, the first derivatives of $G(h,Q)$ vanish, giving the same equations of state as eqs. (2.9) and (2.11). The state of equilibrium is stable if and only if the Hessian of $G(h,Q)$ is positive-definite. The second derivatives of the function $G(h,Q)$ are

$$\frac{\partial^2 G(h,Q)}{\partial h^2}=K,\quad \frac{\partial^2 G(h,Q)}{\partial Q^2}=\frac{h}{\epsilon_0 A},\quad \frac{\partial^2 G(h,Q)}{\partial h\partial Q}=\frac{Q}{\epsilon_0 A}.$$

A state of equilibrium (h,Q) is stable if and only if

$$\frac{Kh}{\epsilon_0 A}>\left(\frac{Q}{\epsilon_0 A}\right)^2.$$

Thus, the transducer is stable when the spring is stiff and the applied voltage is small.

2.5 Instabilities in Soft Dielectric Actuators

The above described devices can be composed of different types of dielectrics. While all dielectrics deform under voltage, the amount of deformation differs markedly among different materials. Under voltage, piezoelectric ceramics attain strains of typically less than 1%. Glassy and semicrystalline polymers can attain strains of less than 10%. Strains about 30% or more were observed in some elastomers. In the last decade, strains over 100% have been achieved in several ways, by pre-stretching an elastomer, by using an elastomer of interpenetrating networks, by swelling an elastomer with a solvent, and by spraying charge on an electrode-free elastomer [27]. These experimental advances have prompted a theoretical question: what is the fundamental limit of deformation that can be induced by voltage? After all, one can easily increase the length of a rubber band several times by using a mechanical force. Why is it difficult to do so by using voltage? The answer to these questions is strongly related to the various instabilities that may arise in an actuator or a generator made of dielectric materials.

For a stiff dielectric, such as a ceramic or a glassy polymer, voltage-induced deformation is limited by electric breakdown, when the voltage mobilizes the charged species in the dielectric to produce a path of electrical conduction. For a compliant dielectric, such as an elastomer, the voltage-induced deformation is often limited by electromechanical instability. Stark and Garton [44] described a model that accounted for the following experimental observation: the breakdown fields of a polymer are reduced when the polymer becomes soft at elevated temperatures. As the applied voltage increases, the polymer thins down, so that the same voltage induces an even higher electric field. This positive feedback results in a mode of instability, known as electromechanical instability or pull-in instability, which causes the polymer to reduce the thickness drastically, often leading to electrical breakdown. Electromechanical instability has been

recognized as a mode of failure for insulators in power transmission cables, for example. Clearly, the quantitative determination of the pull-in voltage is not a simple task for real deformable devices: the failure mechanism of electroactivated thin films depends not only on electro-elastic interactions, but also on the actuator shape and on purely electrical effects.

As a summary, we report a list of all possible instability modes for a dielectric specimen activated electrically:

- **Electric breakdown**: it represents a possible failure mode which occurs when the current electric field reaches the maximum admissible value in the material, beyond it a discharge may destroy the actuator (see Fig. 2.4).

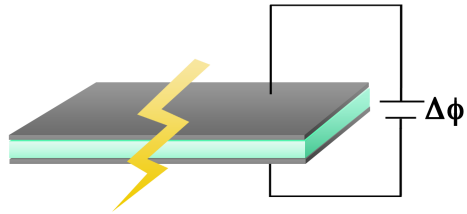

Figure 2.4: Schematization of the phenomenon of electric breakdown for a transducer.

- **Pull-in/electromechanical instability**: in analytical terms, it corresponds to the failure of positive definiteness of the tangent electroelastic constitutive operator. Beyond the threshold set by this criterion, the material is no longer able to sustain the Maxwell pressures transmitted by the electrodes, leading to the collapse of the system or to a snap-through effect. It can be rigorously shown that this criterion is significant only for specimens subjected to traction boundary conditions on the whole boundary, while it does not affect devices with prescribed displacement boundary conditions. In order to describe this type of instability, one may consider a toy model composed of two rigid conducting plates connected by an insulated linear spring,

with a rest distance equal to d. If the plates are subjected to a voltage $\Delta\phi$, the Coulomb forces between the plates will tend to attract them, so that the spring will become compressed (see Fig. 2.5). It is easy to check that there exists a voltage threshold $\Delta\phi^*$, such that for larger voltages no more equilibrium is possible between the elastic and electric forces and the top plate slams onto the bottom plate. For stiffening polymers, the pull-in instability may trigger a snap-through instability (see Fig. 2.6).

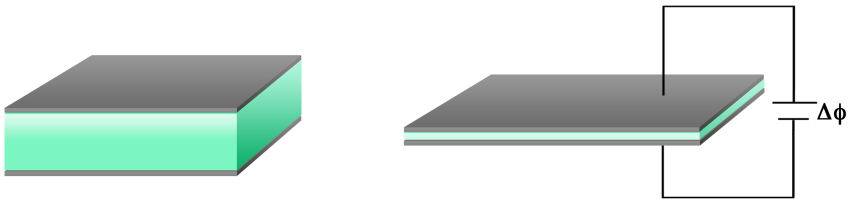

Figure 2.5: Representation of the pull-in instability, where plates are connected by a dielectric device.

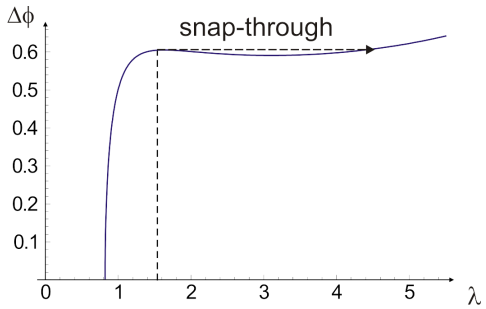

Figure 2.6: The shape of the voltage-stretch curve $\Delta\phi(\lambda)$ indicates a snap-trough electromechanical instability.

- **Diffuse modes of bifurcation**: under compression, buckling-like instabilities may be induced. This is typical of prestretched actuators, where the initial longitudinal tensile prestress may diminish due to the

electrical activation. These instabilities are exploited in buckling-like actuators (see Fig. 2.7 and Chap. 7)

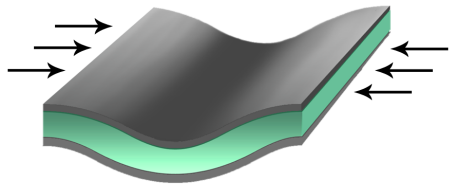

Figure 2.7: A transducer, under lateral compression, exhibits the characteristic deformation of buckling mode.

- **Loss of strong ellipticity/band localization modes**: these modes correspond to the onset of a localized deformation in the form of a band, having a precise inclination. Analytically, it corresponds to the loss of ellipticity of the governing equations of the coupled electromechanical problem (see Fig. 2.8 and Chap. 7).

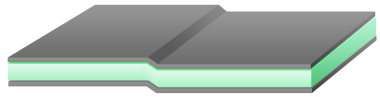

Figure 2.8: Localized deformation, appearing in the form of a band.

Chapter 3

Basic Elements of Solid Mechanics

A brief account of the theory of Continuum Mechanics is given in this Chapter. For additional information, the interested reader is referred to Truesdell and Noll [50], Gurtin [20], Ogden [35].

3.1 Mathematical Basis

In this section the main notions of vector and tensor analysis, that are fundamental tools in the description of deformation of continuous media, are recalled.

3.1.1 Euclidean Vector Spaces

The mechanical behaviour of continuous media is most conveniently described in terms of a scalars, vectors and tensors which in general vary from point to point in the material, and may therefore be regarded as functions of position in the physical space occupied by the solid. In order to express this formally in mathematical terms, the notion of Euclidean point space is required. Let $\mathcal{E}$ be a set of elements which we refer to as *points*. If, for each pair (x, y) of points x, y of $\mathcal{E}$ there exists a vector, denoted $\mathbf{v}(x, y)$,

in $\mathbb{E}$, which indicates the Euclidean vector space, such that

$$\mathbf{v}(x, y) = \mathbf{v}(x, z) + \mathbf{v}(z, y)$$

for all x, y, z in $\mathcal{E}$, and

$$\mathbf{v}(x, y) = \mathbf{v}(x, z) \quad \text{if and only if } y = z$$

for each $\mathbf{x} \in \mathcal{E}$, then $\mathcal{E}$ is said to be a *Euclidean point space* (it is *not* a vector space). It can be easily shown that

$$\mathbf{v}(x, x) = \mathbf{0} \quad \text{for all } x \text{ in } \mathcal{E},$$

and hence that

$$\mathbf{v}(y, x) = -\mathbf{v}(x, y) \quad \text{for all } x, y \text{ in } \mathcal{E}.$$

Then, if a fixed (but arbitrary) point o of $\mathcal{E}$ is chosen for reference $\mathbf{x}(o)$ is called the *position vector* of the point x relative to o, and o is referred to as *origin*. The distance $d(x, y)$ between two points x, y of $\mathcal{E}$ is defined making use of the dot product on $\mathbb{E}$, according to

$$d(x, y) = |\mathbf{x} - \mathbf{y}| = \{(\mathbf{x} - \mathbf{y}) \cdot (\mathbf{x} - \mathbf{y})\}^{1/2}.$$

It is straightforward to establish that the bilinear mapping d from $\mathcal{E} \times \mathcal{E}$ to $\mathbb{R}$ is a *metric*, that is

$$\begin{aligned}
&(a)\ d(x, y) = d(y, x),\\
&(b)\ d(x, y) \neq d(x, z) + d(z, y),\\
&(c)\ d(x, y) \geq 0 \quad \text{with equality if and only if } \ x = y,
\end{aligned}$$

for all x, y, z in $\mathcal{E}$. Properties $(a), (b), (c)$ can be verified from the definition of distance and from some properties of scalar product.

Since $\mathcal{E}$ is endowed with a metric it is a *metric space*. The angle θ between the lines joining o to x and o to y in $\mathcal{E}$ is also defined through the scalar product on $\mathbb{E}$. Thus, we have

$$\cos\theta = \frac{\mathbf{x} \cdot \mathbf{y}}{|\mathbf{x}||\mathbf{y}|}$$

for an arbitrary choice of the origin o.

With an origin o fixed in $\mathcal{E}$, an arbitrary point x of $\mathcal{E}$ corresponds to a unique position vector $\mathbf{x}$ in $\mathbb{E}$. Let $\{\mathbf{i}_k\}$ be an orthonormal basis for $\mathbb{E}$. Then, the components x_k of $\mathbf{x}$ are given by $x_k = \mathbf{x} \cdot \mathbf{i}_k$. They may alternatively be defined by three scalar fields over $\mathbb{E}$, $i_k : \mathcal{E} \to \mathbb{R}$, such that $i_k(x) = \mathbf{x} \cdot \mathbf{i}_k$ $(k = 1, 2, 3)$ for every $x \in \mathcal{E}$. The origin o, together with the collection of mapping i_k is denoted by $\{0, i_k\}$ and this is said to form a *(rectangular) Cartesian coordinates system* on $\mathcal{E}$. The components x_k are called *(rectangular) Cartesian coordinates* of the point x in the coordinate system $\{0, i_k\}$.

Consider an infinitesimal element of surface area dS in a continuous medium. Let $\mathbf{n}$ be the unit normal to dS. In general, the material on one side of dS exerts a force on the material on the other side. We denote the force by $\mathbf{t}(\mathbf{n})dS$, where $\mathbf{t}(\mathbf{n})$ is called the *stress vector* and is such that $\mathbf{t}(-\mathbf{n}) = -\mathbf{t}(\mathbf{n})$. It has dimension of force per unit area and it depends on the orientation of dS, that is on $\mathbf{n}$. In fact, $\mathbf{t}(\mathbf{n})$ depends linearly on $\mathbf{n}$ (Cauchy Theorem). We express this dependence by writing

$$\mathbf{t}(\mathbf{n}) = \mathbf{T}\mathbf{n}, \tag{3.1}$$

where $\mathbf{T}$, which is independent of $\mathbf{n}$, is a *linear mapping* from $\mathbb{E}$ into $\mathbb{E}$. When referred to the orthonormal basis $\{\mathbf{i}_k\}$, however, (3.1) is decomposed as

$$t_k(\mathbf{n}) = T_{kj} n_j,$$

where T_{kj} are the *components* of $\mathbf{T}$ relative to the basis $\{\mathbf{i}_k\}$. The linear mapping $\mathbf{T}$ is called a *second order tensor* on $\mathbb{E}$, and in this context it is a *stress tensor* on $\mathbb{E}$.

We define the *tensor product* in $\mathbb{E}$

$$(\mathbf{u} \otimes \mathbf{v})\mathbf{w} = (\mathbf{v} \cdot \mathbf{w})\mathbf{u}$$

for all $\mathbf{u}, \mathbf{v}, \mathbf{w} \in \mathbb{E}$.

3.1.2 Cartesian Tensors

Let $\mathcal{D}$ be a subset of an Euclidean point space $\mathcal{E}$ and let $\mathcal{L}$ be the space of real-valued linear functions whose domain is the Euclidean space $\mathbb{E}^n$. A *scalar field* $\Phi : \mathcal{D} \to \mathbb{R}$ is a real–valued function over $\mathcal{D}$, a *vector field* $\mathbf{v} : \mathcal{D} \to \mathbb{R}$ and a *tensor field* $\mathbf{T}$ of order n is a mapping $\mathbf{T} : \mathcal{D} \to \mathcal{L}(\underbrace{\mathbb{E} \times \cdots \times \mathbb{E}}_{n \text{ times}}, \mathbb{R})$. Let $\boldsymbol{\psi} : \mathcal{D} \to \mathbb{R}^3$ be a *continuous, one–to–one* mapping whose inverse $\boldsymbol{\psi}^{-1}$, defined on $\boldsymbol{\psi}(\mathcal{D})$, is also continuous. If $\mathbf{x} \in \mathcal{D}$ we write

$$\boldsymbol{\psi}(\mathbf{x}) = (x^1, x^2, x^3), \quad \mathbf{x} = \boldsymbol{\psi}^{-1}(x^1, x^2, x^3).$$

Such a $\boldsymbol{\psi}$ is called a *homeomorphism.*

Given $\boldsymbol{\psi}$ and $\mathcal{D}$ there are three scalar fields $\psi^i : \mathcal{D} \to \mathbb{R}$ such that

$$\boldsymbol{\psi}(\mathbf{x}) = (\psi^1(\mathbf{x}), \psi^2(\mathbf{x}), \psi^3(\mathbf{x})), \quad \mathbf{x} \in \mathcal{D}.$$

The fields ψ^i are called the *coordinate functions* of $\boldsymbol{\psi}$ on $\mathcal{D}$, $\boldsymbol{\psi}$ is a *coordinate system* on $\mathcal{D}$ and $\mathcal{D}$ is a *coordinate neighbourhood.* The coordinates x^i of the point $\mathbf{x}$ in the coordinate system $\boldsymbol{\psi}$ are given by

$$x^i = \psi^i(\mathbf{x}). \tag{3.2}$$

They are called *curvilinear* coordinates covering $\mathcal{D}$, and it is important to distinguish the curvilinear coordinates x^i (superscript) from the Cartesian coordinates x_i (subscript). The equation

$$x^i \equiv \psi^i = \text{constant}$$

defines a subset of $\mathcal{D}$ called a x^i *–coordinate surface* of $\boldsymbol{\psi}$ in $\mathcal{D}$. The intersection of coordinate surfaces corresponding to two different values of i defines a *coordinate curve* in $\mathcal{D}$. The *tangent vector* to the x^i–coordinate curve at $\mathbf{x} = \boldsymbol{\psi}^{-1}(x^1, x^2, x^3)$ is defined as $\partial\mathbf{x}/\partial x^i$. For a field $f : \mathcal{D} \to \mathcal{I}$, we define the mapping $f_\psi : \boldsymbol{\psi}(\mathcal{D}) \to \mathcal{I}$ by

$$f(\mathbf{x}) = f\{\boldsymbol{\psi}^{-1}(x^1, x^2, x^3)\} = f_\psi(x^1, x^2, x^3), \quad \mathbf{x} \in \mathcal{D}.$$

Thus, the *gradient* of f is defined as follow

$$\begin{aligned}(\mathrm{grad}f(\mathbf{x}))\mathbf{a} &= \frac{d}{dt}f_\psi(x^1+ta^1, x^2+ta^2, x^3+ta^3)\\ &= \frac{\partial f_\psi}{\partial x^i}(x^1,x^2,x^3)a^i = \frac{\partial f}{\partial x^i}(\mathbf{x})a^i, \end{aligned} \tag{3.3}$$

where the a^i are defined by $x^i+ta^i = \psi^i(\mathbf{x}+t\mathbf{a})$, recalling (3.2). Application (3.3) to the scalar field ψ^i shows that

$$a^i = (\mathrm{grad}\psi^i(\mathbf{x}))\cdot\mathbf{a}, \tag{3.4}$$

while in respect of the position vector field $\mathbf{r}$ relative to some chosen origin we obtain

$$\mathrm{grad}(\mathbf{r}(\mathbf{x})) = \frac{\partial \mathbf{x}}{\partial x^i}a^i, \tag{3.5}$$

since $\mathbf{r}_\psi(x^1,x^2,x^3) = \mathbf{r}(\mathbf{x}) = \mathbf{x}$. Observing that, we have $\mathrm{grad}(\mathbf{r}(\mathbf{x})) = \mathbf{I}$, where $\mathbf{I}$ is the identity on $\mathbb{E}$. Hence (3.5) gives

$$\mathbf{a} = \frac{\partial \mathbf{x}}{\partial x^i}a^i, \tag{3.6}$$

and since $\mathbf{a}$ is an arbitrary vector on $\mathbb{E}$, the three vectors $\partial\mathbf{x}/\partial x^i$ form a basis $\{\partial\mathbf{x}/\partial x^i\}$ at each point $\mathbf{x}$ of $\mathcal{D}$. It is called the *natural basis* of $\boldsymbol{\psi}$ at $\mathbf{x}$ and we write

$$\mathbf{g}_i(\mathbf{x}) = \frac{\partial \mathbf{x}}{\partial x^i}, \quad (i=1,2,3), \tag{3.7}$$

where $\mathbf{g}_i$ is a vector field on $\mathcal{D}$. Note that $\mathbf{g}_i(\mathbf{x})$ is tangent to the x^i–coordinate curve of $\boldsymbol{\psi}$.

3.2 Representation of Isotropic Functions

Definition 3.2.1. *We say f, $\mathbf{h}$ and $\mathbf{S}$ are scalar, vector and tensor invariants relative to the group $\mathcal{G} \subseteq \mathcal{O}(\mathbb{E})$ (where $\mathcal{O}(\mathbb{E})$ is the orthogonal group*

on $\mathbb{E}$*), respectively, if for any vector* $\mathbf{v}$ *and tensor* $\mathbf{A}$ *we have*

$$\begin{aligned} f(\mathbf{Qv}, \mathbf{QAQ}^T) &= f(\mathbf{v}, \mathbf{A}), && \forall \mathbf{Q} \in \mathscr{G}, \\ \mathbf{h}(\mathbf{Qv}, \mathbf{QAQ}^T) &= \mathbf{Qh}(\mathbf{v}, \mathbf{A}), && \forall \mathbf{Q} \in \mathscr{G}, \\ \mathbf{S}(\mathbf{Qv}, \mathbf{QAQ}^T) &= \mathbf{QS}(\mathbf{v}, \mathbf{A})\mathbf{Q}^T, && \forall \mathbf{Q} \in \mathscr{G}. \end{aligned}$$

If $\mathscr{G} = \mathscr{O}(V)$, the invariants are usually called *isotropic invariants* or *isotropic functions*, otherwise they are called *anisotropic invariants*. We show here some useful examples:

1. isotropic scalar invariant: $\det(\mathbf{A})$; in fact

$$\det(\mathbf{QAQ}^T) = \det(\mathbf{Q})\det(\mathbf{A})\det(\mathbf{Q}^T) = \det(\mathbf{A}),$$

   having used Binet Theorem [42] and the fact that the inverse of a orthogonal tensor coincides with the transpose;

2. Isotropic scalar invariant: $\mathrm{tr}(\mathbf{A}^m\mathbf{B}^n)$; in fact

$$\mathrm{tr}(\underbrace{\mathbf{QAQ}^T \dots \mathbf{QAQ}^T}_{m}\underbrace{\mathbf{QBQ}^T \dots \mathbf{QBQ}^T}_{n}) = \mathrm{tr}(\mathbf{QA}^m\mathbf{B}^n\mathbf{Q}^T) = \mathrm{tr}(\mathbf{A}^m\mathbf{B}^n),$$

   having used the the well-known property for orthogonal tensors ($\mathbf{QQ}^T = \mathbf{I}$) and the invariance of the trace;

3. isotropic tensor invariant: $\mathbf{A}^m\mathbf{v} \otimes \mathbf{B}^n\mathbf{v}$; in fact

$$(\mathbf{QAQ}^T)^m\mathbf{Qv} \otimes (\mathbf{QBQ}^T)^n\mathbf{Qv} = \mathbf{Q}(\mathbf{A}^m\mathbf{v} \otimes \mathbf{B}^n)\mathbf{Q}^T.$$

The goal of representation problems is to find the sets of invariants of scalar such that are basic invariants, and to achieve vector and tensor functions, such that are generating invariants: the full set of scalar and generating invariants ensures the requirement of objectivity. A set of basic invariants or a generating set is called *functional basis* if it is *irreducible*, namely that elements of the basic invariants are not functionally related, and the elements of the generating set are linearly independent with respect to

Variables: $\mathbf{v}, \mathbf{A}$	
Isotropic scalar invariants	$1, \mathrm{tr}\mathbf{A}, \mathrm{tr}\mathbf{A}^2, \mathrm{tr}\mathbf{A}^3, \mathbf{v}\cdot\mathbf{v}, \mathbf{v}\cdot\mathbf{A}\mathbf{v}, \mathbf{v}\cdot\mathbf{A}^2\mathbf{v}$
Isotropic vector generators	$\mathbf{v}, \mathbf{A}\mathbf{v}, \mathbf{A}^2\mathbf{v}$
Isotropic tensors generators	$\mathbf{v}\otimes\mathbf{v}, \mathbf{I}, \mathbf{A}, \mathbf{A}^2, \mathbf{v}\otimes\mathbf{A}\mathbf{v}+\mathbf{A}\mathbf{v}\otimes\mathbf{v}, \mathbf{A}\mathbf{v}\otimes\mathbf{A}\mathbf{v}$

Table 3.1: List of isotropic invariants, for the couple ($\mathbf{v}$, $\mathbf{A}$) vector and symmetric tensor as variables.

the isotropic functions. Functional bases for isotropic functions have been extensively studied in the literature [50]. The functional bases for a space generated by a vector and by a symmetric tensor are presented in table (3.1) where we find all the isotropic invariants [1].

3.3 Large-strain Solid Mechanics

An elastic body undergoing motion occupies different regions of the three dimensional Euclidean space at different times. It is convenient to choose a fixed region, $\mathcal{B}^0$ say, as reference, and to identify points of the body with their position vectors $\mathbf{x}^0$ in $\mathcal{B}^0$, which is then called the *reference configuration*. We denoted by $\mathcal{B}$ the actual configuration then occupied by the body. This is called the *current configuration*.

[1] We can observe that using Cayley-Hamilton, the principal invariants can be defined as a function of $\mathrm{tr}\mathbf{A}, \mathrm{tr}\mathbf{A}^2, \mathrm{tr}\mathbf{A}^3$ and viceversa, in fact

$$\mathrm{tr}\mathbf{A}^2 = I_1^2 - 2I_2, \quad \mathrm{tr}\mathbf{A}^3 = I_1^3 - 3I_2I_1 + 3I_3.$$

Deformation and Strain

We consider the mapping from the reference configuration $\mathcal{B}^0$ to a current configuration $\mathcal{B}$ as a deformation or motion of the body. It carries each point $\mathbf{x}^0$ in the reference configuration $\mathcal{B}^0$ into a point in the current configuration $\mathcal{B}$. The point in $\mathcal{B}^0$ is denoted by the position vector $\mathbf{x}^0$ and the point in $\mathcal{B}$ by $\mathbf{x}$, relative to arbitrarily chosen origins. The deformation may be regarded as a one parameter mapping $\boldsymbol{\chi} : \mathcal{B}^0 \to \mathcal{B}$, which is differentiable, invertible, with the inverse $\boldsymbol{\chi}^{-1}$ invertible too. We write

$$\mathbf{x} = \boldsymbol{\chi}(\mathbf{x}^0), \quad \mathbf{x}^0 \in \mathcal{B}^0. \tag{3.8}$$

On taking the differential of equation (3.8), we obtain

$$d\mathbf{x} = \mathrm{Grad}\boldsymbol{\chi}\ d\mathbf{x}^0$$

where Grad is the gradient operator in $\mathcal{B}^0$. The second-order tensor $\mathrm{Grad}\boldsymbol{\chi}$ is known as the deformation gradient tensor, which will be denoted here by $\mathbf{F}$. A deformation with $\mathbf{F}$ constant is homogeneous. In general, $\mathbf{F}$ depends on $\mathbf{x}^0$. We choose bases vectors $\mathbf{i}_k^0$ and $\mathbf{i}_k$ $(k = 1, 2, 3)$ in the reference and current configurations, respectively. When the bases $\mathbf{i}_k^0$ in $\mathcal{B}^0$ are Cartesian rectangular coordinates, we may express $\mathbf{F}$ in the form

$$\mathbf{F} = \left(\mathbf{i}_1^0 \frac{\partial}{\partial x_1^0} + \mathbf{i}_2^0 \frac{\partial}{\partial x_2^0} + \mathbf{i}_3^0 \frac{\partial}{\partial x_3^0}\right)\mathbf{x}. \tag{3.9}$$

We adopt the conventional assumption that the Jacobian

$$J = \det\mathbf{F}, \tag{3.10}$$

is positive at each point of $\mathcal{B}_0$. According to Nanson's formula, we have

$$\mathbf{n}dA = J\mathbf{F}^{-T}\mathbf{n}^0 dA^0. \tag{3.11}$$

The corresponding volumes dV^0 in $\mathcal{B}^0$ and dV in $\mathcal{B}$ are related by

$$dV = JdV^0.$$

For this reason, if the volume in $\mathcal{B}^0$ is unchanged during the deformation $J = 1$ and the deformation is said to be *isochoric*. Furthermore, a material for which the volume of any region in $\mathcal{B}^0$ is unchanged during any deformation is said to be *incompressible*, and it is said to be compressible if there is no such constraint on the body during any possible motion. Since the tensor $\mathbf{F}$ is non-singular by assumption, from the *Polar Decomposition Theorem* it follows that

$$\mathbf{F} = \mathbf{RU} = \mathbf{VR},$$

where $\mathbf{U}$ and $\mathbf{V}$ are symmetric, positive definite tensors and $\mathbf{R}$ is a proper orthogonal tensor. $\mathbf{U}$ and $\mathbf{V}$ are called the *right* and *left stretch tensor*, respectively, and $\mathbf{R}$ satisfies

$$\mathbf{R}\mathbf{R}^T = \mathbf{R}^T\mathbf{R} = \mathbf{I}, \quad \det\mathbf{R} = 1, \tag{3.12}$$

where $\mathbf{I}$ is the identity and the superscript T denotes the transpose. With the help of equation (3.12), it turns out that $\det\mathbf{F} = \det\mathbf{U}$. If $\mathbf{R} = \mathbf{I}$, we have $\mathbf{F} = \mathbf{U} = \mathbf{V}$ and the deformation is known as a *pure strain*. We use the notation $\mathbf{B} = \mathbf{F}\mathbf{F}^T$ and $\mathbf{C} = \mathbf{F}^T\mathbf{F}$ for the *left* and *right Cauchy-Green deformation tensor*, respectively. They are easily related to $\mathbf{U}$ and $\mathbf{V}$ through

$$\mathbf{B} = \mathbf{V}^2, \quad \mathbf{C} = \mathbf{U}^2. \tag{3.13}$$

Since $\mathbf{U}$ is symmetric and positive definite, its principal values λ_j ($j = 1, 2, 3$) are positive. Let $\mathbf{u}^{(j)}$ ($j = 1, 2, 3$) be the principal axes of $\mathbf{U}$. Then, we have the spectral decomposition

$$\mathbf{U} = \sum_{j=1}^{3} \lambda_j \mathbf{u}^{(j)} \otimes \mathbf{u}^{(j)}.$$

The coefficients λ_j are also the principal values of $\mathbf{V}$ corresponding to principal axes $\mathbf{v}^{(j)} = \mathbf{R}\mathbf{u}^{(j)}$ ($j = 1, 2, 3$), and it turns out that

$$\mathbf{V} = \sum_{j=1}^{3} \lambda_j \mathbf{v}^{(j)} \otimes \mathbf{v}^{(j)}.$$

We refer to λ_j as the *principal stretches*, $\mathbf{u}^{(j)}$ and $\mathbf{v}^{(j)}$ as *Lagrangian and Eulerian principal axes* of the deformation, respectively. From (3.13), we deduce that $\mathbf{B}$ has the same principal axes as $\mathbf{V}$, and $\mathbf{C}$ as $\mathbf{U}$, and

$$\mathbf{B} = \sum_{j=1}^{3} \lambda_j^2 \mathbf{v}^{(j)} \otimes \mathbf{v}^{(j)}, \tag{3.14}$$

$$\mathbf{C} = \sum_{j=1}^{3} \lambda_j^2 \mathbf{u}^{(j)} \otimes \mathbf{u}^{(j)}. \tag{3.15}$$

The principal stretches $\lambda_1, \lambda_2, \lambda_3$ are scalar quantities which are independent of the choice of the coordinate system. The principal invariants of $\mathbf{U}$ (or $\mathbf{V}$) are defined as

$$\begin{aligned} \bar{I}_1 &= \lambda_1 + \lambda_2 + \lambda_3 = \mathrm{tr}\mathbf{U}, \\ \bar{I}_2 &= \lambda_1\lambda_2 + \lambda_1\lambda_3 + \lambda_2\lambda_3 = \frac{1}{2}[(\mathrm{tr}\mathbf{U})^2 - \mathrm{tr}(\mathbf{U}^2)], \\ \bar{I}_3 &= \lambda_1\lambda_2\lambda_3 = \det\mathbf{U}. \end{aligned} \tag{3.16}$$

Similarly, the principal invariants of $\mathbf{B}$ (or $\mathbf{C}$) are denoted by

$$\begin{aligned} I_1 &= \lambda_1^2 + \lambda_2^2 + \lambda_3^2 = \mathrm{tr}\mathbf{B}, \\ I_2 &= \lambda_1^2\lambda_2^2 + \lambda_1^2\lambda_3^2 + \lambda_2^2\lambda_3^2 = \frac{1}{2}[(\mathrm{tr}\mathbf{B})^2 - \mathrm{tr}(\mathbf{B}^2)], \\ I_3 &= \lambda_1^2\lambda_2^2\lambda_3^2 = \det\mathbf{B}. \end{aligned} \tag{3.17}$$

Analysis of Stress and Equation of Equilibrium

Let V be the region occupied by an arbitrary part of the body in the current configuration $\mathcal{B}$, and A be the closed surface bounding V, the outward unit normal to which is denoted by $\mathbf{n}$. We use the notation $\mathbf{t}$ as the traction per unit area of A, and $\mathbf{b}$ as the body force per unit volume of V. From Cauchy's theorem that $\mathbf{t}$ depends linearly on $\mathbf{n}$, we may deduce that there exists a second order tensor $\mathbf{T}$, which is symmetric and independent of $\mathbf{n}$, such that

$$\mathbf{t}(\mathbf{x}, \mathbf{n}) = \mathbf{T}(\mathbf{x})\mathbf{n},$$

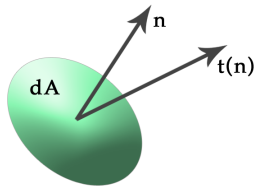

Figure 3.1: Traction forces in Cauchy continuous body.

for all $\mathbf{t}$ in $\mathcal{B}$ and each unit vector $\mathbf{n}$. Thus, $\mathbf{T}$ is said to be the *Cauchy stress tensor*. A consequence of the objectivity and isotropy is that the stress $\mathbf{T}$ must be coaxial with the Eulerian principal axes $\mathbf{v}^{(j)}$. Thus, if t_1, t_2, t_3 denote the principal values of $\mathbf{T}$, then we write

$$\mathbf{T} = \sum_{j=1}^{3} t_j \mathbf{v}^{(j)} \otimes \mathbf{v}^{(j)}.$$

In some situations it is more convenient to introduce a concept of *first Piola-Kirchhoff tensor* $\mathbf{S}$, as the traction per unit reference area, which can be expressed as

$$\mathbf{t}dA = \mathbf{T}\mathbf{n}dA = \mathbf{S}\mathbf{n}^0 dA^0.$$

The area elements dA^0 and dA are related by Nanson's formula (3.11). We then have

$$\mathbf{S} = J\mathbf{T}\mathbf{F}^{-T}. \tag{3.18}$$

Sometimes it is more convenient to use the *nominal stress*, which is defined as

$$\mathbf{S}^T = J\mathbf{F}^{-1}\mathbf{T}. \tag{3.19}$$

The (Eulerian) equation of motion is given by

$$\text{div } \mathbf{T} + \mathbf{b} = \rho\mathbf{a}, \tag{3.20}$$

where ρ is the density in $\mathcal{B}$, $\mathbf{b}$ represents the body force per unit volume in $\mathcal{B}$ and $\mathbf{a}$ denotes the acceleration. In the static case, $\mathbf{a}$ is vanishing and

equation (3.20) is referred to as the *equilibrium equation*. If, furthermore, there is no body force, the equilibrium equation reduces to

$$\text{div } \mathbf{T} = \mathbf{0}. \tag{3.21}$$

Let ρ_0 denotes the density per unit volume in $\mathcal{B}^0$. Then, the mass conservation equation may be expressed in the form

$$J = \frac{\rho_0}{\rho}.$$

The corresponding Lagrangian equilibrium equation of motion is given by

$$\text{Div } \mathbf{S} + \mathbf{b}^0 = \mathbf{0}, \tag{3.22}$$

where Div is the divergence operator in $\mathcal{B}^0$.

3.3.1 Strain-energy Functions

We recall that $\mathbf{S} \cdot \frac{d\mathbf{F}}{dt}$ represents the stress power per unit volume. If there exists a scalar function $W(\mathbf{F})$ such that

$$\frac{d}{dt}W(\mathbf{F}) = \mathbf{S} \cdot \frac{d\mathbf{F}}{dt}$$

the material is said to be a *Green elastic material* or a *hyperelastic material*. Physically, $W(\mathbf{F})$ measures the energy stored in the material during deformation and we refer to it as the *strain-energy function*. When such a function exists, we have

$$\frac{d}{dt}W(\mathbf{F}) = \frac{\partial W(\mathbf{F})}{\partial \mathbf{F}} \cdot \frac{d\mathbf{F}}{dt},$$

so that

$$\mathbf{S} = \frac{\partial W(\mathbf{F})}{\partial \mathbf{F}}. \tag{3.23}$$

For the linear case, the elastic constitutive law may now be written as

$$\mathbf{T} = \mathbb{C}\mathbf{E} \tag{3.24}$$

where $\mathbf{E} = 1/2(\nabla\mathbf{u} + (\nabla\mathbf{u})^T)$ and $\mathbb{C}$ is the fourth order tensor which has the following symmetries

$$C_{ijkl} = C_{jikl} = C_{ijlk},$$

that are the minor symmetries. For a Green-elastic material the additional symmetry

$$C_{ijkl} = C_{klij}$$

holds, and the strain-energy function is given by

$$W = \frac{1}{2}\mathrm{tr}\left[(\mathbb{C}\mathbf{E}) \cdot \mathbf{E}\right]. \tag{3.25}$$

In general, for a homogeneous objective, isotropic hyperelastic material, $W(\mathbf{F})$ must satisfy all properties valid for constitutive equations (material objectivity, material simmetry and so on). From the polar decomposition theorem and the spectral decomposition (for $\mathbf{F}$) we may regard W as a function of $\lambda_1, \lambda_2, \lambda_3$, namely

$$W = W(\lambda_1, \lambda_2, \lambda_3), \tag{3.26}$$

satisfying the symmetry requirement

$$W(\lambda_1, \lambda_2, \lambda_3) = W(\lambda_2, \lambda_3, \lambda_1) = W(\lambda_3, \lambda_1, \lambda_2).$$

When the natural configuration is taken as the reference configuration, we may assume that W vanishes in such a configuration, and set

$$W(1, 1, 1) = 0, \tag{3.27}$$

because in the underformed state $\lambda_1 = \lambda_2 = \lambda_3 = 1$. Analogously, the value of the stress is zero in the natural state, that is

$$\frac{\partial W}{\partial \lambda_j}(1, 1, 1) = 0, \quad (j = 1, 2, 3). \tag{3.28}$$

For a homogeneous objective, isotropic, hyperelastic material, $W(\mathbf{F})$ satisfies

$$W(\mathbf{F}) = W(\mathbf{QF}) = W(\mathbf{FP}), \tag{3.29}$$

for arbitrary rotations $\mathbf{Q}$ and $\mathbf{P}$. From (3.29), it is easily shown (using the polar decomposition theorem) that

$$W(\mathbf{Q}\mathbf{V}\mathbf{Q}^T) = W(\mathbf{V}),$$

which holds for arbitrary $\mathbf{Q}$. By choosing $\mathbf{Q} = \mathbf{R}$ we deduce that

$$W(\mathbf{F}) = W(\mathbf{U}) = W(\mathbf{V}).$$

From (3.19), we calculate $\mathbf{T} = J^{-1}\mathbf{F}\mathbf{S}$, so from (3.23) we have

$$\mathbf{T} = J^{-1}\mathbf{F}\frac{\partial W}{\partial \mathbf{F}}. \tag{3.30}$$

Choosing a system in which $\mathbf{F}$ is in a diagonal form, from spectral decomposition theorem and from (3.30) it turns out

$$\mathbf{T} = J^{-1}\sum_{i=1}^{3}\lambda_i\frac{\partial W}{\partial \lambda_i}\mathbf{v}^{(i)}\otimes\mathbf{v}^{(i)}. \tag{3.31}$$

With the help of (3.31), we calculate

$$\begin{aligned}\frac{\partial W}{\partial \lambda_j} &= \frac{\partial W}{\partial I_1}\frac{\partial I_1}{\partial \lambda_j} + \frac{\partial W}{\partial I_2}\frac{\partial I_2}{\partial \lambda_j} + \frac{\partial W}{\partial I_3}\frac{\partial I_3}{\partial \lambda_j} \\ &= 2\lambda_j W_1 + 2\lambda_j^{-1}[W_2 I_2 + W_3 I_3] - 2\lambda_j^{-3}W_2 I_3, \end{aligned} \tag{3.32}$$

where $W_j = \partial W/\partial I_j$ $(j = 1, 2, 3)$. Eq. (3.31) is rewritten as

$$\mathbf{T} = 2I_3^{-\frac{1}{2}}\sum_{j=1}^{3}[I_2W_2 + I_3W_3 + \lambda_j^2 W_1 - \lambda_j^{-2}W_2I_3]\mathbf{v}^{(j)}\otimes\mathbf{v}^{(j)}.$$

From (3.14), it follows that

$$\mathbf{T} = 2I_3^{-\frac{1}{2}}(I_2W_2 + I_3W_3)\mathbf{I} + 2I_3^{-\frac{1}{2}}W_1\mathbf{B} - 2I_3^{\frac{1}{2}}W_2\mathbf{B}^{-1}, \tag{3.33}$$

or, as it is usual to see,

$$\mathbf{T} = \alpha_0\mathbf{I} + \alpha_1\mathbf{B} + \alpha_{-1}\mathbf{B}^{-1}, \tag{3.34}$$

where the elastic response functions $\alpha_s = \alpha_s(I_1, I_2, I_3)$, $(s = 0, 1, -1)$ from (3.33) are given by

$$\alpha_0 = 2I_3^{-1/2}[I_2W_2 + I_3W_3], \quad \alpha_1 = 2I_3^{-1/2}W_1, \quad \alpha_{-1} = -2I_3^{1/2}W_2.$$

3.4 Incremental Deformations in Solid Mechanics

The mechanics of incremental deformations superimposed upon a given strain allows the investigation of the response of a solid body subject to prestress. The classical way to investigate this problem consists in the introduction of a boundary-value problem and a set of solving incremental linear relationships. All the equations take into account the presence of a given pre-stress state. As pointed out by Biot, if we restrict attention to incremental deformations, the circumstances that lead to a specific distribution of pre-stress within the body are not required to be known. Therefore, equations valid for any material model are established. Biot developed the corresponding theory in the late thirties collecting it in a famous monograph [4]. The topic received much attention in relation to the developments of numerical techniques designed to solve nonlinear problems [33], [43]. On the other hand, from the theoretical point of view, several works have been published concerning criteria of stability and uniqueness of incremental boundary-value problems [21] that provide useful tools in understanding the effective behaviour of loaded structures. In Ogden [35] several aspects of the theory of incremental deformations are touched on, comprising discussion about global and incremental uniqueness and stability in finite elasticity.

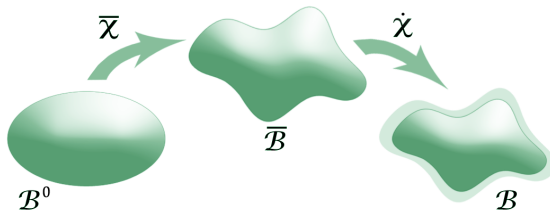

Figure 3.2: Incremental deformation for a body.

Let $\boldsymbol{\chi}(\mathbf{x}^0, t)$ be the motion of a body that is subject to prescribed initial and boundary conditions. Let us consider the problem of finding solutions near $\boldsymbol{\chi}$ when the boundary conditions are perturbed. Let $\overline{\boldsymbol{\chi}}$ be a solution of the perturbed boundary value problem (3.22), with $\mathbf{F} = \mathrm{Grad}\boldsymbol{\chi}(\mathbf{x}^0)$ and recalling that $\mathbf{S}\mathbf{F}^T = \mathbf{F}\mathbf{S}^T$. To specify the boundary conditions, let us consider the motion and surface traction area of the boundary: introducing two subsets $\partial\mathcal{B}_v^0$,$\partial\mathcal{B}_s^0 \in \partial\mathcal{B}^0$ [2], we have

$$\begin{aligned} &\boldsymbol{\chi}(\mathbf{x}^0) = \boldsymbol{\psi}(\mathbf{x}^0) \quad \text{on } \partial\mathcal{B}_v^0, \\ &\mathbf{S}\mathbf{n}^0 = \mathbf{s}(\mathbf{x}^0, \mathbf{x}, \mathbf{F}) \quad \text{on } \partial\mathcal{B}_s^0, \end{aligned} \tag{3.35}$$

where $\boldsymbol{\psi}$ and $\mathbf{s}$ are prescribed vector fields. The condition (3.35) is quite general and allows for a wide variety of assigned tractions, including dead-loading and pressure loading. Let $\overline{\mathbf{x}} = \overline{\boldsymbol{\chi}}(\mathbf{x}^0)$. The displacement of a material particle due to this change is

$$\dot{\mathbf{x}} = \mathbf{x} - \overline{\mathbf{x}} = \boldsymbol{\chi}(\mathbf{x}^0) - \overline{\boldsymbol{\chi}}(\mathbf{x}^0) \equiv \dot{\boldsymbol{\chi}}(\mathbf{x}^0),$$

which serves to define the dot operator $(\dot{\ })$. If the displacement is small for each $\mathbf{x}^0 \in \mathcal{B}^0$, so that the terms of order $|\dot{\mathbf{x}}|^2$ can be neglected, then we refer to $\dot{\mathbf{x}}$ as an incremental (linear) deformation from the current configuration $\mathcal{B}$.

The change in the deformation gradient, brought by the incremental deformation $\dot{\mathbf{x}}$, is given by

$$\dot{\mathbf{F}} = (\dot{\mathrm{Grad}}\boldsymbol{\chi}) = \mathrm{Grad}\overline{\boldsymbol{\chi}} - \mathrm{Grad}\boldsymbol{\chi} = \mathrm{Grad}\dot{\boldsymbol{\chi}}, \tag{3.36}$$

where the property of linearity of the Grad operator has been used. Equation (3.36) is exact and is valid even if $\dot{\mathbf{x}}$ is not small in the sense defined above.

The formulation of incremental boundary-value problems directly derives from that relative to finite deformation. Let the boundary conditions be subjected to the increments

$$\begin{aligned} &\dot{\boldsymbol{\chi}}(\mathbf{x}^0) = \dot{\boldsymbol{\psi}}(\mathbf{x}^0) \quad \text{on } \partial\mathcal{B}_v^0, \\ &\dot{\mathbf{S}}\mathbf{n}^0 = \dot{\mathbf{s}}(\mathbf{x}^0, \mathbf{x}, \dot{\mathbf{F}}) \quad \text{on}\partial\mathcal{B}_s^0, \end{aligned} \tag{3.37}$$

[2] $\partial\mathcal{B}_v^0 \cup \partial\mathcal{B}_s^0 = \partial\mathcal{B}^0$, $\partial\mathcal{B}_v^0 \cap \partial\mathcal{B}_s^0 = \emptyset$

where the increment in $\mathbf{s}$ depends in general on $\dot{\mathbf{x}} = \dot{\boldsymbol{\chi}}(\mathbf{x}^0)$ and $\dot{\mathbf{F}} = \mathrm{Grad}\dot{\boldsymbol{\chi}}(\mathbf{x}^0)$ in addition to the increments in any loading parameters included in $\mathbf{s}$.

The incremental equation of the motion is, from (3.22),

$$\mathrm{Div}\dot{\mathbf{S}} + \rho_0\dot{\mathbf{b}} = \mathbf{0}, \tag{3.38}$$

and the condition of symmetry of $\mathbf{S}\mathbf{F}^T$ becomes

$$\dot{\mathbf{S}}\mathbf{F}^T + \mathbf{S}\dot{\mathbf{F}}^T = \dot{\mathbf{F}}\mathbf{S}^T + \mathbf{F}\dot{\mathbf{S}}^T. \tag{3.39}$$

The linearized constitutive equations may be obtained as

$$\dot{\mathbf{S}} = \mathbb{C}\dot{\mathbf{F}}, \quad \mathbb{C}^0 = \frac{\partial \mathbf{S}}{\partial \mathbf{F}},$$

or, when the material is incompressible ($J = 1$, (3.10)), since $\mathbf{S} = \partial W/\partial \mathbf{F} - p\mathbf{F}^{-T}$,

$$\dot{\mathbf{S}} = \mathbb{C}^0\dot{\mathbf{F}} + p\mathbf{L}^T\mathbf{F}^{-T} - \dot{p}\mathbf{F}^{-T}, \tag{3.40}$$

where

$$\mathbf{L} = \dot{\mathbf{F}}\mathbf{F}^{-1}. \tag{3.41}$$

$\mathbb{C}^0$ is the fourth–order tensor of elastic moduli relative to the reference configuration. In solving incremental boundary–value problems, it is usually convenient to refer to the current configuration. Then, we introduce the new incremental stress quantity

$$\boldsymbol{\Sigma} = J^{-1}\dot{\mathbf{S}}\mathbf{F}^T \tag{3.42}$$

such that, using the Piola Identity

$$\mathrm{Div}(J\mathbf{A}\mathbf{F}^{-T}) = J(\mathrm{div}\mathbf{A}),$$

where $\mathbf{A}$ is a tensor, equation (3.38) and (3.39) take the form, respectively,

$$\mathrm{div}\boldsymbol{\Sigma} + \rho\dot{\mathbf{b}} = \mathbf{0},$$

$$\boldsymbol{\Sigma} - \boldsymbol{\Sigma}^T = \mathbf{L}\mathbf{T} - \mathbf{T}\mathbf{L}^T.$$

Using Nanson's formula (3.11), we remind that $\mathbf{A}\mathbf{n}^0 dA^0 = J^{-1}\mathbf{A}\mathbf{F}^{-T}\mathbf{n}dA$ for every tensor $\mathbf{A}$. So it turns out that

$$\dot{\mathbf{S}}\mathbf{n}^0 dA^0 = J^{-1}\dot{\mathbf{S}}\mathbf{F}^{-T}\mathbf{n}dA = \boldsymbol{\Sigma}\mathbf{n}dA,$$

so the boundary conditions (3.37) become

$$\begin{aligned} &\mathbf{u}(\mathbf{x}) = \dot{\mathbf{x}}(\mathbf{x}) = \dot{\boldsymbol{\psi}}(\mathbf{x}) \quad \text{on } \partial\mathcal{B}_v, \\ &\boldsymbol{\Sigma}\mathbf{n} = \dot{\mathbf{s}}(\mathbf{x}, \mathbf{L}) \quad \text{on } \partial\mathcal{B}_s, \end{aligned} \tag{3.43}$$

where $\mathbf{u}(\mathbf{x})$ is the incremental displacement.
In case of *pressure loading*

$$\mathbf{t} = -P\mathbf{n},$$

where P is the given pressure, so in the reference, using Nanson formula, we find

$$\mathbf{s} = -PJ\mathbf{F}^{-T}\mathbf{n}^0.$$

The corresponding incremental quantity is given by

$$\dot{\mathbf{s}} = -\dot{P}J\mathbf{F}^{-T}\mathbf{n}^0 - P\dot{J}\mathbf{F}^{-T}\mathbf{n}^0 - PJ\dot{(\mathbf{F}^{-T})}\mathbf{n}^0,$$

and considering that $\dot{J} = J\mathrm{tr}(\dot{\mathbf{F}}\mathbf{F}^{-1}) = J\mathrm{tr}(\mathbf{L})$ and $\dot{(\mathbf{F}^{-T})} = -\mathbf{L}^T\mathbf{F}^{-T}$, we obtain

$$\dot{\mathbf{s}} = -\dot{P}J\mathbf{F}^{-T}\mathbf{n}^0 - JP\mathrm{tr}(\mathbf{L})\mathbf{F}^{-T}\mathbf{n}^0 + JP\mathbf{L}^T\mathbf{F}^{-T}\mathbf{n}^0.$$

In the current configuration (re–applying Nanson formula (3.11))

$$\boldsymbol{\Sigma}\mathbf{n} = -\dot{P}\mathbf{n} - P\mathrm{tr}(\mathbf{L})\mathbf{n} + P\mathbf{L}^T\mathbf{n},$$

so in the incompressible case we have (since $\mathrm{tr}(\mathbf{L}) = 0$)

$$\boldsymbol{\Sigma}\mathbf{n} = -\dot{P}\mathbf{n} + P\mathbf{L}^T\mathbf{n}. \tag{3.44}$$

The "Piola identity" is based on the following analytical result:

$$\mathrm{Div}(J\mathbf{F}^{-T}) = \mathbf{0},$$

obtained using, first, the divergence theorem

$$\int_{\mathcal{B}^0} \mathrm{Div}(J\mathbf{F}^{-T})dV^0 = \int_{\partial\mathcal{B}^0} J\mathbf{F}^{-T}\mathbf{n}^0 dA^0,$$

then using Nanson's formula (3.11)

$$\int_{\partial\mathcal{B}^0} J\mathbf{F}^{-T}\mathbf{n}^0 dA^0 = \int_{\partial\mathcal{B}} \mathbf{n}dA = \int_{\partial\mathcal{B}} \mathbf{I}\mathbf{n}dA,$$

and finally the divergence theorem

$$\int_{\partial\mathcal{B}} \mathbf{I}\mathbf{n}dA = \int_{\mathcal{B}} \mathrm{div}\mathbf{I}dV = \mathbf{0}.$$

Therefore

$$\begin{aligned}\mathrm{Div}\mathbf{S} &= \mathrm{Div}(J\mathbf{T}\mathbf{F}^{-T}) = \mathrm{Div}(\mathbf{T}(J\mathbf{F}^{-T})) \\ &= (\mathrm{Div}\mathbf{T})(J\mathbf{F}^{-T}) + \mathbf{T}\mathrm{Div}(J\mathbf{F}^{-T}) = J\mathrm{Div}\mathbf{T}\mathbf{F}^{-T},\end{aligned}$$

so remembering the pull–back rule $\mathrm{div}\mathbf{A} = \mathrm{Div}(\mathbf{A}\mathbf{F}^{-T})$, we obtain the Piola identity $\mathrm{Div}\mathbf{S} = J\mathrm{Div}(\mathbf{T}\mathbf{F}^{-T}) = J\mathrm{div}\mathbf{T}$.

3.5 Constitutive Models

The aim of this section is to introduce the constitutive model suitable to describe the behaviour of rubber-like polymers. Polymers are studied in the fields of polymer chemistry, polymer physics, and polymer engineering. In the last sixty years, many studies have focused on finding new constitutive relations: in particular, many physicists and chemists focused on the research for forms of strain energy so that they could have a good prediction in large deformations [37], [54], [1], [18]. A good constitutive model should represent the three-dimensional nature of the stress-stretch behaviour using a minimal number of parameters to represent physically the deformation process. Ideally, the parameters should be obtainable from a small number of experiments. Simultaneously, it is hard to find a constitutive model which accurately represents the behaviour of such materials

in various deformation states and satisfies the criterion of requiring only a small number of "physically based" parameters, therefore such material parameters or constants should be independent of the deformation state. The first statistical mechanical approach for describing force on a deforming polymeric network assumed the use of Gaussian statistics, based on the fact that chains never approached their fully extended length $r_L = lN$, where N is the number of statistical links of lenght l in the chain between chemical crosslinks. Gaussian statistics yields to Neo–Hookean constitutive law

$$W = \frac{\mu}{2}(\lambda_1^2 + \lambda_2^2 + \lambda_3^2 - 3), \quad \mu = nk\Theta, \tag{3.45}$$

where λ_i are the applied stretches and whose stiffness modulus is a function of the chain density n, Boltzmann's constant k and temperature Θ. In a fundamental review article on basic rubber elasticity, Gent has outlined some open problems. One of these is to understand the non-Gaussian character of short chain elasticity and another question emphasizes the need for a satisfactory general treatment of networks under large deformations, when the chains approach their fully stretched state. It is suggested that progress in this direction would aid the understanding of work hardening, fatigue and fracture of rubber. It is well known that the chemical structure of a polymeric chain may be of three types: *isotactic*, *syndiotactic* and *atactic*. Natural polymeric substances such as natural rubber or guttapercha have an isotactic structure so that the side groups lie on the same side of the polymeric chain. *Isotactic* polymers always crystallize if the temperature is decreased or if they are stretched, because the corresponding groups of two neighboring chains may match easily to form an ordered structure. In isotactic polymers the presence of crystallites act as large junctions or cross links and this has a *strain-stiffening* effect on the mechanical behavior of the material. Therefore when a piece of natural rubber is stretched, because the side groups of the chains are able to converge, as the stretch increases they crystallize and the material stiffens. This effect is clearly recorded in a simple tension experiment where the stress-extension curves exhibit a rapid rise at high values of stretch. On the other hand the structure of many synthetic polymers is *atactic*, i.e. the side groups

are irregularly placed on each side of the chains. An atactic chain never crystallizes, because the side groups, having different sizes and chemical properties may not match in space due to the irregularity of their position relative to the chain backbone. A severe rise in the stress-extension curves is clearly recorded also in experiments with *atactic* rubber-like materials, but here the stiffening arises from the effects of *finite chain extensibility*. Indeed when the full extension of the polymeric chain is approached the material stiffens because most of the monomers composing the chain become aligned along the direction of stretch, and one has to start stretching the bonds, and changing bond angles, both of which require larger energies that of changing the configurations of the chains. Important atactic polymers are elastin polypeptide chains constituting the protein responsible for soft tissue elasticity. Generally speaking, in nearly all networking-forming bio-molecular systems, the process of strain-stiffening is a major factor in the response to a deforming force because this is the mechanism that allows biological tissue to respond adaptively to varying external mechanical conditions that may damage tissue integrity. Limiting chain extensibility from a phenomenological point of view may be introduced in many ways and a detailed review of some of the possibilities may be found in the paper by Horgan and Saccomandi [24].

3.5.1 Mooney-Rivlin Model

In Continuum Mechanics, a Mooney-Rivlin solid is a hyperelastic material model where the strain energy density function is a linear combination of two invariants of the left Cauchy-Green deformation tensor **B**. It was proposed by Melvin Mooney in 1940 [32] and expressed in terms of invariants by Ronald Rivlin in 1948 [40]. The strain energy density function for an incompressible MooneyRivlin material, which is an extension of the Neo-Hookean model (3.45) is

$$W = \frac{\mu_1}{2}(I_1 - 3) - \frac{\mu_2}{2}(I_2 - 3), \quad \mu = \mu_1 - \mu_2, (\mu_2 < 0). \tag{3.46}$$

The ability of neo-Hookean and Mooney-Rivlin constitutive model is to capture small to moderate stretch behaviour of rubber elastic material is

well-recognized.

3.5.2 Arruda-Boyce Model

The need for a constitutive relationship which possesses mathematical simplicity, requires one test to characterize the material and has a limited number of parameters, has been proposed by Arruda and Boyce [1]. The statistical mechanics approach to rubber elasticity models the rubber chain segment between chemical crosslinks as a number N of rigid links of equal length l. The initial chain length is taken from a random walk consideration of N steps of length l, and is denoted by r^0,

$$r^0 = \sqrt{N}l.$$

The fully extended chain has approximate length lN so that the limiting extensibility (or chain locking stretch), defined as the final length divided by initial length, is given in terms of the statistical parameters as $\lambda_L = \sqrt{N}$. At any value of the chain length the most probable angular distribution of rigid links about the chain vector length may be found, following the use of Langevin statistics. Langevin function takes the form

$$\mathscr{L}(x) = \coth x - \frac{1}{x}$$

and it arises in the context of magnetization of an ideal paramagnet, for statistical analysis of randomly jointed chains. The Arruda-Boyce model has been constructed a representative macromolecular network of eight-chains, where each chain emanated from the center of a cube out of each corner. The cube is deformed such that each face lies along a principal stretch axis.

The network principal stress-stretch behaviour is given by

$$\sigma_i = \frac{nk\Theta}{3}\sqrt{N}\frac{\lambda_i^2}{\lambda_{chain}}\mathscr{L}^{-1}\left(\frac{\lambda_{chain}}{\sqrt{N}}\right) + p, \quad i = 1, 2, 3, \tag{3.47}$$

where $\sqrt{N}$ represents the limiting extensibility of a chain, $\mathscr{L}^{-1}$ is the inverse Langevin function ,p is the hydrostatic pressure, λ_i the principal stretches

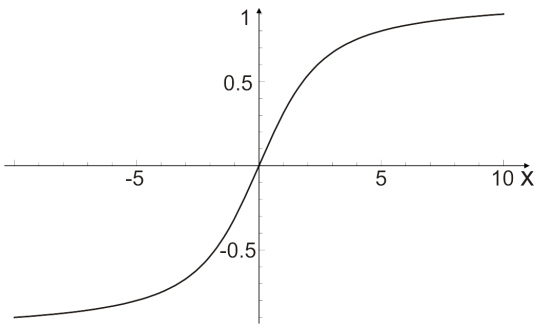

Figure 3.3: Langevin function.

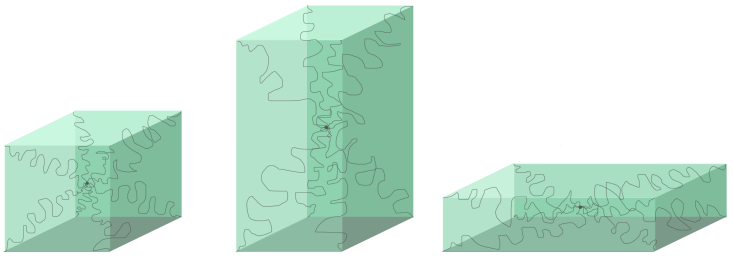

Figure 3.4: Schematic representation of the Arruda-Boyce eight-chain network model in the a) undeformed state, b) in uniaxial tension and c) in uniaxial compression.

and finally

$$\lambda_{chain} = \sqrt{\frac{I_1}{3}} = \frac{1}{\sqrt{3}} \left(\sqrt{\lambda_1^2 + \lambda_2^2 + \lambda_3^2} \right)$$

is the stretch on each chain in the network.
The inverse of Langevin function $\mathscr{L}^{-1}$ is achieved using the methodology of Padé approximation [10] and allows to do a convenient analysis of experimental data and analytical manipulations of a material models: this inverse is given into an approximant Taylor-expansion and takes the form:

$$\mathscr{L}^{-1}(x) = 3x + \frac{9}{5}x^3 + \frac{297}{175}x^5 + \frac{1539}{875}x^7 + \frac{126117}{67375}x^9 + \dots.$$

Then the principal stresses from (3.47) result

$$\begin{aligned}\sigma_i = nk\Theta\frac{\lambda_i^2}{\sqrt{\frac{I_1}{N}}}\Bigg[&\left(\frac{I_1}{N}\right)^{\frac{1}{2}} + \frac{1}{5}\left(\frac{I_1}{N}\right)^{\frac{3}{2}} + \frac{11}{175}\left(\frac{I_1}{N}\right)^{\frac{5}{2}} \\ &+ \frac{19}{875}\left(\frac{I_1}{N}\right)^{\frac{7}{2}} + \frac{519}{67375}\left(\frac{I_1}{N}\right)^{\frac{9}{2}} + \dots\Bigg],\end{aligned} \tag{3.48}$$

and strain energy function was found via integration of eq. (3.48) in the underfomed($I_1 = 3$) and the actual configuration, taking into account that $\sigma_i = \frac{\partial W}{\partial \lambda_i}\lambda_i + p$, giving

$$\begin{aligned}W_{AB} = nk\Theta\Big[&\frac{1}{2}(I_1 - 3) + \frac{1}{20N}(I_1^2 - 9) + \frac{11}{1050N^2}(I_1^3 - 27) \\ &+ \frac{19}{7000N^3}(I_1^4 - 81) + \frac{519}{673750N^4}(I_1^5 - 243) + \dots\Big].\end{aligned} \tag{3.49}$$

3.5.3 Gent Model

Models involve a strain-energy density of the form $W = W(I_1)$, are so *called generalized neo-Hookean models*. The simplest model with limiting chain extensibility is due to Gent. Stress–strain relations for simple, unfilled rubber vulcanizates, are described reasonably well at small and moderate deformations by the Neo–Hookean constitutive relation, which can be rewritten as

$$W = \frac{\mu}{2}J_1 \tag{3.50}$$

where μ is the shear modulus, and J_1 is the first invariant, defined by:

$$J_1 = \lambda_1^2 + \lambda_2^2 + \lambda_3^2 - 3, \tag{3.51}$$

where, as usual, $\lambda_1, \lambda_2, \lambda_3$ are the principal stretch ratios. A number of refinements of equation (3.50) have been proposed, that give even better agreement with experiment at small and moderate strains. However, large discrepancies are found at large strains when the molecular chains become nearly fully stretched. An empirical two–constant relation for W, suitable for use over the entire range of strains, was proposed by A. N. Gent in 1995: it was similar to the Langevin form proposed by James, Guth [52] and Treloar [49] in terms of the maximum strain that a network molecular chain can undergo, but it has a simpler mayhematical form. At the basis of the model is the assumption to have a maximum value of J_1, denoted by J_m, at which the material reaches a limiting state. For a a network of molecular chains, this would be the fully stretched state. At this point W become infinitely large. In order to simulate this behaviour, the following constitutive relation is proposed in place of equation (3.50):

$$W_{Gent} = -\frac{\mu}{2} J_m \log\left(1 - \frac{J_1}{J_m}\right) \tag{3.52}$$

in the limit as a polymeric chain extensibility parameter tends to infinity ($J_m \to \infty$), (3.52), reduces to the classical neo-Hookean form (3.50). Although empirical, this relation has several advantages:

- it involves just two material parameters (μ and J_m), which are given in terms of microscopic properties,
- at small strains equation (3.52) reduces to (3.50),
- since equation (3.52) is expressed in terms of a strain invariant, it can be applied to complex states of deformation,
- it involves only an additional constant respect to (3.50), which is J_m, whose value may be deduced from simple molecular and physical considerations: indeed, because maximum extension ratio of molecular

chains, when they are fully stretched, are propotional to the square root of molecular length, whereas μ is inverserly proportional to the molecula length, the initial constant of (3.52), EJ_m is expeted to be independent of molecular length and hence of the degree of crosslinking,

- (3.52) yields stress–strain relations of remarkably simple mathematical form.

Disadvantages of using this model: predictions of the Gent constitutive law differ somewhat from those given by particular molecular models of rubber network, in particular the differences would have been even more pronounced at large strains because the upturn of "non–affine" displacements of a network occurs at higher extensions.

Comparison between Arruda-Boyce and Gent Model

Returning to the strain energy function of the Gent model given in eq. (3.52), we note that the natural logarithm term can be expanded which yields

$$W_{Gent} = \frac{E}{6} J_m \Big[\frac{J_1}{J_m} + \frac{1}{2}\left(\frac{J_1}{J_m}\right)^2 + \frac{1}{3}\left(\frac{J_1}{J_m}\right)^3 + \frac{1}{4}\left(\frac{J_1}{J_m}\right)^4 + \dots \frac{1}{n+1}\left(\frac{J_1}{J_m}\right)^{n+1} \Big].$$

Furthemore, substituting $J_1 = I_1 - 3$ then gives

$$W_{Gent} = \frac{E}{6} \Big[(I_1 - 3) + \frac{1}{2J_m}(I_1 - 3)^2 + \frac{1}{3J_m^2}(I_1 - 3)^3 + \frac{1}{4J_m^3}(I_1 - 3)^4 + \dots \frac{1}{(n+1)J_m^n}(I_1 - 3)^{n+1} \Big]. \tag{3.53}$$

In other words, the Gent new constitutive model takes the form of a general invariant based representation of the strain energy function

$$W_{Gent} = \sum_{i=1}^{n} c_i (I_1 - 3)^i.$$

However, in the Gent new model, the coefficient c_i are all defined a priori as functions of J_m, which thus provides a physical meaning to the coefficients. The Arruda-Boyce model can also be re-written in a general invariant-based form as

$$W_{AB} = \sum_{i=1}^{n} \tilde{c}_i (I_1^i - 3^i),$$

where the $\tilde{c}_i$ are all determined a priori as functions of the limiting network stretch $N^{1/2}$. As in the Gent model, $\tilde{c}_i$ have physical meaning and do not require additional tests to be fitted. Note that the Arruda-Boyce model was based on a network of eight non-Gaussian chains and was also demonstrated to be predictive of other states of deformation when the two material constants $nk\Theta$ and N were fit to data from a singol test. In other words, when fitting $nk\Theta$ and N to uniaxial tension data, the Arruda-Boyce model was found to predict other states of deformation such as shear and biaxial tension. One can visualize why the Arruda-Boyce is predictive of general three-dimensional states of deformation by observing that each chain in the network stretches and rotates toward the maximum principal stretch axis(es) with deformation much as real molecular network must when deformed.
Comparing eq. (3.53) with eq. (3.49), one can observe that the Gent model emulates the main features of the Arruda-Boyce model. The Gent model recognizes a need for averaged representation of chain stretch (i.e. I_1 based where an average chain stretch is $(I_1/3)^{1/2}$ as shown in Arruda-Boyce), as well as a need for higher order terms in I_1. The Gent model also recognizes the need to weigh the contribution of chain stretch to stress build-up by a limiting network stretch (i.e. the Gent J_1/J_m weighting can be compared to the inverse Langevin based weighting of $\lambda_{chain}/N^{1/2}$ used in the Arruda-Boyce model), where in both models the stress increases in an asymptotic manner as the first invariant approaches a limiting value. In other words, we note that, considering that μ of the Gent model is equal to $6nk\Theta$ of Arruda-Boyce model (or making allowance for μ of (3.52) which is equal to $2nk\Theta$), therefore the limiting stretch can be furnished in the following

approximated formula

$$I_1/3 = N,$$

so for example if we care for uniaxial stretch $\lambda_{lim} = 10$, for Gent model $J_m = 97.2$, then for Arruda-Boyce $N = 33.4$. In Fig. 3.5, the Arruda-Boyce curve exhibits a more gradual approach to the limiting stretch state than does the Gent model, but otherwise the two models show similar behaviour in the case of uniaxial stress.

Indeed, other models have been formulated based on non-Gaussian statis-

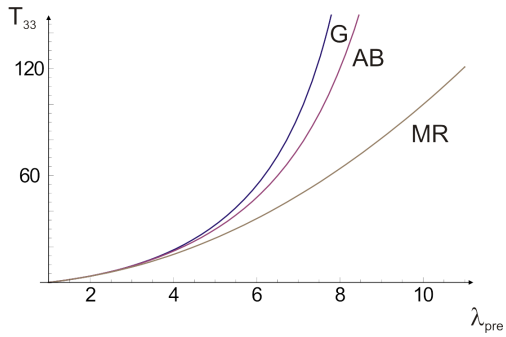

Figure 3.5: Comparison between the three models in uniaxial test (for Gent material $J_m = 97.2$ and for Arruda-Boyce $N = 33.4$).

tics. In one of this [3], Beatty has considered a stretch averaged full-network model of rubber elasticity. On considering a non-Gaussian network of perfectly flexible chains and using the approximate expression for the probability distribution function for the end-to-end distance, it is shown in [3] that the macroscopic constitutive equation for the Cauchy stress tensor for an incompressible material, obtained by averaging in a suitable way, is given by

$$\mathbf{T}_{Beatty} = -p\mathbf{I} + \mu_0 \frac{\mathscr{L}^{-1}(\hat{\lambda}_r)}{3\hat{\lambda}_r}\mathbf{B}, \tag{3.54}$$

where the mean relative chain stretch $\hat{\lambda}_r$ is the ratio of the current chain vector length r_{chain} to its fully extended length $r_L = \sqrt{N}$, defined by

$$\hat{\lambda_r} = \sqrt{\frac{I_1}{3N}}. \tag{3.55}$$

Since the Cauchy stress associated with (3.52) is given by

$$\mathbf{T}_{Gent} = -p\mathbf{I} + \mu \frac{J_m}{J_m - (I_1 - 3)}\mathbf{B}, \tag{3.56}$$

on using (3.55) one obtains $I_1 = 3N\hat{\lambda}_r$, (3.56) can be rewritten as

$$\mathbf{T}_{Gent} = -p\mathbf{I} + \mu \frac{N-1}{N}\frac{1}{1-\hat{\lambda}_r^2}\mathbf{B}, \tag{3.57}$$

where we have used the fact that if the maximum value for I_1 is $3N$, then

$$J_m = 3(N-1).$$

From (3.57), it is clear that Gent model cannot be obtained by a power series approximation of the molecular models based on the inverse Langevin function. The use of a power series to approximate the inverse Langevin function is somewhat misleading because in (3.54) there is a singularity as $\hat{\lambda}_r \to \infty$, and functions with singularities cannot be approximated globally by polynomial expressions. For this reason the comparison carried out in [5] between the eight chain molecular model of [1] and the Gent model is not complete. Then, since the Gent model is remarkably simple, and since analytic closed-form solutions to several benchmark boundary-value problems have been obtained recently on using this model, in [24] authors have shown that the Gent model provides a very good qualitative and quantitative approximation of such models, and they have also seen that the Gent model is closely related to Padé approximants for the inverse Langevin function that arises in the non-Gaussian molecular models. In conclusion, in problems include those of torsion, axial, azimuthal and helical shear, anti-plane shear, mode III crack problems, rotation induced deformation of circular cylinders and fracture, results are radically different from those obtained in the

literature for classical models such as the neo-Hookean and Mooney-Rivlin models for incompressible rubber [25]. Gent model is an attractive alternative to the comparatively complicated molecular models for incompressible rubber involving the inverse Langevin function and warrants inclusion in the libraries of large scale commercial computer codes (e.g., ABAQUS or ANSYS) especially since analytic solutions to benchmark problems are now available for this model.

3.6 Classification of Regimes and Strain Localization

In the purely mechanical case, these materials do not present localizations, as can be deduced from the classical classification of regimes of the governing equations. Considering a deformation of the type $\lambda_1 = \lambda$, $\lambda_2 = 1/\lambda$ and $\lambda_3 = 1$, the ansatz made by Hill and Hutchinson provides the introduction of a stream-function ψ of the type

$$\psi = \psi(c_1 x_1 + c_2 x_2), \tag{3.58}$$

so that $u_1 = \frac{\partial \psi}{\partial x_2}$ and $u_2 = -\frac{\partial \psi}{\partial x_1}$, in this way the incompressibility constraint is automatically verified. Then, the equilibrium equations (3.21) are given by

$$\begin{aligned}
&\Big[c_1^2 c_2 C_{1111} + c_1 c_2^2 C_{1112} - c_1^3 C_{1121} \\
&+ c_2\big(- c_1^2 C_{1122} + c_1 c_2 C_{1211} + c_2^2 C_{1212} \\
&- c_1(c_1 C_{1221} + c_2 C_{1222})\big)\Big]\psi'''(c_1 x_1 + c_2 x_2) - \frac{\partial \dot{p}}{\partial x_1} = 0,
\end{aligned} \tag{3.59}$$

$$\begin{aligned}
&\Big[c_1^2 c_2 C_{2111} + c_1 c_2^2 C_{2112} - c_1^3 C_{2121} \\
&+ c_2\big(- c_1^2 C_{2122} + c_1 c_2 C_{2211} + c_2^2 C_{2212} \\
&- c_1(c_1 C_{2221} + c_2 C_{2222})\big)\Big]\psi'''(c_1 x_1 + c_2 x_2) - \frac{\partial \dot{p}}{\partial x_2} = 0,
\end{aligned} \tag{3.60}$$

differentiating (3.59) respect to x_2, (3.60) respect to x_1 and subtracting the latter, we obtain the fundamental equation

$$\begin{aligned} &c_2^4 C_{1212} + c_1^4 C_{2121} + c_1 c_2^3 (C_{1112} + C_{1211} - C_{1222} - C_{2212}) \\ &+ c_1^3 c_2 (-C_{1121} - C_{2111} + C_{2122} + C_{2221}) \\ &+ c_1^2 c_2^2 (C_{1111} - C_{1122} - C_{1221} - C_{2112} - C_{2211} + C_{2222}) = 0. \end{aligned} \tag{3.61}$$

Eq. (3.61) is equivalent [23] to

$$\{\mu + \frac{1}{2}(\sigma_1 - \sigma_2)\} c_1^4 + 2(2\mu^* - \mu) c_1^2 c_2^2 + \{\mu - \frac{1}{2}(\sigma_1 - \sigma_2)\} c_2^4 = 0, \tag{3.62}$$

where $(\sigma_1 - \sigma_2) = \lambda \frac{dW}{d\lambda}$, $\mu^* = \frac{\lambda}{4} \frac{d}{d\lambda}(\sigma_1 - \sigma_2)$ and $\mu = \frac{1+\lambda^4}{2(\lambda^4-1)}$. In general for (3.62) there are two distinct roots c_1^2/c_2^2. By combining the 4 associated functions of type (3.58) linearly we obtain a general solution of

$$\{\mu + \frac{1}{2}(\sigma_1 - \sigma_2)\} \frac{\partial^4 \psi}{\partial x_1^4} + 2(2\mu^* - \mu) \frac{\partial^4 \psi}{\partial x_1^2 x_2^2} + \{\mu - \frac{1}{2}(\sigma_1 - \sigma_2)\} \frac{\partial^4 \psi}{\partial x_2^4} = 0.$$

Since we are interested only in real ψ, the character of this solution depends on the nature of roots c_1/c_2, if they are real or not. We re-write eq. (3.62), considering $c_1/c_2 = \nu$

$$\{\mu + \frac{1}{2}(\sigma_1 - \sigma_2)\} \nu^4 + 2(2\mu^* - \mu) \nu^2 + \{\mu - \frac{1}{2}(\sigma_1 - \sigma_2)\} = 0, \tag{3.63}$$

the nature of the roots $\pm\nu_1$ and ν_2 of eq. (3.63) defines the regime classification:

- complex conjugate $\pm\nu_1$ and ν_2 in the elliptic complex regime (EC),
- pure imaginary $\pm\nu_1$ and ν_2 in the elliptic imaginary (EI),
- real $\pm\nu_1$ and ν_2 in the hyperbolic (H),
- two real and two pure imaginary $\pm\nu_1$ and ν_2 in the parabolic regime (P).

In Fig. 3.6, the regimes of the three material models employed in the thesis are reported for plain strain deformations, in plots having, in abscissa, the parameter $X = \frac{(\sigma_1 - \sigma_2)}{4\mu^*}$ and in ordinate $Y = \frac{\mu}{2\mu^*}$.

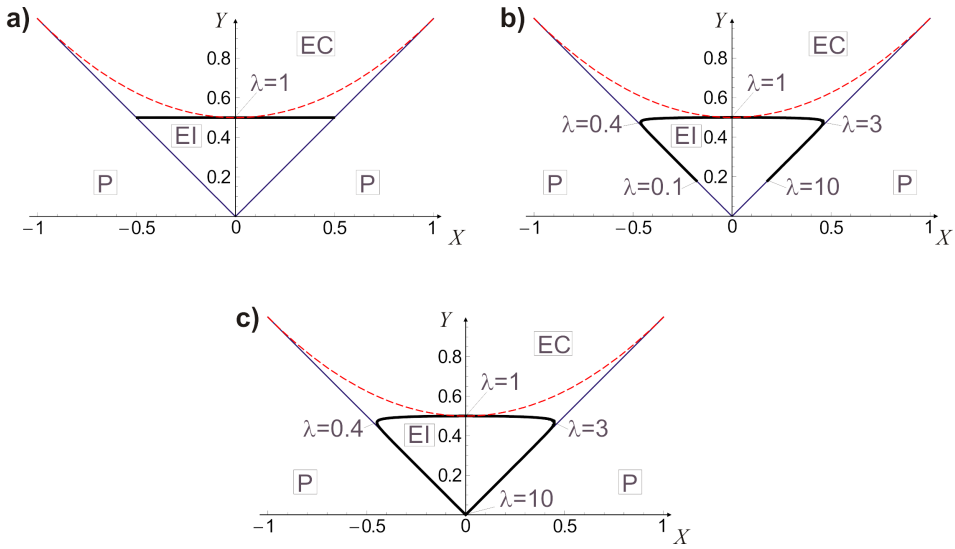

Figure 3.6: Classification of regimes for a) Mooney-Rivlin, b) Arruda-Boyce and c) Gent materials.

Chapter 4

Theory of Elastic Dielectrics

The theory of nonlinear electroelasticity accounts for the coupling of electrical and mechanical material properties of electro-active solids subjected to finite strain. The theory was originally developed by Toupin [47] in 1956 and it is of a great interest because the electromechanical coupling opens the door for the development of new devices: these materials rapidly and reversibly change their mechanical properties in response to the application of an electric field, being capable of large elastic deformations that are much larger than those arising in conventional elasticity. We summarize the basic equations in Eulerian and Lagrangian form for the mechanical and electric field variables and their interactions. We deduce the constitutive law for an isotropic electroelastic material, based on a total energy function that enables expressions for the stress and electric field variable to be cast in particularly simple forms. Two alternative formulations are highlighted: in one formulation the deformation gradient and the electric displacement field vector are taken as the independent variables, while in the other the electric displacement is replaced by the applied electric field vector. Appropriate boundary conditions are specified for the electric field variables and for the total stress tensor. Then, we consider incremental changes in the deformation within the material and in the electric displacement vector, deducing the complete form of electro-elastic tensor moduli.

4.1 Kinematics

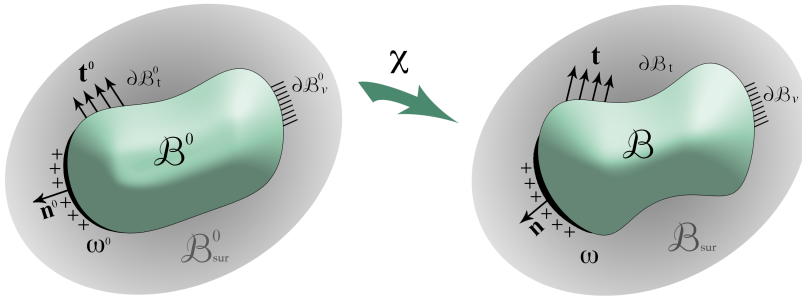

Figure 4.1: A body deformed by electro-mechanical loadings.

Let us consider an isolated system consisting of a multi–phase phase electroelastic body and the complemental surrounding space (see Fig. 4.1) and indicate, as before, by $\mathcal{B}^0$ and $\mathcal{B}^0_{sur} = \mathbb{R}^3 \setminus \mathcal{B}^0$ the underformed stress–free configuration of the body and the surrounding space, respectively. We identify with $\partial\mathcal{B}^0$ the boundary separating $\mathcal{B}^0$ from the surrounding and, in order to specify boundary conditions, the subsets $\partial\mathcal{B}_v$ and $\partial\mathcal{B}_t$ ($\partial\mathcal{B}_v \cup \partial\mathcal{B}_t = \partial\mathcal{B}$, $\partial\mathcal{B}_v \cap \partial\mathcal{B}_t = \emptyset$)are introduced. The application of both mechanical loadings and electric fields deforms quasi statically the body from $\mathcal{B}^0$ to the current configuration $\mathcal{B}$. Such deformation is described by the function $\boldsymbol{\chi}$ that maps a reference point $\mathbf{x}^0$ in $\mathcal{B}^0$ to its deformed position $\mathbf{x} = \boldsymbol{\chi}(\mathbf{x}^0)$ in $\mathcal{B}$. If the surrounding space does not consists of vacuum, the deformation $\boldsymbol{\chi}$ can be extended to $\mathcal{B}^0_{sur}$, yielding $\mathcal{B}_{sur} = \mathbb{R}^3 \setminus \mathcal{B} = \boldsymbol{\chi}(\mathcal{B}^0_{sur})$.

4.2 Maxwell's Equations

In this section, we summarize the specialization of Maxwell's equations for electric field variables in the absence of magnetic fields, free currents and free volume charges and with no time dependence. We use the notation $\mathbf{e}$ for the electric field vector and $\mathbf{d}$ for the electric displacement vector. These are governed by the equations

$$\text{curl}\, \mathbf{e} = \mathbf{0}, \quad \text{div}\, \mathbf{d} = 0, \quad \text{in } \mathcal{B} \cup \mathcal{B}_{sur} \tag{4.1}$$

where curl and div are operators acting in the current domain, with derivatives taken with respect to $\mathbf{x}$. Eqs. $(4.1)_1$ implies that the electric field is conservative, it means that exists a continous scalar function $\phi(\mathbf{x})$, the electric potential, such that

$$\mathbf{e} = -\text{grad}\phi.$$

In vacuo we may regard the electric field $\mathbf{e}$ as the basic variable and then we have simply $\mathbf{d} = \epsilon_0 \mathbf{e}$, where the constant ϵ_0 is the vacuum electric permittivity. For condensed matter, an additional variable is introduced in order to explain the alignement of the dipoles inside the body, caused by the presence of electric field: the polarization density, which is defined as

$$\mathbf{P} = \mathbf{d} - \epsilon_0 \mathbf{e}. \tag{4.2}$$

4.3 Balance Equations

To describe equilibrium of a soft dielectric it is important to introduce the concept of Maxwell stress, often employed in the literature to highlight the effect of the polarization of the material on the total stress distribution. In Toupin [47] and Eringen [15] papers, the total electric field is taken as the sum of three components: one due to the presence of dielectric material, another one due to the effect of polarization charge in the body and on its surface and in addition, the so called local electric field, which is function of the strain and polarization via the constitutive law. The first two fields

together compose the classical Maxwell-Faraday electric field. In McMeeking [31] an innovative way to consider the Maxwell stress is presented, in which the basic physics is not different from that used in [47] and [15], but the structure have a simpler form than used in [47] and [15], identifying different contributions, such as external field, depolarization field or local field: a single electric field is utilized, assuming that it is connected to material strain and polarization by a constitutive law. This formulation is supported by the fact that the electrostatic stress is measurable in experiments either directly through characterization of stress and electric fields or through measurement of the constituive properties of the material. Since the versatility of this formulation, also Ogden [12] and Suo [45] have adopted the structure of Maxwell stress proposed by McMeeking and Landis.

Rinaldi and Brenner [39] highlight the distinction between electrostatic body forces and the associated Maxwell stresses, considering the well-known mathematical relation (see eq. (4.9)), and they emphasize that the equivalence is not supported by physical arguments.

In order to formulate the equilibrium equations, it is instrumental to introduce the notion of *total* (true) stress tensor, $\mathbf{T}$, for which we consider (see eq. (3.21))

$$\operatorname{div} \mathbf{T} = \mathbf{0}, \tag{4.3}$$

and the balance of the angular momentum requires that

$$\mathbf{T} = \mathbf{T}^T. \tag{4.4}$$

The total stress can be formally split into two parts, namely

$$\mathbf{T} = \mathbf{T}_{mec} + \mathbf{T}_e, \tag{4.5}$$

where $\mathbf{T}_{mec}$ is the mechanical stress, while $\mathbf{T}_e$ is the Maxwell stress. Eq. (4.5) must balance the surface traction

$$\mathbf{t} = [\![\mathbf{T}_{mec} + \mathbf{T}_e]\!]\mathbf{n}, \tag{4.6}$$

where $\mathbf{t}$ is now the mechanical (nonelectrical) surface force per unit area acting on $\partial\mathcal{B}$ and the operator $[\![\cdot]\!]$ indicates a jump across the surface $\partial\mathcal{B}$.

Note that eq. (4.6) illustrates why it is difficult to measure separately the mechanical and the Maxwell stresses, since it shows that any traction measured by mechanical means is related to their sum. Since there are no experiments that can separate the effects of the mechanical and the Maxwell stresses unambiguously, it is generally more profitable to consider their sum and not to try to identify them separately. The sum will determine the already introduced total *true* stress $\mathbf{T}$. In addition it can be observed that while $\mathbf{T}$ is symmetric, in general $\mathbf{T}_{mec}$ is not symmetric.

Since mathematically we can separate the two contributions, eq. (4.3) can be rewritten as

$$\mathrm{div}\mathbf{T}_{mec} + \mathbf{f}_e = \mathbf{0}, \tag{4.7}$$

where $\mathbf{T}_{mec}$ can be seen also as the classical Cauchy stress tensor of Continuum Mechanics, in equilibrium with total (both electrical and mechanical) tractions, and $\mathbf{f}_e$ is the electric body force (per unit volume) given by

$$\mathbf{f}_e = (\mathrm{grad}\mathbf{e})^T\mathbf{P}. \tag{4.8}$$

Next we remark that, from (4.2) and (4.1) [1], we have

$$\mathbf{f}_e = \mathrm{div}(\mathbf{e}\otimes\mathbf{d}) - \frac{\epsilon_0}{2}\mathrm{grad}(\mathbf{e}\cdot\mathbf{e}) = \mathrm{div}(\mathbf{e}\otimes\mathbf{d} - \frac{\epsilon_0}{2}(\mathbf{e}\cdot\mathbf{e})\,\mathbf{I}),$$

so we assume that the electric body force can be derived from the Maxwell stress tensor $\mathbf{T}_e$ in this way

$$\mathbf{f}_e = \mathrm{div}\mathbf{T}_e, \tag{4.9}$$

where the electrical body force is the effect of interaction between the electric field and the solid. At the boundary $\partial\mathcal{B}$, the jump in $\mathbf{T}_e$ is linked to the electrical traction $\mathbf{t}_e$ as

$$\mathbf{t}_e = -[\![\mathbf{T}_e]\!]\mathbf{n} \quad \text{on} \quad \partial\mathcal{B}, \tag{4.10}$$

so that eq. (4.6) is satisfied.

[1] Given a vector $\mathbf{v}(\mathbf{x})$, $\mathrm{curl}\mathbf{v}(\mathbf{x})$ is the axial vector corresponding to the skew tensor $\mathrm{grad}\mathbf{v}(\mathbf{x}) - (\mathrm{grad}\mathbf{v}(\mathbf{x}))^T$. It follows that if $\mathrm{curl}\mathbf{v} = \mathbf{0}$ then $\mathrm{grad}\mathbf{v}(\mathbf{x}) = (\mathrm{grad}\mathbf{v}(\mathbf{x}))^T$.

Note that the relationship between $\mathbf{f}_e$ and $\mathbf{T}_e$ is not the only possible within the theory presented above (eq. (4.8), (4.9)). As shown by Bustamante et al. [6], other couples can be determined which fit the general theory based on the total stress. For instance, two of them are reported in Table 4.1.

Energy	Body force $\mathbf{f}_e$	Maxwell Stress $\mathbf{T}_e$
$W(\mathbf{F},\mathbf{e})$	$(\mathbf{grad}\,\mathbf{e})^T\mathbf{P}$	$\mathbf{d}\otimes\mathbf{e}-\frac{1}{2}(\mathbf{d}\cdot\mathbf{e})\mathbf{I}$
$\tilde{W}(\mathbf{F},\mathbf{d})$	$\epsilon_0^{-1}(\mathbf{grad}\,\mathbf{d})^T\mathbf{P}$	$\mathbf{e}\otimes\mathbf{d}+\big[\epsilon_0(\mathbf{d}\cdot\mathbf{d})/2-(\mathbf{d}\cdot\mathbf{e})\big]\mathbf{I}$

Table 4.1: Table of relationships between $\mathbf{f}_e$ and $\mathbf{T}_e$ [6].

4.3.1 Eulerian Formulation

Equilibrium of the dielectric body, in absence of volume forces, is summarized in the following equations

$$\begin{aligned} &\operatorname{div}\mathbf{T}=\mathbf{0}, \quad \mathbf{T}=\mathbf{T}^T \quad \text{in } \mathcal{B}\cup\mathcal{B}_{sur},\\ &\operatorname{div}\mathbf{d}=0, \quad \operatorname{curl}\mathbf{e}=\mathbf{0} \quad \text{in } \mathcal{B}\cup\mathcal{B}_{sur}. \end{aligned} \tag{4.11}$$

4.3.2 Boundary Conditions in the Eulerian Formulation

It remains to prescribe appropriate boundary conditions on the fields $\mathbf{e},\mathbf{d},\mathbf{T}$ and $\boldsymbol{\chi}$, bearing in mind that outside the material, in the case of a vacuum, $\mathbf{P}=\mathbf{0}$. We introduce the subsets $\partial\mathcal{B}_v$ and $\partial\mathcal{B}_t$ ($\partial\mathcal{B}_v\cup\partial\mathcal{B}_t=\partial\mathcal{B}, \partial\mathcal{B}_v\cap\partial\mathcal{B}_t=\oslash$) where displacement and surface tractions are prescribed. Thus the boundary conditions are given by:

$$\begin{aligned} &[\![\mathbf{v}]\!]=\mathbf{0}, \quad [\![\mathbf{T}]\!]\mathbf{n}=\mathbf{t} \quad \text{on } \partial\mathcal{B}_t, \quad \mathbf{v}=\tilde{\mathbf{v}} \quad \text{on } \partial\mathcal{B}_v,\\ &[\![\mathbf{d}]\!]\cdot\mathbf{n}=-\omega, \quad \mathbf{n}\times[\![\mathbf{e}]\!]=\mathbf{0} \quad \text{on } \partial\mathcal{B}, \end{aligned} \tag{4.12}$$

where ω is the surface charge density. By convention $\mathbf{n}$ is taken as the outward pointing normal at the material boundary. In the particular case

of surrounding space consisting of vacuum, the boundary conditions $(4.12)_2$ and $(4.12)_4$ specialize to

$$\mathbf{T}\mathbf{n} = \mathbf{t} + \mathbf{T}^*\mathbf{n}, \quad \mathbf{d}\cdot\mathbf{n} = -\omega + \epsilon_0\mathbf{e}^*\cdot\mathbf{n},$$

respectively, where $\mathbf{T}$ and $\mathbf{d}$ are evaluated in the body, whereas * denotes quantities evaluated in the vacuum. It turns out that

$$\mathbf{T}^* = \epsilon_0\left(\mathbf{e}^*\otimes\mathbf{e}^* - \frac{1}{2}\left(\mathbf{e}^*\cdot\mathbf{e}^*\right)\mathbf{I}\right), \quad \mathbf{d}^* = \epsilon_0\mathbf{e}^* \tag{4.13}$$

ϵ_0 being the permittivity of vacuum ($\epsilon_0 = 8.85$ pF/m). In vacuum the Maxwell stress $\mathbf{T}_e$ coincides with $\mathbf{T}^*$.

4.3.3 Lagrangian Formulation

Integration of (4.3), (4.1) over $\mathcal{B}$, considering (4.4) and a change of variable from $\mathbf{x}$ to $\mathbf{x}^0$ yield

$$\begin{aligned} &\text{Div}\,\mathbf{S} = \mathbf{0}, \quad \mathbf{S}\mathbf{F} = (\mathbf{S}\mathbf{F})^T \quad \text{in } \mathcal{B}^0\cup\mathcal{B}^0_{sur},\\ &\text{Div}\,\mathbf{d}^0 = 0, \quad \text{Curl}\,\mathbf{e}^0 = \mathbf{0} \quad \text{in } \mathcal{B}^0\cup\mathcal{B}^0_{sur}, \end{aligned} \tag{4.14}$$

which represent the Lagrangian formulation of the field eqs. for the electroelastic response of the system, where Curl is the curl operator in the reference configuration $\mathcal{B}^0$. In the eq. (4.14), $\mathbf{S} = J\mathbf{T}\mathbf{F}^{-T}$ is the total first Piola-Kirchhoff stress, $\mathbf{d}^0$ and $\mathbf{e}^0$ are respectively the Lagrangian electric displacement and electric field, given by

$$\mathbf{d}^0 = J\mathbf{F}^{-1}\mathbf{d}, \tag{4.15}$$

and

$$\mathbf{e}^0 = \mathbf{F}^T\mathbf{e}. \tag{4.16}$$

Eq. (4.15) follows from $(4.14)_3$, using the divergence theorem and the Nanson's formula (3.11):

$$\int_{\mathcal{B}}\text{div}\,\mathbf{d}\,dV = \int_{\partial\mathcal{B}}\mathbf{d}\cdot\mathbf{n}\,dA = \int_{\partial\mathcal{B}^0}\mathbf{d}\cdot J\mathbf{F}^{-T}\mathbf{n}^0 dA^0 = \int_{\mathcal{B}^0}\text{Div}(J\mathbf{F}^{-1}\mathbf{d})dV^0.$$

Eq. (4.16) follows from $(4.14)_4$, using Kelvin-Stokes theorem and the fact that $\mathrm{d}\mathbf{x} = \mathbf{F}\mathrm{d}\mathbf{x}^0$:

$$\int_{\mathcal{S}} \operatorname{curl} \mathbf{e}\, dA = \int_{\partial\mathcal{S}} \mathbf{e}\cdot \mathrm{d}\mathbf{x} = \int_{\partial\mathcal{S}^0} \mathbf{F}^T\mathbf{e}\cdot \mathrm{d}\mathbf{x}^0 = \int_{\mathcal{S}^0} \operatorname{Curl}(\mathbf{F}^T\mathbf{e}) dA^0,$$

where $\mathcal{S}_0$ is the surface in the reference configuration that deforms into $\mathcal{S}$, and the closed curve $\partial\mathcal{S}_0$ is its boundary that deforms into $\partial\mathcal{S}$. Since the electric field is conservative, in the reference configuration $\mathbf{e}^0 = -\mathrm{Grad}\phi^0$, where $\phi^0(\mathbf{x}^0) = \phi(\mathbf{x})$ is the Lagrangian description of the electric potential.

4.3.4 Boundary Conditions in the Lagrangian Formulation

The boundary conditions (4.12) may be written in the Lagrangian form as

$$[\![\mathbf{v}^0]\!] = \mathbf{0}, \quad [\![\mathbf{S}]\!]\mathbf{n}^0 = \mathbf{t}^0 \quad \text{on } \partial\mathcal{B}_t^0, \quad \mathbf{v}^0 = \tilde{\mathbf{v}}^0 \quad \text{on } \partial\mathcal{B}_v^0, \tag{4.17}$$

$$[\![\mathbf{d}^0]\!]\cdot\mathbf{n}^0 = -\omega^0, \quad \mathbf{n}^0 \times [\![\mathbf{e}^0]\!] = \mathbf{0} \qquad \text{on } \partial\mathcal{B}^0, \tag{4.18}$$

where $\mathbf{v}^0(\mathbf{x}^0) = \mathbf{v}(\mathbf{x})$.

4.4 Constitutive Equations

We follow the procedure described in McMeeking and Landis [31] to formulate the constitutive relationships for a nonlinear dielectrics excluding here thermal and kinetic effects. The conservation of energy can written as

$$\dot{E} = P_{ext}, \tag{4.19}$$

where E is the total energy of the system and a superimposed dot (or the symbol $\frac{d}{dt}$) indicates the rate of the relevant quantity, P_{ext} denotes the external power that depends on mechanical and electrical effects. In particular, in the absence of body forces and volume free charge

$$P_{ext} = \int_{\partial\mathcal{B}_t} \mathbf{t}\cdot\dot{\mathbf{x}} dS + \int_{\partial\mathcal{B}_e} \phi\dot{\overline{(\omega dS)}}.$$

For the mechanical part, using Cauchy's theorem, the symmetry of the stress tensor and the divergence theorem, the following expression is obtained

$$\int_{\partial\mathcal{B}_t} \mathbf{t}\cdot\dot{\mathbf{x}}\, dS = \int_{\mathcal{B}} (\mathbf{T}\cdot \operatorname{grad}\dot{\mathbf{x}} + \dot{\mathbf{x}}\cdot \operatorname{div}\mathbf{T}) dV,$$

which can be reduced to

$$\int_{\partial\mathcal{B}_t} \mathbf{t}\cdot\dot{\mathbf{x}} dS = \int_{\mathcal{B}} \mathbf{T}\cdot\mathbf{L} dV,$$

making use of (3.41) and exploiting equilibrium eq. (4.3). For the electric part, using the jump condition, we have

$$\int_{\partial\mathcal{B}_e} \phi\dot{\overline{(\omega dS)}} = -\int_{\partial\mathcal{B}_e} \phi[\![\dot{\mathbf{d}}]\!]\cdot\mathbf{n} dS - \int_{\partial\mathcal{B}_e} \phi[\![\mathbf{d}]\!]\cdot\dot{\overline{(\mathbf{n}dS)}},$$

where the first integral, using divergence theorem, the relation

$$\dot{\mathbf{d}} = \hat{\mathbf{d}} - \mathbf{d}\mathrm{tr}\mathbf{L} + \mathbf{L}\mathbf{d}$$

and equilibrium equation, reduces to

$$\begin{aligned} -\int_{\partial\mathcal{B}_e} \phi[\![\dot{\mathbf{d}}]\!]\cdot\mathbf{n} dS &= -\int_{\mathcal{B}_e} \left(\phi \mathrm{div}\dot{\mathbf{d}} + \dot{\mathbf{d}}\mathrm{grad}\phi\right) dV \\ &= -\int_{\mathcal{B}_e} \phi\left(\mathbf{L}^T\cdot\mathrm{grad}\mathbf{d}\right) dV + \int_{\mathcal{B}_e} \dot{\mathbf{d}}\cdot\mathbf{e} dV, \end{aligned}$$

while the second integral, using Nanson's formula (3.11) and then the divergence theorem and equilibrium equation becomes

$$\begin{aligned} &-\int_{\partial\mathcal{B}_e} \phi[\![\mathbf{d}]\!]\cdot(\mathbf{n}\dot{dS}) = -\int_{\partial\mathcal{B}_e} \phi[\![\mathbf{d}]\!]\cdot(\mathrm{tr}\mathbf{L})\mathbf{n}\, dS + \int_{\partial\mathcal{B}_e} \phi[\![\mathbf{d}]\!]\cdot\mathbf{L}^T\mathbf{n}\, dS \\ &= \int_{\mathcal{B}_e} [(\mathrm{tr}\mathbf{L})\mathbf{d}\cdot\mathbf{e} - \phi\,\mathbf{d}\cdot\operatorname{grad}(\operatorname{div}\dot{\mathbf{x}})] dV \\ &\quad + \int_{\mathcal{B}_e} \left[\mathbf{L}^T\cdot(\phi\operatorname{grad}\mathbf{d} - \mathbf{d}\otimes\mathbf{e}) + \phi\,\mathbf{d}\cdot\operatorname{div}(\operatorname{grad}\dot{\mathbf{x}})^T\right] dV \\ &= \int_{\mathcal{B}_e} \{[(\mathbf{d}\cdot\mathbf{e})\,\mathbf{I} - \mathbf{e}\otimes\mathbf{d}]\cdot\mathbf{L} + \phi\mathbf{L}^T\cdot\operatorname{grad}\mathbf{d}\} dV. \end{aligned}$$

Therefore, for the electric part, it turns out that

$$\int_{\partial\mathcal{B}_e} \phi\dot{\overline{(\omega dS)}} = \int_{\mathcal{B}_e} \{\dot{\mathbf{d}}\cdot\mathbf{e} + [(\mathbf{d}\cdot\mathbf{e})\,\mathbf{I} - \mathbf{e}\otimes\mathbf{d}]\cdot\mathbf{L}\}dV,$$

or it can be seen as

$$\int_{\partial\mathcal{B}_e} \phi\dot{\overline{(\omega dS)}} = \int_{\mathcal{B}_e} \{[\hat{\mathbf{d}} + \mathbf{L}\mathbf{d}]\cdot\mathbf{e} - (\mathbf{e}\otimes\mathbf{d})\cdot\mathbf{L}\}dV.$$

So

$$\begin{aligned} P_{ext} = &\int_{\mathcal{B}} \{\dot{\mathbf{d}}\cdot\mathbf{e} + [\mathbf{T} + (\mathbf{d}\cdot\mathbf{e})\,\mathbf{I} - \mathbf{e}\otimes\mathbf{d}]\cdot\mathbf{L}\}dV \\ &+ \int_{\mathcal{B}_{sur}} \{\dot{\mathbf{d}}\cdot\mathbf{e} + [\mathbf{T}^* + (\mathbf{d}\cdot\mathbf{e})\,\mathbf{I} - \mathbf{e}\otimes\mathbf{d}]\cdot\mathbf{L}\}dV \end{aligned} \tag{4.20}$$

and since in vacuum $\mathbf{d} = \epsilon_0\mathbf{e}$ and taking into account (4.2), we obtain

$$\begin{aligned} P_{ext} = &\int_{\mathcal{B}} \{\dot{\mathbf{d}}\cdot\mathbf{e} + [\mathbf{T} + (\mathbf{d}\cdot\mathbf{e})\,\mathbf{I} - \mathbf{e}\otimes\mathbf{d}]\cdot\mathbf{L}\}dV \\ &+ \int_{\mathcal{B}_{sur}} \{\epsilon_0\dot{\mathbf{e}}\cdot\mathbf{e} + [\mathbf{T}^* + (\epsilon_0\mathbf{e}\cdot\mathbf{e})\,\mathbf{I} - \epsilon_0\mathbf{e}\otimes\mathbf{e}]\cdot\mathbf{L}\}dV. \end{aligned}$$

Remembering (4.13) and $\frac{d}{dt}\int_{\mathcal{B}} \frac{\epsilon_0}{2}\mathbf{e}\cdot\mathbf{e}\,dV = \epsilon_0\left[\int_{\mathcal{B}}\left(\dot{\mathbf{e}} + \frac{\mathbf{e}}{2}\right)\cdot\mathbf{e}\,dV\right]$, we have that

$$\begin{aligned} P_{ext} = &\int_{\mathcal{B}} \{\dot{\mathbf{P}}\cdot\mathbf{e} + [\mathbf{T} - \mathbf{T}^* + (\mathbf{P}\cdot\mathbf{e})\,\mathbf{I} - \mathbf{e}\otimes\mathbf{P}]\cdot\mathbf{L}\}dV \\ &+ \frac{d}{dt}\int_{\mathbb{R}^3} \frac{\epsilon_0}{2}\mathbf{e}\cdot\mathbf{e}\,dV. \end{aligned} \tag{4.21}$$

In vacuum $\mathbf{T} = \mathbf{T}^*$, $\mathbf{P} = \mathbf{0}$ and P_{ext} simply reduces to the last integral. The total energy is the sum of internal and electrostatic energies. If we indicate by $\tilde{W}$ the Helmholtz free-energy per unit reference volume of each phase, we have

$$\dot{E} = \frac{d}{dt}\int_{\mathcal{B}^0} \tilde{W}dV^0 + \frac{d}{dt}\int_{\mathbb{R}^3} \frac{\epsilon_0}{2}\mathbf{e}\cdot\mathbf{e}\,dV,$$

so that change of variables of the first integral gives

$$\dot{E} = \int_{\mathcal{B}} \{J^{-1}\dot{\tilde{W}}\}\, dV + \frac{d}{dt}\int_{\mathbb{R}^3} \frac{\epsilon_0}{2}\mathbf{e}\cdot\mathbf{e}\, dV.$$

The use of the last and (4.21) in the balance (4.19) provides

$$\dot{\tilde{W}} = J\dot{\mathbf{P}}\cdot\mathbf{e} + J\left[\mathbf{T} - \mathbf{T}^* + (\mathbf{P}\cdot\mathbf{e})\,\mathbf{I} - \mathbf{e}\otimes\mathbf{P}\right]\cdot\mathbf{L}. \tag{4.22}$$

Assuming that the Helmholtz free-energy will depend on deformation gradient and polarization, so that

$$\dot{\tilde{W}} = \frac{\partial\tilde{W}}{\partial\mathbf{F}}\cdot\dot{\mathbf{F}} + \frac{\partial\tilde{W}}{\partial\mathbf{P}}\cdot\dot{\mathbf{P}},$$

the substitution in (4.22) yields the constitutive equations

$$J\left[\mathbf{T} - \mathbf{T}^* + (\mathbf{P}\cdot\mathbf{e})\,\mathbf{I} - \mathbf{e}\otimes\mathbf{P}\right] = \frac{\partial\tilde{W}}{\partial\mathbf{F}}\mathbf{F}^T, \tag{4.23}$$

and

$$J\mathbf{e} = \frac{\partial\tilde{W}}{\partial\mathbf{P}}.$$

An alternative possibility is the introduction of the electric free energy $Y = Y(\mathbf{F},\mathbf{e})$, given by $Y = \tilde{W} - J\mathbf{e}\cdot\mathbf{P}$, so that a straightforward substitution provides

$$J\left[\mathbf{T} - \mathbf{T}^* - \mathbf{e}\otimes\mathbf{P}\right] = \frac{\partial Y}{\partial\mathbf{F}}\mathbf{F}^T,$$

and

$$J\mathbf{P} = -\frac{\partial Y}{\partial\mathbf{e}}.$$

A procedure parallel to that described in the previous subsection can be followed to obtain the form of the constitutive equations in terms Lagrangian variables. To this end, we note that, based on relation $\mathbf{d} = J^{-1}\mathbf{F}\mathbf{d}^0$, it follows that $J\dot{\mathbf{d}} = \mathbf{F}\dot{\mathbf{d}}^0 + (\mathbf{L} - (\mathrm{tr}\mathbf{L})\mathbf{I})\mathbf{F}\mathbf{d}^0$, the Lagrangian counterpart of (4.20) is

$$P_{ext} = \int_{\mathcal{B}^0} \mathbf{e}^0\cdot\dot{\mathbf{d}}^0 + \mathbf{S}\cdot\dot{\mathbf{F}}\, dV^0 + \int_{\mathcal{B}^0_{sur}} \mathbf{e}^0\cdot\dot{\mathbf{d}}^0 + \mathbf{S}^*\cdot\dot{\mathbf{F}}\, dV^0,$$

where $\mathbf{S}^* = J\mathbf{T}^*\mathbf{F}^{-T}$. The rate of the total energy can be reformulated as

$$\dot{E} = \frac{d}{dt}\int_{\mathcal{B}^0} \tilde{W} + J\frac{\epsilon_0}{2}\mathbf{C}^{-1}\mathbf{e}^0 \cdot \mathbf{e}^0 dV^0 + \frac{d}{dt}\int_{\mathcal{B}^0_{sur}} J\frac{\epsilon_0}{2}\mathbf{C}^{-1}\mathbf{e} \cdot \mathbf{e}\, dV^0,$$

where the two contributions relative to each phase of the body (due to the polarization of the material and to the electric field) have been separated from that of the external vacuum. If we introduce the modified Helmholtz free-energy function $W = W(\mathbf{F}, \mathbf{d}^0)$, such that

$$W = \tilde{W} + J\frac{\epsilon_0}{2}\mathbf{C}^{-1}\mathbf{e}^0 \cdot \mathbf{e}^0,$$

considering

$$\dot{W} = \frac{\partial W}{\partial \mathbf{F}}\dot{\mathbf{F}} + \frac{\partial W}{\partial \mathbf{d}^0} \cdot \dot{\mathbf{d}}^0,$$

then the energy balance (4.19) is satisfied if

$$\dot{W} = \mathbf{e}^0 \cdot \dot{\mathbf{d}}^0 + \mathbf{S} \cdot \dot{\mathbf{F}},$$

that yields the constitutive prescriptions

$$\mathbf{S} = \frac{\partial W}{\partial \mathbf{F}}, \quad \mathbf{e}^0 = \frac{\partial W}{\partial \mathbf{d}^0}. \tag{4.24}$$

On the other hand, the electric enthalpy $H(\mathbf{F}, \mathbf{e}^0)$ [30] can be introduced, defined as

$$H = W - \mathbf{d}^0 \cdot \mathbf{e}^0,$$

providing the following expression of the energy balance

$$\dot{H} = -\mathbf{d}^0 \cdot \mathbf{e}^0 + \mathbf{S} \cdot \dot{\mathbf{F}},$$

which implies that Lagrangian constitutive equations can be reformulated as

$$\mathbf{S} = \frac{\partial H}{\partial \mathbf{F}}, \quad \mathbf{d}^0 = -\frac{\partial H}{\partial \mathbf{e}^0}. \tag{4.25}$$

4.4.1 The Incompressible Case

The constitutive equations for an incompressible soft dielectric material are similar to the that obtained before. As $\mathrm{tr}\mathbf{L} = 0$ expression (4.20) simplifies to

$$\begin{aligned} P_{ext} = &\int_{\mathcal{B}} \{\dot{\mathbf{d}} \cdot \mathbf{e} + (\mathbf{T} - \mathbf{e} \otimes \mathbf{d}) \cdot \mathbf{L}\} dV \\ &+ \int_{\mathcal{B}_{sur}} \{\dot{\mathbf{d}} \cdot \mathbf{e} + (\mathbf{T}^* - \mathbf{e} \otimes \mathbf{d}) \cdot \mathbf{L}\} dV. \end{aligned} \tag{4.26}$$

Incompressibility could be enforced introducing the Lagrange multiplier p, associated with the constraint $\psi(\mathbf{F}) = J - 1 = 0$, directly into the Helmholtz free-energy W, which is now replaced by the expression $\tilde{W} - p\psi(\mathbf{F})$. Taking into account that $\frac{d\psi(\mathbf{F})}{d\mathbf{F}} = p\mathbf{F}^{-T}$, the same procedure followed above (4.23) provides the following constitutive equations for an incompressible material:

$$\mathbf{T} - \mathbf{T}^* - \mathbf{e} \otimes \mathbf{P} = \frac{\partial \tilde{W}}{\partial \mathbf{F}} \mathbf{F}^T - p\mathbf{I}, \quad \mathbf{e} = \frac{\partial \tilde{W}}{\partial \mathbf{P}},$$

while

$$\mathbf{S} = \frac{\partial W}{\partial \mathbf{F}} - p\mathbf{F}^{-T}, \quad \mathbf{e}^0 = \frac{\partial W}{\partial \mathbf{d}^0}. \tag{4.27}$$

Considering (4.25), equivalently we have

$$\mathbf{S} = \frac{\partial H}{\partial \mathbf{F}} - p\mathbf{F}^{-T}, \quad \mathbf{d}^0 = -\frac{\partial H}{\partial \mathbf{e}^0}. \tag{4.28}$$

4.5 Constitutive Equations for Isotropic Soft Dielectrics: Part 1

In this first part we want to consider a conservative material whose response is described by a free-energy function whose independent variables are the gradient of deformation (3.9) and the reference electric displacement (4.15), $W = W(\mathbf{F}, \mathbf{d}^0)$. The Eulerian total stress can be obtained recalling $(4.24)_1$ and (3.18)

$$\mathbf{T} = \frac{1}{J} \frac{\partial W}{\partial \mathbf{F}} \mathbf{F}^T, \tag{4.29}$$

and from $(4.24)_2$, the Eulerian electric field is

$$\mathbf{e} = \mathbf{F}^{-T}\frac{\partial W}{\partial \mathbf{d}^0}.$$

For an incompressible material, for which $J = 1$ (3.10), eq. (4.29) modifies as (see (4.24))

$$\mathbf{T} = \frac{\partial W}{\partial \mathbf{F}}\mathbf{F}^T - p\mathbf{I}. \tag{4.30}$$

The representation theorem for incompressible bodies becomes

$$\mathbf{T} = -p\mathbf{I} + \alpha_1\mathbf{B} - \alpha_{-1}(I_1\mathbf{B} - \mathbf{B}^2), \tag{4.31}$$

and, using Cayley-Hamilton theorem, $\mathbf{B}^{-1} = \mathbf{B}^2 - I_1\mathbf{B} + I_2\mathbf{I}$, so eq. (4.31) can be equivalently represented as

$$\begin{aligned}\mathbf{T} &= -(p + \alpha_{-1}I_2)\mathbf{I} + \alpha_1\mathbf{B} - \alpha_{-1}(I_1\mathbf{B} - \mathbf{B}^2)\\ &= -\pi\mathbf{I} + \alpha_1\mathbf{B} + \alpha_{-1}\mathbf{B}^{-1},\end{aligned} \tag{4.32}$$

where α_1 and α_{-1} are the material response functions. The unknown hydrostatic pressure is given in two equivalent ways[2] through p and through π, which are related by

$$p = \pi - \alpha_{-1}I_2.$$

In (4.32) we can identify, recalling eq. (3.35), $\alpha_1 = 2\frac{\partial W}{\partial I_1}$ and $\alpha_{-1} = -2\frac{\partial W}{\partial I_2}$. If we consider the total first Piola–Kirchhoff we have, from eq. (4.31),

$$\mathbf{S} = -\pi\mathbf{F}^{-T} + \alpha_1\mathbf{F} + \alpha_{-1}\mathbf{F}^{-T}\mathbf{C}^{-1}, \tag{4.33}$$

or from (4.32)

$$\mathbf{S} = -p\mathbf{F}^{-T} + \alpha_1\mathbf{F} - \alpha_{-1}(I_1\mathbf{F} - \mathbf{F}\mathbf{C}). \tag{4.34}$$

[2]If we consider a pure homogeneous plane–strain deformation, we can write the principal stresses as

$$t_i = \lambda_i\frac{\partial W}{\partial \lambda_i} - \tilde{\pi}$$

and can be easily shown that pressure term $\tilde{\pi}$ coincides with pressure term p in (4.31).

For an isotropic hyperelastic dielectric the free–energy $W = W(\mathbf{F}, \mathbf{d}^0)$ can be expressed as a function of the invariants (3.17) of the right Cauchy–Green tensor $\mathbf{C} = \mathbf{F}^T\mathbf{F}$

$$I_1 = \mathrm{tr}\mathbf{C}, \quad I_2 = \frac{1}{2}(I_1^2 - \mathrm{tr}(\mathbf{C}^2)), \quad I_3 = \det\mathbf{C} = J^2 \tag{4.35}$$

and (as we can see in the table 3.1) three additional invariants that depend on $\mathbf{d}^0$, namely

$$I_4 = \mathbf{d}^0 \cdot \mathbf{d}^0, \quad I_5 = \mathbf{d}^0 \cdot \mathbf{C}\mathbf{d}^0, \quad I_6 = \mathbf{d}^0 \cdot \mathbf{C}^2\mathbf{d}^0. \tag{4.36}$$

For an incompressible material $I_3 = 1$, so that W depends only on five independent scalars. Due both to the lack of available experimental data and to the desire of a simple enough formalism that allows a better understanding of the material response, an uncoupled form for the free energy is often considered

$$W(I_i) = W_{elas}(I_1, I_2) + W_{pol}(I_4, I_5, I_6),$$

where W_{elas} is the strain energy when electric effect are ignored while W_{pol} represents the contribution of the polarization of the solid. Several investigations showed that the uncoupled free energy well captures the behaviour of large classes of soft dielectrics such as ideal dielectrics and electrostrictive materials. We will focus on a particular form of free–energy (for incompressible material)

$$W(I_i) = W_{elas}(I_1, I_2) + \frac{1}{2\epsilon_0\bar{\epsilon}_r}(\bar{\gamma}_0 I_4 + \bar{\gamma}_1 I_5 + \bar{\gamma}_2 I_6), \tag{4.37}$$

where $\bar{\gamma}_i$ $(i = 0, 1, 2)$ are dimensionless constant coefficients and $\bar{\epsilon}_r$ is the relative dielectric constant in the unstretched configuration. We introduce other dimensionless coefficients, recalling (3.35) $\bar{\alpha}_1$ and $\bar{\alpha}_{-1}$, that for Mooney-Rivlin material (3.46) specialize as

$$\bar{\alpha}_1 = \frac{\mu_1}{\mu}, \quad \bar{\alpha}_{-1} = \frac{\mu_2}{\mu}, \tag{4.38}$$

and for Gent model (3.52) they become

$$\bar{\alpha}_1 = \frac{J_m}{J_m - (I_1 - 3)}, \quad \bar{\alpha}_{-1} = 0. \tag{4.39}$$

As shown in Table 3.1, the total Cauchy stress and the electric field, in terms of $\mathbf{F}$ and $\mathbf{d}$ can be expressed in terms of left Cauchy–Green tensor $\mathbf{B}$ and the Eulerian electric displacement $\mathbf{d}$ as follows

$$\mathbf{T} = -\pi\mathbf{I} + \mu\left[\bar{\alpha}_1\mathbf{B} + \bar{\alpha}_{-1}\mathbf{B}^{-1}\right] + \frac{1}{\epsilon_0\bar{\epsilon}_r}\Big[\bar{\gamma}_1\mathbf{d}\otimes\mathbf{d} + \bar{\gamma}_2(\mathbf{d}\otimes\mathbf{B}\mathbf{d} + \mathbf{B}\mathbf{d}\otimes\mathbf{d})\Big], \tag{4.40}$$

or better

$$\mathbf{T} = -p\,\mathbf{I} + \mu\left[\bar{\alpha}_1\mathbf{B} - \bar{\alpha}_{-1}(I_1\mathbf{B} - \mathbf{B}^2)\right] + \frac{1}{\epsilon_0\bar{\epsilon}_r}\Big[\bar{\gamma}_1\mathbf{d}\otimes\mathbf{d} + \bar{\gamma}_2(\mathbf{d}\otimes\mathbf{B}\mathbf{d} + \mathbf{B}\mathbf{d}\otimes\mathbf{d})\Big], \tag{4.41}$$

and

$$\mathbf{e} = \mathcal{E}^{-1}\mathbf{d}, \qquad \mathcal{E}^{-1} = \frac{1}{\epsilon_0\bar{\epsilon}_r}(\bar{\gamma}_0\mathbf{B}^{-1} + \bar{\gamma}_1\mathbf{I} + \bar{\gamma}_2\mathbf{B}), \tag{4.42}$$

where $\mathcal{E}$ is the Eulerian tensor of dielectric constants. In the lagrangian formulation, (4.40) and (4.42) become:

$$\begin{aligned}\mathbf{S} &= -\pi\mathbf{F}^{-T} + \mu\left(\alpha_1\mathbf{F} + \alpha_{-1}\mathbf{F}^{-T}\mathbf{C}^{-1}\right)\\ &\quad + \frac{1}{\epsilon_0\bar{\epsilon}_r}\Big[\bar{\gamma}_1\mathbf{F}\mathbf{d}^0\otimes\mathbf{d}^0 + \bar{\gamma}_2(\mathbf{F}\mathbf{d}^0\otimes\mathbf{C}\mathbf{d}^0 + \mathbf{F}\mathbf{C}\mathbf{d}^0\otimes\mathbf{d}^0)\Big],\end{aligned} \tag{4.43}$$

or better

$$\begin{aligned}\mathbf{S} &= -p\,\mathbf{F}^{-T} + \mu\left[\bar{\alpha}_1\mathbf{F} - \bar{\alpha}_{-1}(I_1\mathbf{F} - \mathbf{F}\mathbf{C})\right]\\ &\quad + \frac{1}{\epsilon_0\bar{\epsilon}_r}\Big[\bar{\gamma}_1\mathbf{F}\mathbf{d}^0\otimes\mathbf{d}^0 + \bar{\gamma}_2(\mathbf{F}\mathbf{d}^0\otimes\mathbf{C}\mathbf{d}^0 + \mathbf{F}\mathbf{C}\mathbf{d}^0\otimes\mathbf{d}^0)\Big],\end{aligned} \tag{4.44}$$

and

$$\mathbf{e}^0 = (\mathcal{E}^0)^{-1}\mathbf{d}^0, \qquad (\mathcal{E}^0)^{-1} = \frac{1}{\epsilon_0\bar{\epsilon}_r}(\bar{\gamma}_0\mathbf{I} + \bar{\gamma}_1\mathbf{C} + \bar{\gamma}_2\mathbf{C}^2), \tag{4.45}$$

where $\mathcal{E}^0$ is the Lagrangian tensor of dielectric constants. For an ideal dielectric we can observe that $\bar{\gamma}_0 = \bar{\gamma}_2 = 0$ and $\bar{\gamma}_1 = 1$, so that $\mathcal{E}^{-1} = \frac{1}{\epsilon_0\bar{\epsilon}_r}\mathbf{I}$.

4.6 Constitutive Equations for Isotropic Soft Dielectrics: Part 2

In this second part, we consider the constitutive law (4.25), whose independent quantities are the gradient deformation (3.9), as before, and the reference electric field (4.16), $H = H(\mathbf{F}, \mathbf{e}^0)$. The Eulerian total stress, from $(4.25)_1$ and (3.18)

$$\mathbf{T} = \frac{1}{J}\frac{\partial H}{\partial \mathbf{F}}\mathbf{F}^T \tag{4.46}$$

and from $(4.25)_2$, the true electric displacement is

$$\mathbf{d} = -\frac{1}{J}\mathbf{F}\frac{\partial H}{\partial \mathbf{e}^0}. \tag{4.47}$$

For an incompressible material, eqs. (4.46) and (4.47) modify as (see $(4.28)_2$)

$$\mathbf{T} = \frac{\partial H}{\partial \mathbf{F}}\mathbf{F}^T - p\mathbf{I}, \quad \mathbf{d} = -\mathbf{F}\frac{\partial H}{\partial \mathbf{e}^0}.$$

The mechanical invariants (4.35) result the same, while the electric invariants are defined as

$$K_4 = \mathbf{e}^0 \cdot \mathbf{e}^0, \quad K_5 = \mathbf{e}^0 \cdot \mathbf{C}^{-1}\mathbf{e}^0, \quad K_6 = \mathbf{e}^0 \cdot \mathbf{C}^{-2}\mathbf{e}^0.$$

Our assumption for the free energy (for incompressible material) is, as before,

$$H(I_1, I_2, K_4, K_5, K_6) = H_{elas}(I_1, I_2) + \frac{\epsilon_0 \bar{\epsilon}_r}{2}(\bar{\eta}_0 K_4 + \bar{\eta}_1 K_5 + \bar{\eta}_2 K_6), \tag{4.48}$$

where $\bar{\eta}_i$, $(i = 0, 1, 2)$ are dimensionless constant coefficients. Note that K_4, K_5 and K_6 can also be written, respectively, as $\mathbf{e}\cdot\mathbf{B}\mathbf{e}$, $\mathbf{e}\cdot\mathbf{e}$ and $\mathbf{e}\cdot(\mathbf{B}^{-1}\mathbf{e})$. The choice (4.48) is not unique (referring to Cayley-Hamilton theorem) and one could, for example, replace $\mathbf{C}^{-1}$ by $\mathbf{C}$ in I_5 and I_6 [12], [30]. The total first Piola-Kirchhoff is therefore

$$\begin{aligned}\mathbf{S} = &-p\,\mathbf{F}^{-T} + \mu\,[\bar{\alpha}_1\mathbf{F} - \bar{\alpha}_{-1}(I_1\mathbf{F} - \mathbf{F}\mathbf{C})] \\ &- \epsilon_0\bar{\epsilon}_r\{\bar{\eta}_1(\mathbf{F}^{-T}\mathbf{e}^0 \otimes \mathbf{C}^{-1}\mathbf{e}^0) + \bar{\eta}_2(\mathbf{F}^{-T}\mathbf{e}^0 \otimes \mathbf{C}^{-2}\mathbf{e}^0 + \mathbf{B}^{-1}\mathbf{F}^{-T}\mathbf{e}^0 \otimes \mathbf{C}^{-1}\mathbf{e}^0)\},\end{aligned}$$

and the electric displacement is

$$\mathbf{d}^0 = \mathcal{E}^0\mathbf{e}^0, \quad \mathcal{E}^0 = -\epsilon_0\bar{\epsilon}_r(\bar{\eta}_0\mathbf{I} + \bar{\eta}_1\mathbf{C}^{-1} + \bar{\eta}_2\mathbf{C}^{-2}).$$

Consequently, the total stress tensor is

$$\begin{aligned}\mathbf{T} = &-p\,\mathbf{I} + \mu\left[\bar{\alpha}_1\mathbf{B} - \bar{\alpha}_{-1}(I_1\mathbf{B} - \mathbf{B}^2)\right]\\ &- \epsilon_0\bar{\epsilon}_r\Big[\{\bar{\eta}_1\mathbf{e}\otimes\mathbf{e} + \bar{\eta}_2(\mathbf{e}\otimes\mathbf{B}^{-1}\mathbf{e} + \mathbf{B}^{-1}\mathbf{e}\otimes\mathbf{e})\Big],\end{aligned} \tag{4.49}$$

and the true electric displacement is

$$\mathbf{d} = \mathcal{E}\mathbf{e}, \quad \mathcal{E} = -\epsilon_0\bar{\epsilon}_r(\bar{\eta}_0\mathbf{B} + \bar{\eta}_1\mathbf{I} + \bar{\eta}_2\mathbf{B}^{-1}).$$

For an ideal dielectric, we can observe that $\bar{\eta}_0 = \bar{\eta}_2 = 0$ and $\bar{\eta}_1 = -1$, so that $\mathcal{E} = \epsilon_0\bar{\epsilon}_r\mathbf{I}$. We note that $\mathcal{E}$ is the same operator presented in (4.42), but written in terms of different "dielectric" coefficients.

4.7 Electroelastic Incremental Constitutive Equations: Part 1

Recalling sect. 3.4, here incremental equations related to the dielectric are presented, considering a free-energy of the type $W = W(\mathbf{F}, \mathbf{d}^0)$, presented in sect. 4.5.

4.7.1 Lagrangian Formulation

We start considering a perturbation $\dot{\mathbf{t}}^0$ and $\dot{\omega}^0$ of the tractions and the surface charges applied on $\partial\mathcal{B}^0$ that takes the body to a new equilibrium configuration where eqs. (4.14), (4.12) are still satisfied and leaves the body force density $\mathbf{b}^0$ unchanged. Likewise in (3.4), the incremental problem is governed by

$$\begin{aligned}&\text{Div}\,\dot{\mathbf{S}} = \mathbf{0},\\ &\text{Div}\,\dot{\mathbf{d}}^0 = 0, \quad \text{in } \mathcal{B}^0 \cup \mathcal{B}^0_{sur},\\ &\text{Curl}\,\dot{\mathbf{e}} = \mathbf{0},\end{aligned} \tag{4.50}$$

where $\dot{\mathbf{S}}, \dot{\mathbf{d}}^0$ and $\dot{\mathbf{e}}^0$ denote the increments of total first Piola-Kirchhoff stress, nominal electric displacement and nominal electric field caused by the perturbation. The incremental jump conditions at the external boundary of the body take the form

$$\begin{aligned} &[\![\dot{\mathbf{x}}^0]\!] = \mathbf{0}, \quad [\![\dot{\mathbf{S}}]\!]\mathbf{n}^0 = \dot{\mathbf{t}}^0 \quad \text{on } \partial\mathcal{B}_t^0, \qquad \dot{\mathbf{x}} = \mathbf{0} \quad \text{on } \partial\mathcal{B}_v^0, \\ &[\![\dot{\mathbf{d}}^0]\!] \cdot \mathbf{n}^0 = -\dot{\omega}^0, \quad \mathbf{n}^0 \times [\![\dot{\mathbf{e}}^0]\!] = \mathbf{0} \quad \text{on } \partial\mathcal{B}^0, \end{aligned} \tag{4.51}$$

$\dot{\mathbf{x}} = \dot{\boldsymbol{\chi}}(\mathbf{x}^0)$ denoting the incremental deformation. Similar boundary conditions hold at $\partial\mathcal{B}_{int}^0$, namely

$$\begin{aligned} &[\![\dot{\mathbf{x}}^0]\!] = \mathbf{0}, \quad [\![\dot{\mathbf{S}}]\!]\mathbf{n}^0 = \mathbf{0}, \\ &[\![\dot{\mathbf{d}}^0]\!] \cdot \mathbf{n}^0 = 0, \quad \mathbf{n}^0 \times [\![\dot{\mathbf{e}}^0]\!] = \mathbf{0} \quad \text{on } \partial\mathcal{B}_{int}^0. \end{aligned}$$

Assuming that all incremental quantities are sufficiently small, the constitutive equations

$$\mathbf{S} = \frac{\partial W}{\partial \mathbf{F}}, \quad \mathbf{e}^0 = \frac{\partial W}{\partial \mathbf{d}^0}$$

can be linearized; for the total Piola Kirchhoff stress as from (4.57)

$$\dot{\mathbf{S}} = \mathbb{C}^0\dot{\mathbf{F}} + \mathbb{B}^0\dot{\mathbf{d}}^0, \quad \dot{S}_{iJ} = C_{iJkL}^0\dot{F}_{kL} + B_{iJM}^0\dot{d}_M^0, \tag{4.52}$$

while for the electric field we have

$$\dot{\mathbf{e}}^0 = \mathbb{B}^{0T^*}\dot{\mathbf{F}} + \mathbb{A}^0\dot{\mathbf{d}}^0, \quad \dot{e}_M^0 = B_{iJM}^0\dot{F}_{iJ} + A_{MN}^0\dot{d}_M^0, \tag{4.53}$$

where $\dot{\mathbf{F}} = \text{Grad}\dot{\boldsymbol{\chi}}$, $(B^{0T^*})_{MiJ} = B_{iJM}^0$ and the electroelastic moduli tensors $\mathbb{C}^0$, $\mathbb{B}^0$ and $\mathbb{A}^0$ are given by

$$\begin{aligned} C_{iJkL}^0 &= \frac{\partial^2 W}{\partial F_{iJ}\partial F_{kL}}, \\ B_{iJM}^0 &= \frac{\partial^2 W}{\partial F_{iJ}\partial d_M^0}, \\ A_{MN}^0 &= \frac{\partial^2 W}{\partial d_M^0 \partial d_N^0}, \end{aligned}$$

which imply the following symmetries (given by regularity of the strain energy)

$$C^0_{iJkL} = C^0_{kLiJ}, \quad A^0_{MN} = A^0_{NM}.$$

For incompressible materials the incremental total first Piola-Kirchhoff stress tensor and Lagrangian electric field are given by

$$\dot{\mathbf{S}} = -\dot{p}\mathbf{F}^{-T} + p(\mathbf{F}^{-T}\dot{\mathbf{F}}^T\mathbf{F}^{-T}) + \mathbb{C}^0\dot{\mathbf{F}} + \mathbb{B}^0\dot{\mathbf{d}}^0$$

and

$$\dot{\mathbf{e}}^0 = \mathbb{B}^{0T^*}\dot{\mathbf{F}} + \mathbb{A}^0\dot{\mathbf{d}}^0,$$

where the Lagrange multiplier $\dot{p}$ has been introduced by the incompressibility constraint $\mathrm{tr}(\dot{\mathbf{F}}\mathbf{F}^{-1}) = 0$. Explicitly, indicating with C_{SL} the right Cauchy-Green tensor, the fourth order tensor $\mathbb{C}^0$, in the incompressible case, is given by

$$\begin{aligned} C^0_{iJkL} \;=\; & 2\Bigg[\frac{\partial W}{\partial I_1}\delta_{ik}\delta_{JL} + 2F_{iJ}F_{kL}\left(\frac{\partial^2 W}{\partial I_1^2} + \frac{\partial W}{\partial I_2}\right) \\ & +2\frac{\partial^2 W}{\partial I_2^2}(I_1F_{iJ} - F_{iR}C_{RJ})(I_1F_{kL} - F_{kS}C_{SL}) \\ & +\frac{\partial W}{\partial I_2}[\delta_{ik}(I_1\delta_{JL} - C_{JL}) - F_{iL}F_{kJ} - B_{ik}\delta_{JL}] \\ & +2\frac{\partial^2 W}{\partial I_1\partial I_2}\left(2I_1F_{iJ}F_{kL} - C_{JM}F_{iM}F_{kL} - F_{iJ}F_{kM}C_{ML}\right)\Bigg] \\ & +\frac{1}{\epsilon_0\bar{\epsilon}_r}\Bigg\{\bar{\gamma}_1\delta_{ik}d^0_Jd^0_L + \bar{\gamma}_2\left[\delta_{ik}d^0_S(C_{JS}d^0_L + C_{LS}d^0_J)\right. \\ & \left. +F_{iR}d^0_R(\delta_{JL}F_{kS}d^0_S + F_{kJ}d^0_L) + F_{iL}F_{kS}d^0_Sd^0_J + B_{ik}d^0_Jd^0_L\right]\Bigg\}. \end{aligned} \tag{4.54}$$

Explicitly, the third order tensor is given by

$$B^0_{iJM} = \frac{1}{\epsilon_0\bar{\epsilon}_r}\Big[\bar{\gamma}_1(F_{iM}d^0_J + F_{iS}d^0_S\delta_{JM}) + \bar{\gamma}_2(F_{iM}C_{JS}d^0_S + F_{iS}C_{JM}d^0_S + F_{iS}C_{SM}d^0_J + F_{iR}C_{RS}d^0_S\delta_{JM})\Big],$$

and the second order tensor by

$$A^0_{MN} = \frac{1}{\epsilon_0\bar{\epsilon}_r}\Big[\bar{\gamma}_0\delta_{MN} + \bar{\gamma}_1 C_{MN} + \bar{\gamma}_2 C^2_{MN}\Big].$$

4.7.2 Pressure Terms for the Incompressible Case

For an incompressible material, starting from (4.34) we can consider the incremental first Piola–Kirchhoff (only "mechanical" contributions)

$$\begin{aligned}\dot{\mathbf{S}} &= -\dot{p}\mathbf{F}^{-T} + p(\mathbf{F}^{-T}\dot{\mathbf{F}}^T\mathbf{F}^{-T}) + \alpha_1\dot{\mathbf{F}} - \alpha_{-1}\dot{\overline{(I_1\mathbf{F} - \mathbf{FC})}} \\ &= -\dot{p}\mathbf{F}^{-T} + p(\mathbf{F}^{-T}\dot{\mathbf{F}}^T\mathbf{F}^{-T}) + \mathbb{C}^{0,p}\dot{\mathbf{F}}\end{aligned} \tag{4.55}$$

or, considering (4.33),

$$\begin{aligned}\dot{\mathbf{S}} = &-\dot{\pi}\mathbf{F}^{-T} + \pi(\mathbf{F}^{-T}\dot{\mathbf{F}}^T\mathbf{F}^{-T}) - \alpha_{-1}I_2(\mathbf{F}^{-T}\dot{\mathbf{F}}^T\mathbf{F}^{-T}) \\ &+ \alpha_{-1}\left(\frac{\partial I_2}{\partial\mathbf{F}}\cdot\dot{\mathbf{F}}\right)\mathbf{F}^{-T} + \mathbb{C}^{0,p}\dot{\mathbf{F}},\end{aligned} \tag{4.56}$$

where $\frac{\partial I_2}{\partial\mathbf{F}} = 2(I_1\mathbf{F} - \mathbf{FC})$. So taking into account (4.33)

$$\mathbb{C}^{0,\pi}\dot{\mathbf{F}} = \mathbb{C}^{0,p}\dot{\mathbf{F}} + \alpha_{-1}\left[2(I_1\mathbf{F} - \mathbf{FC})\cdot\dot{\mathbf{F}} - I_2\mathbf{F}^{-T}\dot{\mathbf{F}}^T\right]\mathbf{F}^{-T}$$

where $\mathbb{C}^{0,\pi}$ is the fourth order tensor considering π as pressure term and $\mathbb{C}^{0,p}$ is the fourth order tensor considering p. In indices we have:

$$\begin{aligned}C^{0,p}_{iJkL} = &\alpha_1\delta_{ik}\delta_{JL} - 2\alpha_{-1}F_{iJ}F_{kL} \\ &- \alpha_{-1}\left(I_1\delta_{ik}\delta_{JL} - \delta_{ik}C_{JL} - F_{iL}F_{kJ} - \delta_{JL}B_{ik}\right)\end{aligned}$$

and it follows that

$$C^{0,\pi}_{iJkL} = C^{0,p}_{iJkL} + \alpha_{-1}\left[2(I_1 F^{-1}_{Ji} F_{kL} - F^{-1}_{Ji} F_{kJ} C_{JL}) - I_2 F^{-1}_{Jk} F^{-1}_{Li}\right].$$

So from (4.55) we have

$$\dot{\mathbf{S}} = \mathbb{C}^{0,p}\dot{\mathbf{F}} - \dot{p}\mathbf{F}^{-T} + p(\mathbf{F}^{-T}\dot{\mathbf{F}}^{T}\mathbf{F}^{-T}) \tag{4.57}$$

or, from (4.56), equivalently

$$\dot{\mathbf{S}} = \mathbb{C}^{0,\pi}\dot{\mathbf{F}} - \dot{\pi}\mathbf{F}^{-T} + \pi(\mathbf{F}^{-T}\dot{\mathbf{F}}^{T}\mathbf{F}^{-T}). \tag{4.58}$$

We can note that $C^{0,\pi}_{iJkL}$ doesn't have major symmetries because of its derivation starting from (4.56). For this reason the tensor we consider is that associated with the pressure p and dependence on the latter will be omitted henceforth.

4.7.3 Updated Lagrangian Formulation

In solving incremental boundary-values problems, it is usually convenient to refer to the current configuration. Push-forward transformations based on linear momentum balance and divergence theorem (see Appendix (10.1) and (10.2)) allow the introduction of the mechanical quantity (3.42) and for the electrical quantities we obtain

$$\hat{\mathbf{d}} = \frac{1}{J}\mathbf{F}\dot{\mathbf{d}}^{0}, \quad \hat{\mathbf{e}} = \mathbf{F}^{-T}\dot{\mathbf{e}}^{0}.$$

Introduction of the incremental updated quantities into eqs. (4.50) yields

$$\begin{aligned} &\operatorname{div} \boldsymbol{\Sigma} = \mathbf{0}, \\ &\operatorname{div} \hat{\mathbf{d}} = 0, \quad \text{in } \mathcal{B} \cup \mathcal{B}_{sur}, \\ &\operatorname{curl} \hat{\mathbf{e}} = \mathbf{0}, \end{aligned} \tag{4.59}$$

which represent the updated Lagrangian formulation of the field equations governing the incremental problem. The incremental boundary conditions

relating the jumps in the updated Lagrangian formulation to the perturbations in the reference configuration (recalling eq. (3.43)) can be written as

$$\begin{aligned} &[\![\mathbf{u}]\!] = \mathbf{0}, \quad [\![\dot{\boldsymbol{\Sigma}}]\!]\mathbf{n}dA = \dot{\mathbf{t}}^0 dA^0 \quad \text{on } \partial\mathcal{B}_t, \qquad \mathbf{u} = \mathbf{0} \quad \text{on } \partial\mathcal{B}_v, \\ &[\![\hat{\mathbf{d}}]\!] \cdot \mathbf{n}dA = -\dot{\omega}^0 dA^0, \quad \mathbf{n}^0 \times [\![\hat{\mathbf{e}}]\!] = \mathbf{0} \quad \text{on } \partial\mathcal{B}. \end{aligned} \tag{4.60}$$

Introduction of eq. (3.42) into eqs. (4.52) and (4.53) yields

$$\boldsymbol{\Sigma} = \mathbb{C}\mathbf{L} + \mathbb{B}\hat{\mathbf{d}}, \tag{4.61}$$

and

$$\hat{\mathbf{e}} = \mathbb{B}^{T*}\mathbf{L} + \mathbb{A}\hat{\mathbf{d}}, \tag{4.62}$$

where the components of the updated constitutive tensors are given by

$$C_{iqkp} = \frac{1}{J} C^0_{iJkL} F_{pL} F_{qJ}, \quad B_{iqa} = B^0_{iJM} F_{qJ} F^{-1}_{Ma}, \quad A_{ab} = J A^0_{MN} F^{-1}_{Ma} F^{-1}_{Nb}. \tag{4.63}$$

For an incompressible material eq. (4.61) modifies as

$$\boldsymbol{\Sigma} = \mathbb{C}\mathbf{L} + p\mathbf{L}^T - \dot{p}\mathbf{I} + \mathbb{B}\hat{\mathbf{d}},$$

whereas eq. (4.63) are still valid, substituting $J = 1$. Analogously to $\mathbb{C}^0$ and $\mathbb{A}^0$, the updated constitutive tensors $\mathbb{C}$ and $\mathbb{A}$ possess major symmetries

$$C_{iqkp} = C_{kpiq}, \quad A_{ab} = A_{ba}.$$

In the incompressible case, the straightforward components of the updated fourth order tensor are

$$\begin{aligned} C_{iqkp} = 2\Bigg[& \frac{\partial W}{\partial I_1}\delta_{ik}B_{pq} + 2B_{iq}B_{kp}\left(\frac{\partial^2 W}{\partial I_1^2} + \frac{\partial W}{\partial I_2}\right) \\ & + 2\frac{\partial^2 W}{\partial I_2^2}\left(I_1 B_{iq} - B_{ia}B_{qa}\right)\left(I_1 B_{kp} - B_{tk}B_{pt}\right) \\ & + \frac{\partial W}{\partial I_2}(\delta_{ik}B_{pq}(I_1 - B_{pq}) - B_{ip}B_{kq} - B_{ik}B_{pq}) \\ & + 2\frac{\partial^2 W}{\partial I_1 \partial I_2}\left(2I_1 B_{iq}B_{kp} - B_{ia}B_{qa}B_{kp} - B_{iq}B_{ap}B_{ka}\right)\Bigg] \\ & + \frac{1}{\epsilon_0 \bar{\epsilon}_r}\Bigg\{\bar{\gamma}_1\delta_{ik}d_p d_q + \bar{\gamma}_2\Bigg[\delta_{ik}d_s(B_{qs}d_p + B_{ps}d_q) \\ & + d_i(B_{pq}d_k + B_{qk}d_p) + d_q(B_{pi}d_k + B_{ik}d_p)\Bigg]\Bigg\}, \end{aligned} \tag{4.64}$$

and for the third and second order tensors we have explicitly

$$B_{iqa} = \frac{1}{\epsilon_0 \bar{\epsilon}_r}\Big[\bar{\gamma}_1(\delta_{ia}d_q + d_i\delta_{qa}) + \bar{\gamma}_2(\delta_{ia}B_{qs}d_s + B_{qa}d_i + B_{ia}d_q + B_{is}d_s\delta_{qa})\Big], \tag{4.65}$$

and

$$A_{ab} = \frac{1}{\epsilon_0 \bar{\epsilon}_r}\Big(\bar{\gamma}_0 B_{ab}^{-1} + \bar{\gamma}_1\delta_{ab} + \bar{\gamma}_2 B_{ab}\Big). \tag{4.66}$$

4.8 Electroelastic Incremental Constitutive Equations: Part 2

Recalling sect. 3.4, here incremental equations related to the dielectric are presented, considering a free-energy $H = H(\mathbf{F}, \mathbf{e}^0)$, where the electric field is the independent quantity, as presented in sect. 4.6.

4.8.1 Lagrangian Formulation

The incremental problem is governed by (4.50), with the boundary conditions given by (4.51). Assuming that all quantities are sufficiently small, the linearized constitutive equations are:

$$\dot{\mathbf{S}} = \mathbb{C}^{0,H}\dot{\mathbf{F}} - \mathbb{B}^{0,H}\dot{\mathbf{e}}^0, \quad \dot{S}_{iJ} = C^{0,H}_{iJkL}\dot{F}_{kL} - B^{0,H}_{iJM}\dot{e}^0_M \tag{4.67}$$

and for the electric displacement

$$\dot{\mathbf{d}}^0 = \mathbb{B}^{0,HT^*}\dot{\mathbf{F}} + \mathbb{A}^{0,H}\dot{\mathbf{e}}^0, \quad \dot{d}^0_M = B^{0,H}_{iJM}\dot{F}_{iJ} + A^{0,H}_{MN}\dot{e}^0_M, \tag{4.68}$$

where $(B^{0,HT^*})_{MiJ} = B^{0,H}_{iJM}$. The electroelastic moduli tensors $\mathbb{C}^{0,H}$, $\mathbb{B}^{0,H}$ and $\mathbb{A}^{0,H}$ are given by

$$\begin{aligned} C^{0,H}_{iJkL} &= \frac{\partial^2 H}{\partial F_{iJ}\partial F_{kL}}, \\ B^{0,H}_{iJM} &= -\frac{\partial^2 H}{\partial F_{iJ}\partial e^0_M} \\ A^{0,H}_{MN} &= -\frac{\partial^2 H}{\partial e^0_M \partial e^0_N}, \end{aligned} \tag{4.69}$$

which imply the following symmetries (given by regularity of strain-energy)

$$C^{0,H}_{iJkL} = C^{0,H}_{kLiJ}, \quad A^{0,H}_{MN} = A^{0,H}_{NM}.$$

For incompressible materials the incremental total first Piola-Kirchhoff stress tensor and Lagrangian electric field are given by

$$\dot{\mathbf{S}} = -\dot{p}\mathbf{F}^{-T} + p(\mathbf{F}^{-T}\dot{\mathbf{F}}^T\mathbf{F}^{-T}) + \mathbb{C}^{0,H}\dot{\mathbf{F}} - \mathbb{B}^{0,H}\dot{\mathbf{e}^0}$$

and

$$\dot{\mathbf{d}}^0 = \mathbb{B}^{0,HT^*}\dot{\mathbf{F}} + \mathbb{A}^{0,H}\dot{\mathbf{e}}^0,$$

where the Lagrange multiplier $\dot{p}$ has been introduced by the incompressibility constraint $\mathrm{tr}(\dot{\mathbf{F}}\mathbf{F}^{-1}) = 0$. In detail, in components we have

$$
\begin{aligned}
C^{0,H}_{iJkL} \;=\; & 2\Bigg[\frac{\partial H}{\partial I_1}\delta_{ik}\delta_{JL} + 2F_{iJ}F_{kL}\left(\frac{\partial^2 H}{\partial I_1^2} + \frac{\partial H}{\partial I_2}\right) \\
& +2\frac{\partial^2 H}{\partial I_2^2}(I_1F_{iJ} - F_{iR}C_{RJ})(I_1F_{kL} - F_{kS}C_{SL}) \\
& +\frac{\partial H}{\partial I_2}[\delta_{ik}(I_1\delta_{JL} - C_{JL}) - F_{iL}F_{kJ} - B_{ik}\delta_{JL}] \\
& +2\frac{\partial^2 H}{\partial I_1 \partial I_2}\left(2I_1F_{iJ}F_{kL} - C_{JM}F_{iM}F_{kL} - F_{iJ}F_{kM}C_{ML}\right)\Bigg] \\
& +\epsilon_0\bar{\epsilon}_r\Bigg\{\bar{\eta}_1 e^0_P e^0_S\Big[C^{-1}_{JS}F^{-1}_{Pk}F^{-1}_{Li} + F^{-1}_{Pi}(C^{-1}_{JL}F^{-1}_{Sk} + C^{-1}_{SL}F^{-1}_{Jk})\Big] \\
& +\bar{\eta}_2 e^0_S e^0_R\Big[F^{-1}_{Li}F^{-1}_{Sk}C^{-2}_{JR} + F^{-1}_{Si}F^{-1}_{Jk}C^{-2}_{LR} \\
& +F^{-1}_{Si}(C^{-1}_{JL}F^{-1}_{Pk}C^{-1}_{PR} + C^{-1}_{JP}F^{-1}_{Pk}C^{-1}_{LR} + C^{-2}_{JL}F^{-1}_{Rk}) \\
& +F^{-1}_{Li}F^{-1}_{Pk}C^{-1}_{PR}C^{-1}_{JS} + B^{-1}_{ik}C^{-1}_{LR}C^{-1}_{JS} \\
& +B^{-1}_{it}(F^{-1}_{Lt}F^{-1}_{Rk}C^{-1}_{JS} + F^{-1}_{Rt}F^{-1}_{Jk}C^{-1}_{LS} + F^{-1}_{Rt}C^{-1}_{JL}F^{-1}_{Sk})\Big]\Bigg\},
\end{aligned}
$$

and the third order tensor becomes

$$
\begin{aligned}
B^{0,H}_{iJM} = \epsilon_0\bar{\epsilon}_r\Big[&\bar{\eta}_1 F^{-1}_{Jl}e^0_P(F^{-1}_{Mi}F^{-1}_{Pl} + F^{-1}_{Ml}F^{-1}_{Pi}) \\
&+ \bar{\eta}_2 e^0_P(F^{-1}_{Mi}C^{-2}_{JP} + C^{-1}_{MJ}F^{-1}_{Ti}C^{-1}_{TL} + C^{-1}_{MT}F^{-1}_{Ti}C^{-1}_{JP} + C^{-2}_{MJ}F^{-1}_{Pi})\Big],
\end{aligned}
$$

while the second order tensor takes the form

$$
A^{0,H}_{MN} = -\epsilon_0\bar{\epsilon}_r(\bar{\eta}_0\delta_{MN} + \bar{\eta}_1 C^{-1}_{MN} + \bar{\eta}_2 C^{-2}_{MN}).
$$

4.8.2 Updated Lagrangian Formulation

Considering the governing eqs. (4.59) for the incremental problem, the constitutive equations become

$$\boldsymbol{\Sigma} = \mathbb{C}^H \mathbf{L} - \mathbb{B}^H \hat{\mathbf{e}}, \tag{4.70}$$

and

$$\hat{\mathbf{d}} = \mathbb{B}^{H,T*} \mathbf{L} + \mathbb{A}^H \hat{\mathbf{e}}, \tag{4.71}$$

where the components of the updated constitutive tensors are given by

$$C^H_{iqkp} = \frac{1}{J} C^{0,H}_{iJkL} F_{pL} F_{qJ}, \quad B^H_{iqa} = \frac{1}{J} B^{0,H}_{iJM} F_{qJ} F_{aM}, \quad A^H_{ab} = \frac{1}{J} A^{0,H}_{MN} F_{aM} F_{bN}. \tag{4.72}$$

The correspondent boundary conditions are the same as seen in eqs. (4.60). For an incompressible material eq. (4.70) modifies as

$$\boldsymbol{\Sigma} = \mathbb{C}^H \mathbf{L} + p\mathbf{L}^T - \dot{p}\mathbf{I} - \mathbb{B}^H \hat{\mathbf{e}},$$

whereas eq (4.72) are still valid, substituting $J = 1$. Analogously to $\mathbb{C}^{0,H}$ and $\mathbb{A}^{0,H}$, the updated constitutive tensors $\mathbb{C}^H$ and $\mathbb{A}^H$ possess major symmetries

$$C^H_{iqkp} = C^H_{kpiq}, \quad A^H_{ab} = A^H_{ba}.$$

In the incompressible case, the components of the updated fourth order tensor are

$$\begin{aligned}
C^H_{iqkp} = 2\Bigg[&\frac{\partial H}{\partial I_1}\delta_{ik}B_{pq} + 2B_{iq}B_{kp}\left(\frac{\partial^2 H}{\partial I_1^2} + \frac{\partial H}{\partial I_2}\right)\\
&+ 2\frac{\partial^2 H}{\partial I_2^2}\left(I_1 B_{iq} - B_{ia}B_{qa}\right)\left(I_1 B_{kp} - B_{tk}B_{pt}\right)\\
&+ \frac{\partial H}{\partial I_2}(\delta_{ik}B_{pq}(I_1 - B_{pq}) - B_{ip}B_{kq} - B_{ik}B_{pq})\\
&+ 2\frac{\partial^2 H}{\partial I_1 \partial I_2}\left(2I_1 B_{iq}B_{kp} - B_{ia}B_{qa}B_{kp} - B_{iq}B_{ap}B_{ka}\right)\Bigg]\\
&+ \epsilon_0\bar{\epsilon}_r\Bigg\{\bar{\eta}_1\big(\delta_{ip}e_k e_q + \delta_{qp}e_i e_k + \delta_{qk}e_i e_p\big) + \bar{\eta}_2\Bigg[e_t\Big(\delta_{ip}e_k B^{-1}_{qt}\\
&+ \delta_{kq}e_i B^{-1}_{pt} + (\delta_{pq}e_i + \delta_{ip}e_q)B^{-1}_{kt} + (\delta_{kq}e_p + \delta_{pq}e_k)B^{-1}_{it}\Big)\\
&+ e_i(B^{-1}_{kq}e_p + B^{-1}_{qp}e_k) + e_q(B^{-1}_{ik}e_p + B^{-1}_{pi}e_k)\Bigg]\Bigg\}
\end{aligned} \tag{4.73}$$

that of the third order tensor are

$$\begin{aligned}
B^H_{iqa} = \epsilon_0\bar{\epsilon}_r\Big[&\bar{\eta}_1(\delta_{ia}e_q + \delta_{aq}e_i)\\
&+ \bar{\eta}_2(\delta_{ia}B^{-1}_{qt}e_t + \delta_{aq}B^{-1}_{it}e_t + B^{-1}_{ia}e_q + B^{-1}_{aq}e_i)\Big],
\end{aligned} \tag{4.74}$$

while the second order tensor becomes

$$A^H_{ab} = -\epsilon_0\bar{\epsilon}_r\Big[\bar{\eta}_0 F_{aM}F_{bM} + \bar{\eta}_1\delta_{ab} + \bar{\eta}_2 B^{-1}_{ba}\Big]. \tag{4.75}$$

Chapter 5

Electric-induced Deformations in Solid Mechanics

This chapter aims at providing a clarification on a couple of well-known phenomena in Solid Mechanics at that can be described using the notion of electro-elasticity presented previously: piezoelectricity and electrostriction.

5.1 Piezoelectricity and Electrostriction at Small Deformations

"Piezo" in Greek means "pressure". In 1880 the Curie brothers discovered that by applying a pressure (mechanical stress) to a crystal of quartz, a surface electric charge was developed, thus induced by an electric field ("direct piezo-electric effect"); other natural materials with this property are tourmaline and Rochelle salt. Around 1930, it was discovered that "ferroelectric ceramics", developed to realize devices such as capacitors, had this property when subjected to the process of "polarization", i.e. when a strong electric field (1-2 kV/mm) was applied; the best known of these (developed in 1945) are the Barium titanate, $BaTiO_3$, and the Lead zirconate titanate (PZT), suitably doped. Piezoelectric materials have been recently developed in a plastic matrix (PVDF) and continuing developments are underway to find

new materials and more advanced manufacturing processes.

While "piezoelectricity" is a first-order coupling between electric field and stress/strain, "electrostriction" is a second-order coupling between electrical and mechanical variables. At small strains, it is possible to separate these two contributions expanding the total first Piola-Kirchhoff stress $S_{iJ} = S_{iJ}(\mathbf{F}, \mathbf{d}^0)$ and the nominal electric field $e^0_N = e^0_N(\mathbf{F}, \mathbf{d}^0)$ into a second-order Taylor series about the natural configuration:

$$\begin{aligned}\dot{S}_{iJ} = &\frac{\partial S_{iJ}}{\partial F_{kL}}\dot{F}_{kL} + \frac{\partial S_{iJ}}{\partial d^0_M}\dot{d}^0_M + \frac{1}{2}\dot{F}_{qR}\frac{\partial^2 S_{ij}}{\partial F_{qR}\partial F_{kL}}\dot{F}_{kL} \\ &+ \dot{F}_{kL}\frac{\partial^2 S_{ij}}{\partial F_{kL}\partial d^0_M}\dot{d}^0_M + \frac{1}{2}\dot{d}^0_S\frac{\partial^2 S_{ij}}{\partial d^0_S\partial d^0_M}\dot{d}^0_M,\end{aligned} \tag{5.1}$$

$$\begin{aligned}\dot{e}^0_N = &\frac{\partial e^0_N}{\partial F_{kL}}\dot{F}_{kL} + \frac{\partial e^0_N}{\partial d^0_M}\dot{d}^0_M + \frac{1}{2}\dot{F}_{qR}\frac{\partial^2 e^0_N}{\partial F_{qR}\partial F_{kL}}\dot{F}_{kL} \\ &+ \dot{F}_{kL}\frac{\partial^2 e^0_N}{\partial F_{kL}\partial d^0_M}\dot{d}^0_M + \frac{1}{2}\dot{d}^0_S\frac{\partial^2 e^0_N}{\partial d^0_S\partial d^0_M}\dot{d}^0_M,\end{aligned} \tag{5.2}$$

or, in terms of the electro-elastic density energy,

$$\begin{aligned}\dot{S}_{iJ} = &\frac{\partial^2 W}{\partial F_{kL}\partial F_{iJ}}\dot{F}_{kL} + \frac{\partial^2 W}{\partial d^0_M\partial F_{iJ}}\dot{d}^0_M + \frac{1}{2}\dot{F}_{qR}\frac{\partial}{\partial F_{qR}}\left(\frac{\partial^2 W}{\partial F_{kL}\partial F_{iJ}}\right)\dot{F}_{kL} \\ &+ \dot{F}_{kL}\frac{\partial}{\partial d^0_M}\left(\frac{\partial^2 W}{\partial F_{iJ}\partial F_{kL}}\right)\dot{d}^0_M + \frac{1}{2}\dot{d}^0_S\frac{\partial}{\partial d^0_S}\left(\frac{\partial^2 W}{\partial F_{iJ}\partial d^0_M}\right)\dot{d}^0_M,\end{aligned}$$

and

$$\begin{aligned}\dot{e}^0_N = &\frac{\partial^2 W}{\partial F_{kL}\partial d^0_N}\dot{F}_{kL} + \frac{\partial^2 W}{\partial d^0_M\partial d^0_N}\dot{d}^0_M + \frac{1}{2}\dot{F}_{qR}\frac{\partial}{\partial F_{qR}}\left(\frac{\partial^2 W}{\partial F_{kL}\partial d^0_N}\right)\dot{F}_{kL} \\ &+ \dot{F}_{kL}\frac{\partial}{\partial F_{kL}}\left(\frac{\partial^2 W}{\partial d^0_M\partial d^0_N}\right)\dot{d}^0_M + \frac{1}{2}\dot{d}^0_S\frac{\partial}{\partial d^0_S}\left(\frac{\partial^2 W}{\partial d^0_N\partial d^0_M}\right)\dot{d}^0_M.\end{aligned}$$

The tensors of incremental moduli can still be introduced. The elastic coefficients (at constant electric field) are

$$C^0_{iJkL} = \frac{\partial^2 W}{\partial F_{kL}\partial F_{iJ}},$$

the piezoelectric stress coefficients takes the form

$$B^0_{iJM} = \frac{\partial^2 W}{\partial d^0_M \partial F_{iJ}}, \tag{5.3}$$

while the dielectric permittivity coefficients at constant strain are

$$A^0_{MN} = \frac{\partial^2 W}{\partial d^0_M \partial d^0_N}. \tag{5.4}$$

We can define the quadratic stiffness coefficients as

$$\frac{\partial C^0_{iJkL}}{\partial F_{qR}} = \frac{\partial}{\partial F_{qR}} \left(\frac{\partial^2 W}{\partial F_{kL} \partial F_{iJ}} \right), \tag{5.5}$$

and the quadratic dielectric permittivity coefficients as

$$\frac{\partial A^0_{MN}}{\partial d^0_S} = \frac{\partial}{\partial d^0_S} \left(\frac{\partial^2 W}{\partial d^0_N \partial d^0_M} \right). \tag{5.6}$$

The mixed second order derivatives (second-order coupling between mechanical and electrical variables) are

$$\frac{\partial C^0_{iJkL}}{\partial d^0_M} = \frac{\partial}{\partial d^0_M} \left(\frac{\partial^2 W}{\partial F_{kL} \partial F_{iJ}} \right) = \frac{\partial}{\partial F_{kL}} \left(\frac{\partial^2 W}{\partial d^0_M \partial F_{iJ}} \right) = \frac{\partial B^0_{iJM}}{\partial F_{kL}} \tag{5.7}$$

and

$$\frac{\partial B^0_{iJM}}{\partial d^0_S} = \frac{\partial}{\partial d^0_S} \left(\frac{\partial^2 W}{\partial d^0_M \partial F_{iJ}} \right) = \frac{\partial A^0_{MS}}{\partial F_{iJ}}. \tag{5.8}$$

For a piezoelectric material, the constitutive law is that considered from the first-order Taylor series expansion about the undeformed state, assuming that displacements and their gradients are small enough so that there is no need to distinguish between Lagrangian and Eulerian descriptions. Therefore,

$$\sigma_{ij} = C_{ijkl}\epsilon_{kl} + B_{ijm}\delta_m$$
$$e_n = B_{kln}\epsilon_{kl} + A_{nm}\delta_m$$

where $\dot{S}_{iJ}, \dot{e}_N, \dot{F}_{iJ}, \dot{d}^0_M$ become, respectively, σ_{ij}, e_n, ϵ_{ij}, δ_m, taking into account that $C_{ijkl} = \frac{1}{2}(C^0_{iJkL} + C^0_{iJLk})$ as the fourth order elastic tensor has minor and major symmetries. This procedure is analogous to that obtained in (4.52) and (4.53), which became (4.61) and (4.62), respectively.

We provide below an example of how a purely electrostrictive material is treated. For polyurethane materials, for instance, the following assumptions are made:

- they do not exhibit any piezoelectric behaviour and the coefficients B_{ijm} are therefore zero;
- their quadratic stiffness coefficients (5.5) are negligible;
- the variation of the stiffness coefficients with respect to the electric field is negligible and the coefficient (5.7) are therefore ignored.

As a consequence, the only two relevant second-order quantities are the electrostrictive stress coefficients

$$Q_{msij} = \frac{1}{2}\frac{\partial A_{ms}}{\partial \epsilon_{ij}},$$

and the quadratic dielectric permittivity coefficients at constant strain, i.e.

$$O_{nms} = \frac{1}{2}\frac{\partial A_{mn}}{\partial \delta_s};$$

then, the electrostrictive response considered for polyurethanes reduce to

$$\begin{aligned} \sigma_{ij} &= C_{ijkl}\epsilon_{kl} + Q_{msij}\delta_m\delta_s, \\ e_n &= A_{mn}\delta_m + 2Q_{mnkl}\delta_m\epsilon_{kl} + O_{nms}\delta_m\delta_s. \end{aligned}$$

By analogy with piezoelectricity, one can also define electrostrictive strain coefficients M_{msij}, which relate the strains to the square of the electric displacement as

$$\epsilon_{ij} = M_{msij}\delta_m\delta_s.$$

Placing in $(5.9)_1$ $\sigma_{ij} = 0$ [19], then it follows from (5.9) that the electrostrictive coefficients are given by

$$Q_{msij} = -M_{mskl}C_{klij}.$$

Entries M_{msij} are the quantities that are to be experimentally obtained in order to characterize the electrostrictive behaviour of polyurethane [19].

5.2 Deformation-dependent Permittivity: Electrostriction in Soft Dielectric Elastomers

In a dielectric polarized by an external field, two are the effects leading to an electric induced strain: Maxwell effect and electrostriction. Even though both are quadratic in the intensity of electric field (differently form piezoelectricity), Maxwell effect is caused by electrostatic attraction of charges on the electrodes while electrostriction is due to the intrinsic electromechanical response of the material, as previously discussed.

In terms of modelling, electrostriction refers to the change of the dielectric permittivity with the deformation, as suggested also by definition (5.9). DEs deform substantially, so that the role of the electrostriction in these materials cannot in general be neglected. Experimental results show that typical materials for DEAs possess this property (Wissler and Mazza [53]; Li et al. [28]) and therefore it becomes important to investigate its effects to the stability behaviour of such actuators. Even though Suo and Zhao [45] provided a first description of electrostriction for soft dielectrics, our goal is to show that deformation-dependent permittivity is incorporated in the constitutive model (4.41), (4.44). We point out that ideal dielectrics with constant permittivity, for which $\mathbf{e} = \mathbf{d}/(\epsilon_0\epsilon_r)$, are caught in the Eulerian counterpart of $(4.41)_2$ imposing $\bar{\gamma}_0 = \bar{\gamma}_2 = 0$ and $\bar{\gamma}_1 = 1$, with $\bar{\epsilon}_r = \epsilon_r$.

The considered sets of parameters $\bar{\gamma}_i$ $(i = 0, 1, 2)$ have been computed gathering data from experimental tests performed by Wissler and Mazza [53] and Li et al. [28] on 3M VHB4910 equally biaxially prestretched films. To this end, the formula for Eulerian electric field has been specialized accordingly, providing values reported in Table 5.1. The fitting results,

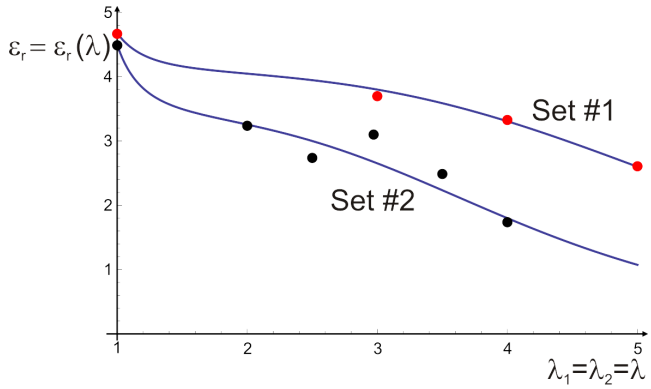

Figure 5.1: Experimental results: biaxial tests, $\epsilon_r = \bar{\epsilon}_r(\bar{\gamma}_0(\lambda_1\lambda_2)^2 + \bar{\gamma}_1 + \bar{\gamma}_2/(\lambda_1\lambda_2)^2)^{-1}$.

Set # (Reference)	$\bar{\epsilon}_r$	$\bar{\gamma}_0$	$\bar{\gamma}_1$	$\bar{\gamma}_2$
1 (Wissler and Mazza) [53]	4.68	0.00104	1.14904	−0.15008
2 (Li et al.) [28]	4.5	0.00458	1.3298	−0.33438

Table 5.1: Sets of electrostrictive parameters employed in the instability analyses in terms of $\bar{\gamma}_0, \bar{\gamma}_1, \bar{\gamma}_2$.

obtained using the least square method, are reported in Fig. 5.1.
The same procedure described above, referring to the constitutive equation (4.49), gives the correspondent values in terms of η_i $(i = 0, 1, 2)$, reported in Table 5.2.

The influence of electrostriction on the deformation of an electrically excited specimen can be inferred specializing the $(4.41)_2$ to a homogeneous deformation of a three-dimensional actuator (see Fig. 5.3), where $\mathbf{F} =$

Set # (Reference)	$\bar{\epsilon}_r$	$\bar{\eta}_0$	$\bar{\eta}_1$	$\bar{\eta}_2$
1 (Wissler and Mazza) [53]	4.68	−0.1468	$-0,853712$	0.000512
2 (Li et al.) [28]	4.5	−0.2952	−0.705973	0.00119971

Table 5.2: Sets of electrostrictive parameters employed in the instability analyses in terms of $\bar{\eta}_0, \bar{\eta}_1, \bar{\eta}_2$.

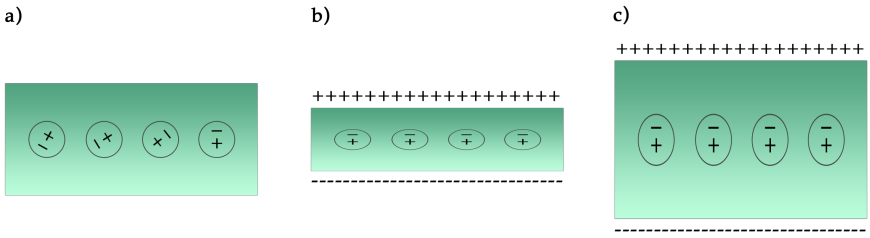

Figure 5.2: In a) a dielectric that is non polar in absence of applied voltage. Subject to a voltage, some dielectrics become thinner b) but other dielectrics become thicker c).

diag$[1/\sqrt{\lambda}, 1/\sqrt{\lambda}, \lambda]$ and the electric displacement is directed along x_3, i.e $\mathbf{d} = (0, 0, d_3)$, namely

$$T_{11} - T_{33} = \mu(\bar{\alpha}_1\lambda - \bar{\alpha}_{-1})\frac{1-\lambda^3}{\lambda^2} - \frac{1}{\epsilon_0\bar{\epsilon}_r}d_3^2(\bar{\gamma}_1 + \bar{\gamma}_2\lambda^2).$$

The "electric part" of the stress difference, which depends on the electrostrictive coefficients, is

$$(T_{11} - T_{33})^{el} = -\frac{1}{\epsilon_0\bar{\epsilon}_r}d_3^2(\bar{\gamma}_1 + \bar{\gamma}_2\lambda^2), \tag{5.9}$$

that can be reformulated in terms of the applied voltage ($\Delta\phi$) introducing the electric field (4.42)

$$e_3 = \frac{1}{\epsilon_0\bar{\epsilon}_r}\left(\frac{\bar{\gamma}_0}{\lambda^2} + \bar{\gamma}_1 + \bar{\gamma}_2\lambda^2\right)d_3,$$

and employing the relationship $e_3 = \frac{\Delta\phi}{h} = \frac{\Delta\phi}{\lambda h^0}$, obtaining

$$\frac{(T_{11} - T_{33})^{el}}{\epsilon_0\bar{\epsilon}_r} = -\frac{\bar{\gamma}_1 + \bar{\gamma}_2\lambda^2}{\left(\frac{\bar{\gamma}_0}{\lambda^2} + \bar{\gamma}_1 + \bar{\gamma}_2\lambda^2\right)^2}\frac{\Delta\phi^2}{(h^0)^2\lambda^2}. \tag{5.10}$$

In Fig. 5.4 the function $\frac{(T_{11}-T_{33})^{el}}{\epsilon_0\bar{\epsilon}_r(\Delta\phi/h^0)^2}$ is reported for the sets of parameters of Table 5.1. It is noted that an increase of electrostriction for the

soft elastomer makes the electric part of the stress difference less intense compared to the case where ϵ_r is constant. This difference can turn positive when the change is particularly pronounced. In this case, the electrostrictive contribution to the global deformation of the actuator overcomes the squeezing effect induced by the Maxwell stress, resulting in an increase of the thickness of the system.

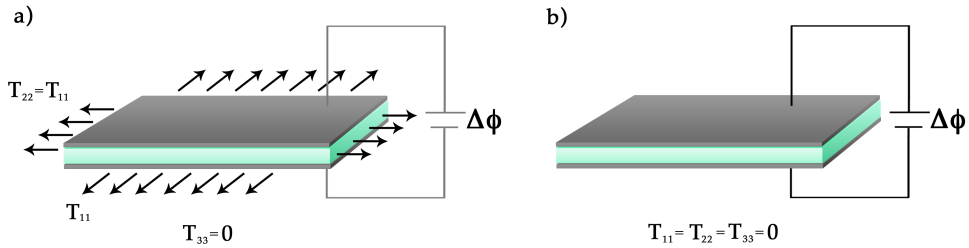

Figure 5.3: In a) the specimen is prestressed with $T_{11} = T_{22}$, $T_{33} = 0$. In b) the specimen is free prestressed ($T_{11} = T_{22} = T_{33} = 0$).

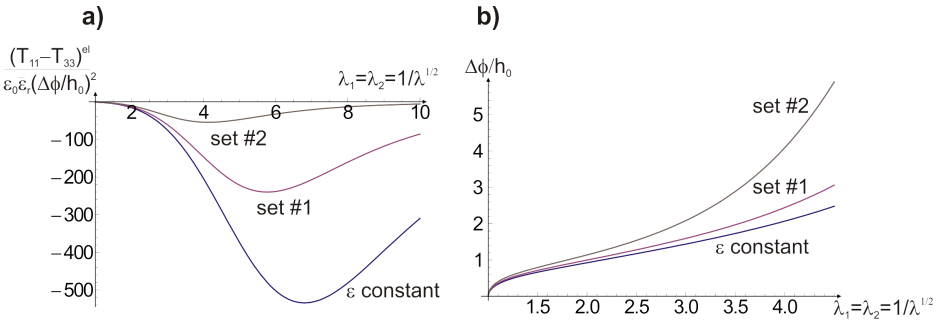

Figure 5.4: In a) plot of "electric part" of the stress (5.10) is reported, in which we can note that after the minimum value, electrostriction takes over Maxwell effect. In b) the voltage (per unit of thickness) in terms of λ_1 is represented, when $T_{11} = T_{33} = 0$.

Chapter 6

Homogeneous Non-linear Electroelastic Deformations for DE Actuators

The homogeneous electroelastic deformations considered as fundamental paths for the instability analysis are here introduced.

6.1 Homogeneous Fundamental Paths: Prestressed and Prestretched DE-layers

Stability of DE actuators are performed considering states obtained deforming homogeneously the initial natural configuration in plane strain by electrical actuation. To this end, we introduce a reference cartesian coordinate system $Ox_1^0x_2^0x_3^0$ with orthonormal basis $\{\mathbf{i}_1, \mathbf{i}_2, \mathbf{i}_3\}$, where x_3^0 is the out of plane axis, x_1^0 the longitudinal axis, and x_2^0 the transverse direction of the layer, such that the boundaries of the layer correspond to $x_2^0 = 0$ and $x_2^0 = h^0$, where h^0 is the initial thickness. In particular, we consider a deformation described by

$$x_1 = \lambda x_1^0, \quad x_2 = \frac{1}{\lambda} x_2^0, \quad x_3 = x_3^0,$$

where λ is the imposed pre–stretch along direction x_1^0, so the deformation gradient is $\mathbf{F} = \mathrm{diag}[\lambda, 1/\lambda, 1]$. The electrical actuation is induced by per-

fectly compliant electrodes on the two boundaries at $x_2^0 = 0, h^0$ where a voltage $\Delta\phi$ is applied, so that electric field and electric displacement are uniquely directed along direction x_2^0 ($\mathbf{e} = e_2\mathbf{i}_2$ and $\mathbf{d} = d_2\mathbf{i}_2$).

Then, the invariants I_1 and I_2 (3.17) are simply

$$I_1 = I_2 = 1 + \lambda^2 + \frac{1}{\lambda^2}, \tag{6.1}$$

while $I_3 = 1$ due to the incompressibility constraint. The current and the reference electric displacements (eq. (4.15)) are linked by

$$d_1 = 0, \quad d_2 = \frac{d_2^0}{\lambda}, \quad d_3 = 0,$$

while the electro-mechanical invariants I_4, I_5, I_6 (4.36) are given by

$$I_4 = (d_2^0)^2, \quad I_5 = \lambda^{-2} I_4, \quad I_6 = \lambda^{-4} I_4. \tag{6.2}$$

We can easily obtain the component of the stress tensor $\mathbf{T}$ (4.41), for which the only non-zero components are:

$$\begin{aligned} T_{11} &= \lambda^2 \mu\bar{\alpha}_1 - \mu\bar{\alpha}_{-1}(\lambda^2 + 1) - p, \\ T_{22} &= \frac{\mu\bar{\alpha}_1}{\lambda^2} - \mu\bar{\alpha}_{-1}\frac{1+\lambda^2}{\lambda^2} + d_2^2\frac{\bar{\gamma}_1}{\epsilon_0\bar{\epsilon}_r} + \frac{2d_2^2\bar{\gamma}_2}{\epsilon_0\bar{\epsilon}_r\lambda^2} - p, \\ T_{33} &= \mu\bar{\alpha}_1 - \mu\bar{\alpha}_{-1}(\frac{1}{\lambda^2} + \lambda^2) - p, \end{aligned} \tag{6.3}$$

while the components of the electric field $\mathbf{e}$ (4.42) are

$$e_1 = 0, \quad e_2 = \frac{d_2}{\epsilon_0\bar{\epsilon}_r}(\bar{\gamma}_1 + \frac{\bar{\gamma}_2}{\lambda^2} + \bar{\gamma}_0\lambda^2), \quad e_3 = 0.$$

6.1.1 Presence of an External Electric Field

Adopting the deformation just described, on the specialization of the boundary conditions

$$(\mathbf{d} - \mathbf{d}^*) \cdot \mathbf{n} = 0, \quad (\mathbf{e} - \mathbf{e}^*) \times \mathbf{n} = \mathbf{0},$$

to the boundary $x_2^0 = x_2 = 0$, we obtain $d_2^* = d_2$ and from $(4.13)_2$ it follows that $d_1^* = d_3^* = 0$ and $e_2^* = \epsilon_0^{-1} d_2^* = \epsilon_0^{-1} d_2$, (see Fig. 6.1). Outside the material we take the electric field to be uniform and equal to its value at $x_2 = 0$. Then, Maxwell's equations are satisfied identically and $\mathbf{d}^*$ and $\mathbf{e}^*$ (eq. (4.13)) have components

$$d_1^* = 0, \quad d_2^* = d_2 = \lambda^{-1} d_2^0, \quad d_3^* = 0,$$

and

$$e_1^* = 0, \quad e_2^* = \epsilon_0^{-1} d_2 = \epsilon_0^{-1} \lambda^{-1} d_2^0, \quad e_3^* = 0,$$

respectively. We deduce from $(4.13)_1$ that the non–zero components of the Maxwell stress are given by

$$T_{11}^* = T_{33}^* = -T_{22}^* = -\frac{d_2^2}{2\epsilon_0}.$$

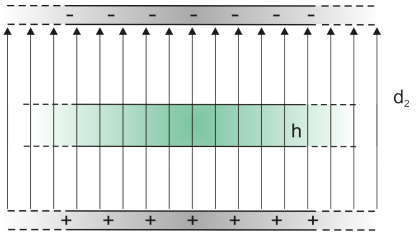

Figure 6.1: A specimen is subjected to an external transverse electric displacement field and deforms accordingly.

Therefore, from $(6.3)_2$, and using the assumption of an external electric field, we compute the pressure

$$p = \left(\frac{\bar{\gamma}_1}{\epsilon_0 \bar{\epsilon}_r} - \frac{1}{2\epsilon_0} \right) d_2^2 + \frac{2 d_2^2 \bar{\gamma}_2}{\epsilon_0 \bar{\epsilon}_r \lambda^2} + \frac{\mu \bar{\alpha}_1}{\lambda^2} - \mu \bar{\alpha}_{-1} \left(1 + \frac{1}{\lambda^2} \right).$$

6.1.2 Expansion with Longitudinal Applied Force

In this case (Fig. 6.2) the actuator is stress free along direction x_2 and subjected to a constant force $\tilde{S}h_0$ along the longitudinal direction, so that the stress state is represented by

$$S_{11} = \tilde{S}, \quad S_{22} = 0,$$

which provide the following implicit relation between λ and $\bar{D} = d_2/\sqrt{\mu\epsilon_0\bar{\epsilon}_r}$, i.e.

$$\frac{\tilde{S}}{\mu}\lambda^2 + (\bar{\alpha}_1 - \bar{\alpha}_{-1})\left(\frac{1}{\lambda} - \lambda^3\right) + \bar{D}^2\left(\bar{\gamma}_1\lambda + \frac{2\bar{\gamma}_2}{\lambda}\right) = 0.$$

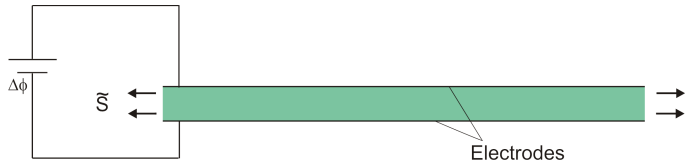

Figure 6.2: A specimen is prestressed and activated electrically at $S_{11} = \tilde{S}$, applying a constant force $\tilde{S}$ along x_2 direction.

6.1.3 Pre-stretched Specimen

Along x_2, the total stress is identically zero throughout the solid, namely $T_{22} = 0$. Denoting by λ_{pre} the imposed pre-stretch, the applied deformation results in an uniaxial tensile state of stress,

$$T_{11}^{\text{pre}} = \mu(\bar{\alpha}_1 - \bar{\alpha}_{-1})\left(\lambda_{\text{pre}}^2 - \frac{1}{\lambda_{\text{pre}}^2}\right).$$

When a varying electric displacement d_2 (see Fig. 6.3) is subsequently applied, the longitudinal stress changes as

$$\frac{T_{11}}{\mu} = \frac{T_{11}^{\text{pre}}}{\mu} - \bar{D}^2\left(\bar{\gamma}_1 + \frac{2\bar{\gamma}_2}{\lambda_{\text{pre}}^2}\right).$$

The electric actuation decreases the longitudinal stress, so that at a certain level of d_2, under compression, a buckling-like instability occurs. The behaviour of T_{11} in terms of $\bar{D}$ is reported in Fig. 6.4 for the sets of parameters #1 and #2. The vanishing of T_{11} is often indicated as 'loss of tension'.

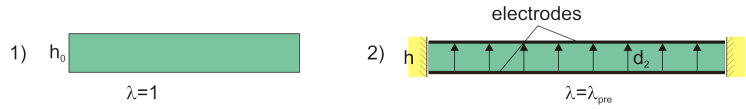

Figure 6.3: A specimen is prestretched, so starting from the natural configuration ($\lambda = 1$), the actual configuration is achieved by imposing, 1) $\lambda = \lambda_{\rm pre}$ and 2) an electric displacement field.

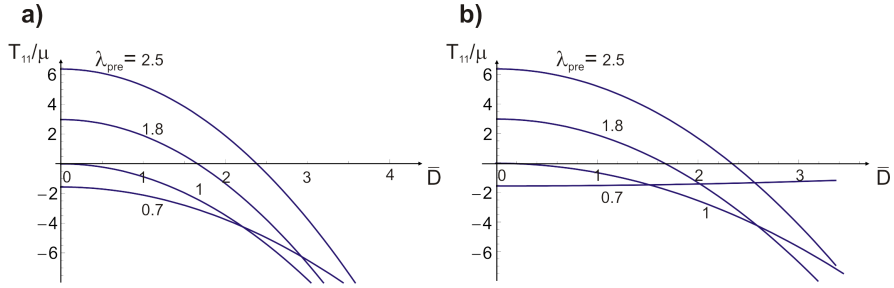

Figure 6.4: Plots of dimensionless uniaxial tensile state of stress for Gent model material (3.52), (4.37), with set #1 in a) and set #2 in b).

Chapter 7

Diffuse Modes and Band Localization of DE Actuators

Bertoldi and Gei [2] have investigated analytically the influence of electromechanical finite deformations on the stability of multilayered soft dielectrics. For homogeneous systems, diffuse mode bifurcations for prestretched actuators and onset of band localization are here investigated, for different geometries (layer and half-space), under plain strain conditions.

7.1 Diffuse Modes of Bifurcation

These instabilities may be detected investigating the propagation of small-amplitude perturbations of arbitrary wavelength superimposed on the current state of deformation [14]. While a real natural frequency corresponds to a propagating wave, a complex natural frequency identifies perturbation exponentially growing with time. Therefore, the transition between a stable and an unstable configuration is observed when the frequency vanishes and can be studied using investigation of zero-speed waves: for electroelastic solids, Dorfmann and Ogden [13] have explored surface instability, revealing that the critical loading parameter is crucially dependent on the magnitude of electric displacement applied.

Diffuse modes are meaningful for partially constrained bodies, then they are investigated here only for prestretched specimens. We will analyse two particular geometries: a half-space and a layer, with different boundary conditions. In the investigation of diffuse modes, along the homogeneous fundamental path, we must consider when band localization occurs as an alternative instability which terminates the homogeneous response of the body. The latter will be discussed deeply in Sect. 7.4.

7.1.1 Surface Instability with an External Electric Field

The study of diffuse modes for a half-space is called *surface instability*. We consider a prestretched half-space and with the presence of an external field, as in Fig. 7.1, assuming as fundamental path the one presented in sect. 6.1.1 , recalling incremental eqs. (4.59) and specializing the constitutive equations for a Mooney-Rivlin electroelastic solid (3.46), (4.37). For the Gent material model a similar procedure can be followed.

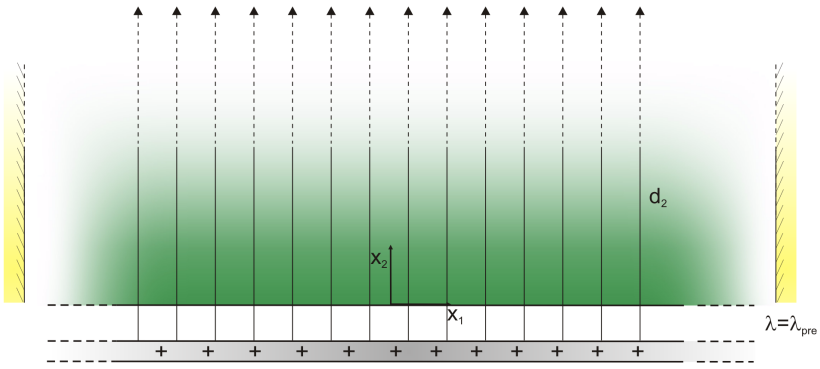

Figure 7.1: A specimen is prestreched and an external electric displacement field is applied in the transversal direction.

Electroelastic Moduli

Since $F_{ij} = 0$ for $i \neq j$ and $d_1^0 = d_3^0 = 0$, significant simplifications occur in the component of the tensors $\mathbb{C}$, $\mathbb{B}$ and $\mathbb{A}$ (see eqns. (4.64),(4.65),(4.66)). In particular, we obtain

$$
\begin{aligned}
&C_{1111} = C_{3131} = \lambda_{\text{pre}}^2 \mu,\\
&C_{1212} = \frac{d_2^2(\bar{\gamma}_1 \lambda_{\text{pre}}^2 + \bar{\gamma}_2(2 + \lambda_{\text{pre}}^4)) + \epsilon_0 \bar{\epsilon}_r \mu}{\epsilon_0 \bar{\epsilon}_r \lambda_{\text{pre}}^2},\\
&C_{1221} = C_{2112} = C_{2332} = C_{3223} = \frac{d_2^2 \bar{\gamma}_2 \lambda_{\text{pre}}^2}{\epsilon_0 \bar{\epsilon}_r},\\
&C_{2323} = \left(\frac{d_2^2 \bar{\gamma}_2 \lambda_{\text{pre}}^2}{\epsilon_0 \bar{\epsilon}_r} + \mu \right), \quad C_{2121} = \lambda_{\text{pre}}^2 C_{2323},\\
&C_{2222} = \frac{d_2^2(6\bar{\gamma}_2 + \bar{\gamma}_1 \lambda_{\text{pre}}^2) + \epsilon_0 \bar{\epsilon}_r \mu}{\epsilon_0 \bar{\epsilon}_r \lambda_{\text{pre}}^2},\\
&C_{3232} = \frac{d_2^2(2\bar{\gamma}_2 + (\bar{\gamma}_1 + \bar{\gamma}_2)\lambda_{\text{pre}}^2) + \epsilon_0 \bar{\epsilon}_r \mu}{\epsilon_0 \bar{\epsilon}_r \lambda_{\text{pre}}^2},\\
&C_{1313} = C_{3333} = \mu,
\end{aligned}
$$

and

$$
\begin{aligned}
&B_{121} = B_{211} = \frac{d_2(\bar{\gamma}_2 + \bar{\gamma}_1 \lambda_{\text{pre}}^2 + \bar{\gamma}_2 \lambda_{\text{pre}}^4)}{\epsilon_0 \bar{\epsilon}_r \lambda_{\text{pre}}^2}\\
&B_{233} = B_{323} = \frac{d_2(\bar{\gamma}_2 \lambda_{\text{pre}}^2 + \bar{\gamma}_1 \lambda_{\text{pre}}^2 + \bar{\gamma}_2)}{\epsilon_0 \bar{\epsilon}_r \lambda_{\text{pre}}^2},\\
&B_{222} = \frac{2d_2(\bar{\gamma}_1 \lambda_{\text{pre}}^2 + 2\bar{\gamma}_2)}{\epsilon_0 \bar{\epsilon}_r \lambda_{\text{pre}}^2}
\end{aligned}
$$

and

$$
A_{11} = \frac{\bar{\gamma}_0 + \bar{\gamma}_1 \lambda_{\text{pre}}^2 + \bar{\gamma}_2 \lambda_{\text{pre}}^4}{\epsilon_0 \bar{\epsilon}_r \lambda_{\text{pre}}^2}, \quad A_{22} = \frac{\bar{\gamma}_0 \lambda_{\text{pre}}^4 + \bar{\gamma}_1 \lambda_{\text{pre}}^2 + \bar{\gamma}_2}{\epsilon_0 \bar{\epsilon}_r \lambda_{\text{pre}}^2}, \quad A_{33} = \frac{\bar{\gamma}_0 + \bar{\gamma}_1 + \bar{\gamma}_2}{\epsilon_0 \bar{\epsilon}_r}.
$$

Incremental Fields and Equations

As for the underlying deformation, we consider the incremental deformation also to have a plane strain character. Thus, we suppose that the components of the incremental displacement (presented in $(3.43)_1$) are such that $u_3 = 0$ and that the in–plane components depend only on x_1 and x_2: $u_i = u_i(x_1, x_2)$, for $i = 1, 2$. Similarly, we assume that $\hat{d}_3 = 0$ and $\hat{d}_i = \hat{d}_i(x_1, x_2)$, for $i = 1, 2$ and $\dot{p} = \dot{p}(x_1, x_2)$. So the incremental field equations

$$\Sigma_{11,1} + \Sigma_{12,2} = 0,$$
$$\Sigma_{21,1} + \Sigma_{22,2} = 0,$$

$$\hat{d}_{1,1} + \hat{d}_{2,2} = 0,$$

$$\hat{e}_{1,2} - \hat{e}_{2,1} = 0,$$

specialize in

$$\begin{aligned}
&u_{1,11}\lambda_{\rm pre}^2\mu + u_{1,11}\left(d_2^2\frac{\bar{\gamma}_1}{\epsilon_0\bar{\epsilon}_r} - \frac{d_2^2}{2\epsilon_0} + \frac{\mu}{\lambda_{\rm pre}^2}\right) - \dot{p}_{,1} \\
&+ \hat{d}_{1,2}d_2\frac{\bar{\gamma}_1\lambda_{\rm pre}^2 + \bar{\gamma}_2(1+\lambda_{\rm pre}^4)}{\epsilon_0\bar{\epsilon}_r\lambda_{\rm pre}^2} + u_{1,22}\left(d_2^2\frac{\bar{\gamma}_1 + \bar{\gamma}_2(2+\lambda_{\rm pre}^4)}{\epsilon_0\bar{\epsilon}_r} + \frac{\mu}{\lambda_{\rm pre}^2}\right) \\
&+ u_{2,12}\left(d_2^2\frac{\bar{\gamma}_1 + \bar{\gamma}_2\lambda_{\rm pre}^2}{\epsilon_0\bar{\epsilon}_r} - \frac{d_2^2}{2\epsilon_0} + \frac{\mu}{\lambda_{\rm pre}^2}\right) = 0, \\
&\hat{d}_{1,1}d_2\frac{\bar{\gamma}_1 + \bar{\gamma}_2(1+\lambda_{\rm pre}^4)}{\epsilon_0\bar{\epsilon}_r\lambda_{\rm pre}^2} + u_{2,11}\mu\lambda_{\rm pre}^2 + u_{1,12}\left(d_2^2\frac{\bar{\gamma}_1}{\epsilon_0\bar{\epsilon}_r} - \frac{d_2^2}{2\epsilon_0} + \frac{\mu}{\lambda_{\rm pre}^2}\right) \\
&+ 2d_2\hat{d}_{2,2}\frac{\bar{\gamma}_1\lambda_{\rm pre}^2 + 2\bar{\gamma}_2}{\epsilon_0\bar{\epsilon}_r\lambda_{\rm pre}^2} + u_{2,22}\left(d_2^2\gamma_1 + \frac{\mu}{\lambda_{\rm pre}^2}\right) \\
&+ u_{2,22}\left(d_2^2\frac{\bar{\gamma}_1}{\epsilon_0\bar{\epsilon}_r} - \frac{d_2^2}{2\epsilon_0} + \frac{\mu}{\lambda_{\rm pre}^2}\right) - \dot{p}_{,2} = 0,
\end{aligned} \tag{7.1}$$

and

$$d_2(u_{1,22}+2u_{2,12})(\bar{\gamma}_2+\bar{\gamma}_1\lambda_{\rm pre}^2+\bar{\gamma}_2\lambda_{\rm pre}^4)+\hat{d}_{1,2}\left(\bar{\gamma}_0+\bar{\gamma}_1\lambda_{\rm pre}^2+\bar{\gamma}_2\lambda_{\rm pre}^4\right)$$
$$-2d_2u_{2,12}(\bar{\gamma}_1\lambda_{\rm pre}^2+2\bar{\gamma}_2)-\hat{d}_{2,1}(\bar{\gamma}_1\lambda_{\rm pre}^2+\bar{\gamma}_0\lambda_{\rm pre}^4+\bar{\gamma}_2)=0. \tag{7.2}$$

Solution

In order to solve the incremental boundary value problem (4.59) and (4.60), we seek small–amplitude solutions in the half space $x_2 \geq 0$ in the form

$$\begin{aligned} u_i(x_1,x_2) &= v_i(x_2)\exp(ik_1x_1),\\ \hat{d}_i(x_1,x_2) &= \Delta_i(x_2)\exp(ik_1x_1),\\ \dot{p}(x_1,x_2) &= q(x_2)\exp(ik_1x_1), \quad \text{for } i=1,2. \end{aligned} \tag{7.3}$$

The incompressibility constrain $u_{1,1}+u_{2,2}=0$ imposes that for $(7.3)_1$ we have

$$ik_1v_1(x_2)+v_2'(x_2)=0 \tag{7.4}$$

and the Maxwell equation $\hat{d}_{1,1}+\hat{d}_{2,2}=0$ imposes that for $(7.3)_2$ we have

$$ik_1\Delta_1(x_2)+\Delta_2'(x_2)=0. \tag{7.5}$$

It's necessary to make other assumptions:

$$\begin{aligned} v_2(x_2) &= U\exp(sk_1x_2),\\ \Delta_2(x_2) &= W\exp(sk_1x_2),\\ q(x_2) &= Q\exp(sk_1x_2), \end{aligned} \tag{7.6}$$

where s is to be determined subject to the restriction

$$\mathrm{Re}(s)<0, \tag{7.7}$$

which ensures that displacement decays away from the boundary with increasing x_2. Then, from (7.4), eq. $(7.6)_1$ becomes

$$v_1(x_2)=iUs\exp(sk_1x_2)$$

and from (7.5), eq. $(7.6)_2$ becomes

$$\Delta_1(x_2) = iWs\exp(sk_1x_2).$$

So substituting all these quantities in (7.1) and (7.2) we obtain a homogeneous system ,in the unknowns U, W, Q, to which is associated a 3×3 matrix. So in order to have a non trivial solution, the determinant of coefficients U, V, Q must vanish. This leads to the equation in the variable s, which in the case of Ogden and Dorfmann ($\bar{\gamma}_2 = 0$), is simply given by

$$\begin{aligned}&\lambda_{\rm pre}^2[s^4 + \lambda_{\rm pre}^4 - s^2(1+\lambda_{\rm pre}^4)]\big[d_2^2 s^2\bar{\gamma}_0\bar{\gamma}_1\lambda_{\rm pre}^2\\ &+ \epsilon_0\bar{\epsilon}_r(s^2\bar{\gamma}_0 + (s^2-1)\bar{\gamma}_1\lambda_{\rm pre}^2 - \bar{\gamma}_0\lambda_{\rm pre}^4)\mu\big] = 0\end{aligned} \tag{7.8}$$

which is cubic in s^2. Let s_1, s_2, s_3 the three negative roots of (7.8), because this ensure that the displacement decays away from the boundary with increasing x_2. So here we write the roots

$$s_1 = -1, \quad s_2 = -\lambda^2, \quad s_3 = -\frac{\lambda_{\rm pre}\sqrt{\epsilon_0\bar{\epsilon}_r(\bar{\gamma}_1 + \bar{\gamma}_0\lambda_{\rm pre}^2)\mu}}{\sqrt{d_2^2\bar{\gamma}_0\bar{\gamma}_1\lambda_{\rm pre}^2 + \epsilon_0\bar{\epsilon}_r(\bar{\gamma}_0 + \bar{\gamma}_1\lambda_{\rm pre}^2)\mu}}.$$

So the general solution for the half–space satisfying the decay condition can be written as

$$\begin{aligned}v_2(x_2) &= \sum_{j=1}^{3} U_j\exp(s_jk_1x_2),\\ \Delta_2(x_2) &= \sum_{j=1}^{3} W_j\exp(s_jk_1x_2),\\ q(x_2) &= \sum_{j=1}^{3} Q_j\exp(s_jk_1x_2).\end{aligned}$$

The constants U_j, W_j and Q_j are not independent and are connected using the equilibrium eqs. $(7.1)_2$ and (7.2) (given in the simple case $\bar{\gamma}_2 = 0$):

$$W_j = -\frac{d_2k_1\bar{\gamma}_1\lambda_{\rm pre}^2 s_j(s_j^2-1)U_j}{\bar{\gamma}_0(s_j^2 - \lambda_{\rm pre}^4) + \bar{\gamma}_1\lambda_{\rm pre}^2(s_j^2-1)}, \quad \text{for } j = 1,2,3, \tag{7.9}$$

and

$$Q_j = \frac{1}{s_j} k_1(-\lambda_{\text{pre}}^4 + s_j^2)\left(\frac{\mu}{\lambda_{\text{pre}}^2} + \frac{d_2^2\bar{\gamma}_0\bar{\gamma}_1 s_j^2}{\epsilon_0\epsilon_r[\bar{\gamma}_0(s_j^2 - \lambda_{\text{pre}}^4) + \bar{\gamma}_1\lambda_{\text{pre}}^2(s_j^2 - 1)]}\right) U_j,$$
$$\text{for } j = 1, 2, 3. \tag{7.10}$$

Incremental Exterior Equations

Outside the material, Maxwell's equations hold for $\mathbf{d}^*$ and $\mathbf{e}^*$. From the equation curl$\mathbf{e}^* = \mathbf{0}$, and the assumption that all fields depend only on x_1 and x_2, we deduce the existence of a scalar function $\varphi^* = \varphi^*(x_1, x_2)$ such that

$$\dot{e_1}^* = -\varphi^*_{,1}, \quad \dot{e_2}^* = -\varphi^*_{,2}, \quad \dot{e_3}^* = 0.$$

Then

$$\dot{d_1}^* = -\epsilon_0\varphi^*_{,1}, \quad \dot{e_2}^* = -\epsilon_0\varphi^*_{,2}, \quad \dot{d_3}^* = 0.$$

and the equation div$\mathbf{d}^* = 0$ gives

$$\varphi^*_{,11} + \varphi^*_{,22} = 0$$

for φ^*. Finally, the incremental Maxwell stress tensor has the following non–zero components

$$\dot{T}^*_{11} = \dot{T}^*_{33} = -\dot{T}^*_{22} = \epsilon_0 e^*_2\varphi^*_{,2}$$
$$\dot{T}^*_{12} = \dot{T}^*_{21} = -\epsilon_0 e^*_2\varphi^*_{,1}.$$

For the vacuum we suppose that

$$\dot{\varphi}^{*-}(x_1, x_2) = F^- \exp(k_1 x_2) \exp(ik_1 x_1)$$

so that the solution decays for $x_2 \to -\infty$, where the subscript minus indicates that we are in the neighbor of $x_2 = 0$. In this way we have

$$\dot{e_1}^{*-} = -iF^- k_1 \exp(ik_1 x_1 + k_1 x_2), \quad \dot{e_2}^{*-} = -F^- k_1 \exp(ik_1 x_1 + k_1 x_2).$$

Incremental Boundary Conditions

Next we specialize the incremental boundary conditions to the present situation. We set the incremental mechanical traction $\dot{\mathbf{t}}$ to $\mathbf{0}$ and the incremental traction boundary condition $(4.60)_{2,4}$ specializes in

$$\dot{\mathbf{\Sigma}}\mathbf{n}dA = \dot{\mathbf{t}^0}dA^0 + \mathbf{\Sigma}^*\mathbf{n}dA, \quad \hat{\mathbf{d}} \cdot \mathbf{n}dA = -\dot{\omega}^0 dA^0 + \hat{\mathbf{d}}^* \cdot \mathbf{n}dA, \tag{7.11}$$

where

$$\mathbf{\Sigma}^* = \dot{\mathbf{T}}^* + \mathbf{T}^*[\mathrm{tr}\mathbf{L}_{|bnd}\mathbf{I} - (\mathbf{L}_{|bnd})^T], \quad \hat{\mathbf{d}}^* = \epsilon_0[\dot{\mathbf{e}}^* + (\mathrm{tr}\mathbf{L}_{|bnd}\mathbf{I} - \mathbf{L}_{|bnd})\mathbf{e}^*],$$

denoting with $\dot{\mathbf{e}}^*$ the increment of the electric field in the vacuum and with $\mathbf{L}_{|bnd} = (\mathrm{grad}\mathbf{u})_{\partial\mathcal{B}}$. Eq. $(7.11)_1$ reduces to the component equations

$$\begin{aligned} &\Sigma_{21} + T^*_{11}u_{2,1} + T^*_{21}u_{2,2} - \dot{T}^*_{21} = 0, \\ &\Sigma_{22} + T^*_{22}u_{2,2} + T^*_{21}u_{2,1} - \dot{T}^*_{22} = 0 \end{aligned} \tag{7.12}$$

on $x_2 = 0$. Then the incremental electric boundary condition $(7.11)_2$ becomes

$$\hat{d_2} + d^*_1 u_{2,1} + d^*_2 u_{2,2} - \dot{d}^*_2 = 0 \tag{7.13}$$

and

$$\hat{e_1} - u_{1,1}e^*_1 - u_{2,1}e^*_2 - \dot{e}^*_1 = 0 \tag{7.14}$$

on $x_2 = 0$. We remind that in this case $T_{12} = T_{21} = 0$, $d^*_1 = 0$ and $e^*_1 = 0$.

Substituting eqs. (7.3), (7.6), (7.9),(7.10) in (7.12), (7.13) and (7.14) we obtain a system of four homogeneous equations. For non–trivial solution, the determinant of coefficients U_j, for $j = 1, 2, 3$ and F^- must vanish. This provides a connection between the four quantities $k_1, \bar{\gamma}_0, \bar{\gamma}_1, \bar{\gamma}_2, d_2$, in which we have to consider the fixed value of μ and ϵ_0. This equation is called *bifurcation equation*.

Results

We can consider a comparison with the Ogden-Dorfmann work. In [13], we find that authors indicate with α and β the electric material coefficients, establishing the next relations with our electrostrictive coefficients

$$\alpha = \frac{\bar{\gamma}_0}{2\bar{\epsilon}_r}, \quad \beta = \frac{\bar{\gamma}_1}{2\bar{\epsilon}_r}.$$

Since it is valid the physical relationships

$$\bar{\gamma}_0 + \bar{\gamma}_1 + \bar{\gamma}_2 = 1, \quad \bar{\epsilon}_r > 1$$

then it follows that for Ogden-Dorfmann coefficients must be verified that

$$\alpha + \beta < \frac{1}{2},$$

but in their work is not taken into account to comply with this condition, so some numerical data, which are presented, have no physical meaning.

Results are reported in Fig. 7.2, where the chosen parameters are consistent with the rest of the thesis (see Table 5.1). Curves pertinent to Sets #1 and #2 terminate at the onset of band-localization (marked with red points) that will be analysed in Sect. 7.4, while set #0 denotes the case $\epsilon_r = \bar{\epsilon}_r$ (constant). When $\bar{D} = 0$, surface instability is achieved at $\lambda_{\text{pre}} \approx 0.544$ as predicted by Biot [4]. It is found that the electric field has a highly nonlinear influence on the stability, and it is evident the strongly dependence on the parameters $\bar{\gamma}_0$, $\bar{\gamma}_1$ and $\bar{\gamma}_2$.

7.2 Surface Instability with Electric Field Induced by a Surface Electrode

We consider a half-space with an external electric field, induced by a surface electrode, so subjected to a fundamental path as presented in sect. 6.1.3, see Fig. 7.3. Study has been made for Mooney-Rivlin electroelastic material model (3.46), (4.37). Analogous calculations have been made for Gent electroelastic material model (3.52), (4.37).

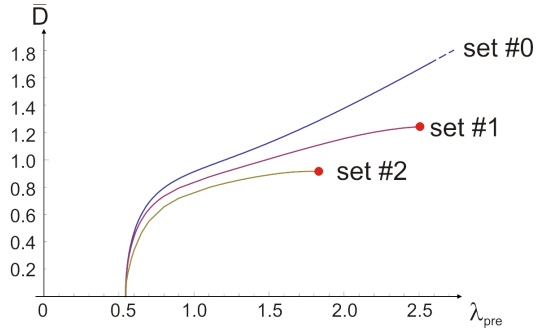

Figure 7.2: Plot of the critical stretch λ_{pre} for an electroelastic Mooney-Rivlin half-space as a function of the dimensionless $\bar{D} = d_2/\sqrt{\mu\epsilon_0\bar{\epsilon}_r}$, with the presence of an external electric field. Results show that the electric field has a highly nonlinear influence on the stability, and it is evident the strongly dependence on the parameters $\bar{\gamma}_0$, $\bar{\gamma}_1$ and $\bar{\gamma}_2$, set #0 stands for $\epsilon_r = \bar{\epsilon}_r$.

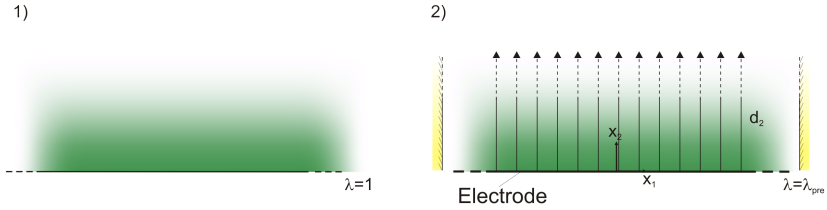

Figure 7.3: A specimen is prestretched, so starting from the natural configuration ($\lambda = 1$), the actual configuration is achieved by imposing 1) $\lambda = \lambda_{\text{pre}}$ and 2) an electric displacement field induced by a surface electrode.

The incremental equations become:

$$
\begin{aligned}
&u_{1,11}\lambda_{\text{pre}}^2\mu + u_{1,11}\left(d_2^2\frac{\bar{\gamma}_1}{\epsilon_0\bar{\epsilon}_r} + \frac{\mu}{\lambda_{\text{pre}}^2}\right) - \dot{p}_{,1} \\
&+ \hat{d}_{1,2}d_2\frac{\bar{\gamma}_1\lambda_{\text{pre}}^2 + \bar{\gamma}_2(1+\lambda_{\text{pre}}^4)}{\epsilon_0\bar{\epsilon}_r\lambda_{\text{pre}}^2} + u_{1,22}\left(d_2^2\frac{\bar{\gamma}_1 + \bar{\gamma}_2(2+\lambda_{\text{pre}}^4)}{\epsilon_0\bar{\epsilon}_r} + \frac{\mu}{\lambda_{\text{pre}}^2}\right) \\
&+ u_{2,12}\left(d_2^2\frac{\bar{\gamma}_1 + \bar{\gamma}_2\lambda_{\text{pre}}^2}{\epsilon_0\bar{\epsilon}_r} + \frac{\mu}{\lambda_{\text{pre}}^2}\right) = 0, \\
&\hat{d}_{1,1}d_2\frac{\bar{\gamma}_1 + \bar{\gamma}_2(1+\lambda_{\text{pre}}^4)}{\epsilon_0\bar{\epsilon}_r\lambda_{\text{pre}}^2} + u_{2,11}\mu\lambda_{\text{pre}}^2 + u_{1,12}\left(d_2^2\frac{\bar{\gamma}_1}{\epsilon_0\bar{\epsilon}_r} + \frac{\mu}{\lambda_{\text{pre}}^2}\right) \\
&+ 2d_2\hat{d}_{2,2}\frac{\bar{\gamma}_1\lambda_{\text{pre}}^2 + 2\bar{\gamma}_2}{\epsilon_0\bar{\epsilon}_r\lambda_{\text{pre}}^2} + u_{2,22}\left(d_2^2\gamma_1 + \frac{\mu}{\lambda_{\text{pre}}^2}\right) \\
&+ u_{2,22}\left(d_2^2\frac{\bar{\gamma}_1}{\epsilon_0\bar{\epsilon}_r} + \frac{\mu}{\lambda_{\text{pre}}^2}\right) - \dot{p}_{,2} = 0
\end{aligned}
\tag{7.15}
$$

and

$$
\begin{aligned}
&d_2(u_{1,22} + 2u_{2,12})(\bar{\gamma}_2 + \bar{\gamma}_1\lambda_{\text{pre}}^2 + \bar{\gamma}_2\lambda_{\text{pre}}^4) + \hat{d}_{1,2}\left(\bar{\gamma}_0 + \bar{\gamma}_1\lambda_{\text{pre}}^2 + \bar{\gamma}_2\lambda_{\text{pre}}^4\right) \\
&- 2d_2u_{2,12}(\bar{\gamma}_1\lambda_{\text{pre}}^2 + 2\bar{\gamma}_2) - \hat{d}_{2,1}(\bar{\gamma}_1\lambda_{\text{pre}}^2 + \bar{\gamma}_0\lambda_{\text{pre}}^4 + \bar{\gamma}_2) = 0.
\end{aligned}
\tag{7.16}
$$

Considering the same solutions seen above for the prevoius half-space problem, we obtain on one hand the same values for s, on the other incremental boundary conditions change as follows: introducing the incremental electric field $\dot{\phi}^{*-}(x_1, x_2) = F^- \exp(k_1 x_2) * \exp(ik_1 x_1)$, we specialize such conditions in $x_2 = 0$ and for the electrical part we have to consider only the incremental Maxwell stress tensor:

$$
\hat{d}_2 - \epsilon_0\dot{e}_2^{*-} = 0, \quad \hat{e}_1 - \dot{e}_1^{*-} = 0.
$$

With the same manipulations seen before, we obtain bifurcation equation, in terms of $k_1, \bar{\gamma}_0, \bar{\gamma}_1, \bar{\gamma}_2, d_2, \mu, \epsilon_0$.

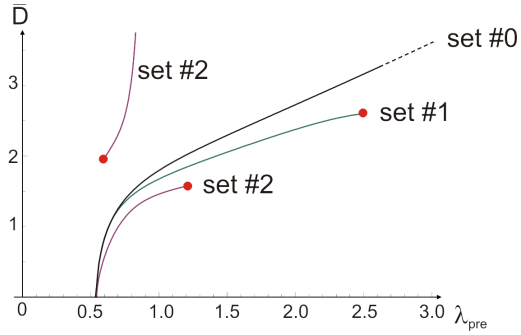

Figure 7.4: Surface instability diagram for a Mooney-Rivlin material, induced by an electric field generated by a surface electrode. For set #2 the solution is composed of two branches, mainly in the compressive range ($\lambda_{\rm pre}$). Red points indicate occurrence of band-localization instability.

Results

Fig. 7.4 is qualitatively similar to Fig. 7.2, even if their quantitative comparison is provided in Fig. 7.8, for set #0 only, for a Mooney Rivlin model (3.46). We observe that, for the same value of strech, a higher value of $\bar{D}$ occurs when the electric field is generated by a surface electrode. In particular Fig. 7.4, for set #2, the solution is composed of two branches: the first is a classical surface instability, the second is a localized mode along the surface of the half-space (see Fig. 7.7 and comments below). In all plots, red points indicate occurrence of band-localization instability. The "stars" in c) denote the two modes sketched in Fig. 7.7.

Figs. 7.2-7.4 exhibit the comparison between surface instabilities for Mooney-Rivlin in blue and Gent material models in purple (recalling (3.52), assuming in the uni-axial test the limiting stretch equal to 10, conseguently $J_m = 97.2$ (3.51)), when the electric field is generated by a surface electrode. At low stretches ($\lambda_{\rm pre} \lesssim 2$, the two material responses are very similar. For sets #1 and #2 the curves are interrupted in the range where the instability is determined by band-localization (Sect. 7.4).

The sketch of instability modes corresponding to the two points marked

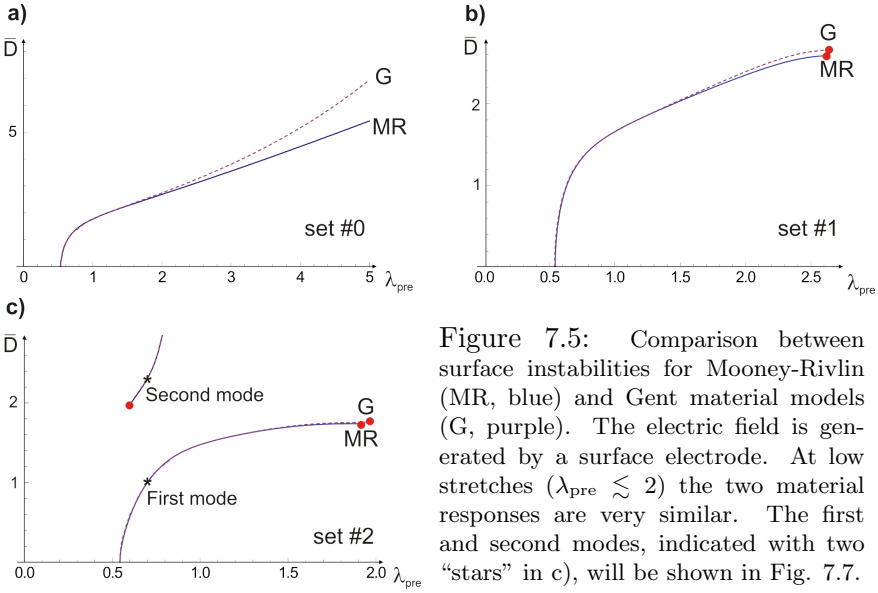

Figure 7.5: Comparison between surface instabilities for Mooney-Rivlin (MR, blue) and Gent material models (G, purple). The electric field is generated by a surface electrode. At low stretches ($\lambda_{\text{pre}} \lesssim 2$) the two material responses are very similar. The first and second modes, indicated with two "stars" in c), will be shown in Fig. 7.7.

by "stars" in the previous figures (set #2, $\lambda_{\text{pre}} = 0.7$) are drawn in Fig. 7.7. Surfaces in a) and b) display, respectively, the functions $|\mathbf{u}(x_1, x_2)|$ and $|\hat{\mathbf{d}}(x_1, x_2)|$ for the first mode, corresponding to the classical Rayleigh mode. Modes have been normalized chosing $\max(|\mathbf{u}(x_1, 0)|) = 1$. Parts b) and d) of Fig. 7.7 report the same functions for the second mode. It can be observed that the latter is very localized along the surface of the half space with high values of the electric quantity compared to the former. We have also noted that $\hat{d}_2$ component is predominant compared to $\hat{d}_1$.

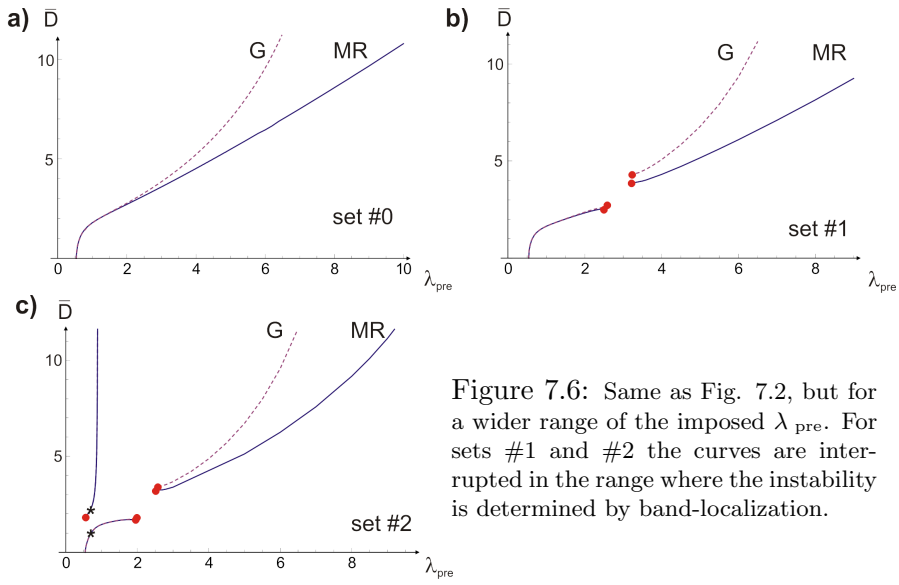

Figure 7.6: Same as Fig. 7.2, but for a wider range of the imposed λ_{pre}. For sets #1 and #2 the curves are interrupted in the range where the instability is determined by band-localization.

7.3 Diffuse modes of Instability in a Homogeneous Layer

The goal of this section is to investigate electrostrictive effects on diffuse (sinusoidal) instability modes for a homogeneous layer under plane strain condition, subjected to the large strain deformation described in Sect. 6.1.3 (see Fig. 6.3): the specimen will be first prestretched homogeneously to $\lambda = \lambda_{\text{pre}}$ and then subject to electric actuation along the transverse direction. These instability modes are important as they comprise buckling instability (a diffuse mode with high wavelength, typical of slender specimens) and surface instability (the limit for short wavelengths) as calculated before. Real actuators exploit buckling modes to induce a snap actuation mechanism [8].

To start, we suppose that the components of the incremental displacement are such that $u_3 = 0$ and that the in–plane components depend only on x_1 and x_2: $u_i = u_i(x_1, x_2)$, for $i = 1, 2$. Similarly, we assume $\hat{d}_3 = 0$

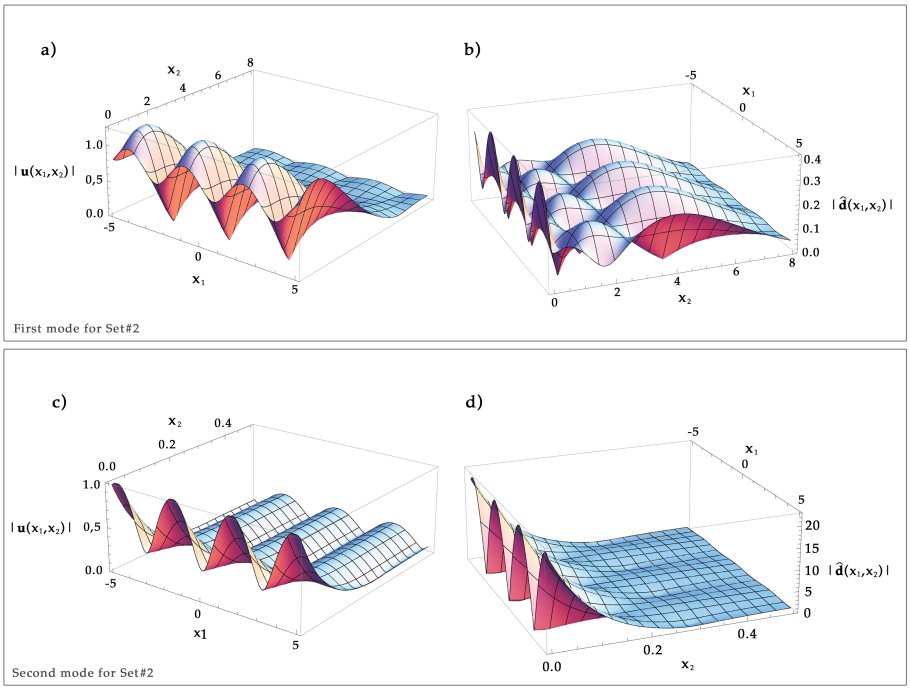

Figure 7.7: Instability modes corresponding to the two "stars" reported in Fig. 7.4 for set #2 ($\lambda_{\text{pre}} = 0.7$). a), c): modulus of incremental displacement $|\mathbf{u}(x_1, x_2)|$; b), d): modulus of updated incremental electric displacement field $|\hat{\mathbf{d}}(x_1, x_2)|$. Note the difference in the amplitudes between d) and b).

and $\hat{d}_i = \hat{d}_i(x_1, x_2)$ for $i = 1, 2$. Moreover, $\dot{p} = \dot{p}(x_1, x_2)$. Under these hypotheses, the incremental field equations are

$$\Sigma_{11,1} + \Sigma_{12,2} = 0, \quad \Sigma_{21,1} + \Sigma_{22,2} = 0, \tag{7.17}$$

$$\hat{d}_{1,1} + \hat{d}_{2,2} = 0, \tag{7.18}$$

$$\hat{e}_{1,2} - \hat{e}_{2,1} = 0, \tag{7.19}$$

while the entries of the constitutive moduli (4.64)-(4.65)-(4.66) simplify accordingly.

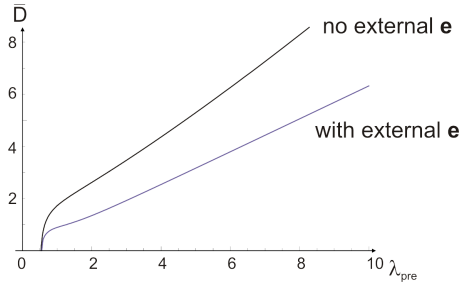

Figure 7.8: Comparison between surface instabilities obtained for the two different fundamental paths considered (Mooney-Rivlin material, set #0).

Incremental boundary conditions

The incremental traction boundary conditions are similar to those employed for the half-space problem, Sect. 7.1.1,

$$\begin{aligned} \Sigma_{21} - \dot{T}^*_{21} &= 0, \\ \Sigma_{22} - \dot{T}^*_{22} &= 0 \end{aligned} \tag{7.20}$$

$$\hat{d}_2 - \dot{d}^*_2 = 0 \tag{7.21}$$

$$\hat{e}_1 - \dot{e}^*_1 = 0 \tag{7.22}$$

but now they are imposed on the two boundary of the layer, $x_2 = 0, h$.

Diffuse modes of instability

Diffuse instability modes correspond to solutions of the incremental equations of the form

$$\begin{aligned} \dot{u}_i(x_1, x_2) &= v_i(x_2) \exp(ik_1 x_1), \\ \hat{\dot{d}}_i(x_1, x_2) &= \Delta_i(x_2) \exp(ik_1 x_1), \\ \dot{p}_i(x_1, x_2) &= q(x_2) \exp(ik_1 x_1), \quad \text{for } i = 1, 2, \end{aligned} \tag{7.23}$$

being k_1 the wavenumber. The incompressibility constraint $u_{1,1} + u_{2,2} = 0$ imposes

$$ik_1 v_1(x_2) + v_2'(x_2) = 0, \tag{7.24}$$

while the Maxwell equation $\hat{d}_{1,1} + \hat{d}_{2,2} = 0$ that

$$ik_1 \Delta_1(x_2) + \Delta_2'(x_2) = 0, \tag{7.25}$$

(see $(7.23)_2$). Admissible form for the x_2–dependent fields in (7.23) are

$$\begin{aligned} v_2(x_2) &= U \exp(sk_1 x_2), \\ \Delta_2(x_2) &= W \exp(sk_1 x_2), \\ q(x_2) &= Q \exp(sk_1 x_2), \end{aligned} \tag{7.26}$$

so that from eqs. $(7.26)_1$ and $(7.26)_2$, (7.24) and (7.25), become, respectively,

$$\begin{aligned} v_1(x_2) &= iUs \exp(sk_1 x_2), \\ \Delta_1(x_2) &= iWs \exp(sk_1 x_2). \end{aligned}$$

Substituting all these quantities in (7.17) and (7.19), we obtain a homogeneous system in the unknowns U, W, Q. A non-trivial solution is found if the determinant of the matrix of coefficients vanishes, leading to an equation in the variable s, which is a cubic in s^2. Let $s_1, s_2, s_3, s_4, s_5, s_6$ be the roots of that equation. The general solution for the incremental fields is

$$\begin{aligned} v_2(x_2) &= \sum_{i=1}^{6} U_i \exp(s_i k_1 x_2), \\ \Delta_2(x_2) &= \sum_{i=1}^{6} W_i \exp(s_i k_1 x_2), \\ q(x_2) &= \sum_{i=1}^{6} Q_i \exp(s_i k_1 x_2). \end{aligned}$$

The constants U_i, W_i and Q_i are not independent and are connected using the equilibrium equations $(7.17)_2$ and (7.19).

Exterior equations

Outside the material, Maxwell equations hold for $\mathbf{d}^*$ and $\mathbf{e}^*$. From $\operatorname{curl}\mathbf{e}^* = \mathbf{0}$ and the assumption that all fields depend only on x_1 and x_2, we deduce the existence of a scalar function $\varphi^* = \varphi^*(x_1, x_2)$ such that

$$\dot{e_1}^* = -\varphi^*_{,1}, \quad \dot{e_2}^* = -\varphi^*_{,2}, \quad \dot{e_3}^* = 0, \tag{7.27}$$

where $\dot{\mathbf{e}}^*$ is the electric field in the vacuum caused by the perturbation. Then, as $\dot{\mathbf{d}} = \epsilon_0 \dot{\mathbf{e}}$,

$$\dot{d_1}^* = -\epsilon_0 \varphi^*_{,1}, \quad \dot{e_2}^* = -\epsilon_0 \varphi^*_{,2}, \quad \dot{d_3}^* = 0,$$

while the condition $\operatorname{div}\dot{\mathbf{d}}^* = 0$ gives

$$\varphi^*_{,11} + \varphi^*_{,22} = 0. \tag{7.28}$$

Finally, the incremental Maxwell stress tensor in vacuum (4.13) has the following non–zero components

$$\begin{aligned} \dot{T}^*_{11} &= \dot{T}^*_{33} = -\dot{T}^*_{22} = \epsilon_0 e^*_2 \varphi^*_{,2}, \\ \dot{T}^*_{12} &= \dot{T}^*_{21} = -\epsilon_0 e^*_2 \varphi^*_{,1}. \end{aligned}$$

The surrounding space consists of vacuum for $x_2 < 0$ and $x_2 > h$. For the vacuum at $x_2 < 0$ an expression for $\dot{\varphi}^{*-}$ satisfying (7.28) and decaying conditions for $x_2 \to -\infty$ is

$$\dot{\varphi}^{*-}(x_1, x_2) = F^- \exp(k_1 x_2) \exp(i k_1 x_1),$$

while for that at $x_2 > h$ similar considerations lead to

$$\dot{\varphi}^{*+}(x_1, x_2) = F^+ \exp(-k_1 x_2) \exp(i k_1 x_1).$$

In this way, eqs. (7.27) provide

$$\dot{e_1}^{*-} = -iF^- k_1 \exp(i k_1 x_1 + k_1 x_2), \quad \dot{e_2}^{*-} = -F^- k_1 \exp(i k_1 x_1 + k_1 x_2),$$

and

$$\dot{e_1}^{*+} = -iF^+k_1 \exp(ik_1x_1 - k_1x_2), \quad \dot{e_2}^{*+} = F^+k_1 \exp(ik_1x_1 - k_1x_2),$$

for the two vacui.

Substituting eqs. (7.23), (7.26), and the expressions of W_i and Q_i in (7.20), (7.21) and (7.22), a system of eight homogeneous equations is obtained. For non–trivial, inhomogeneous solutions, the determinant of coefficients U_i, for $i = 1, \ldots, 6$, and F^-, F^+ must vanish. This is the *bifurcation equation* that can be studied, for a well-defined strain energy function, assigning the following dimensionless quantities: $\lambda_{\rm pre}, k_1h, \bar{\gamma}_0, \bar{\gamma}_1, \bar{\gamma}_2, \bar{D}$.

Results

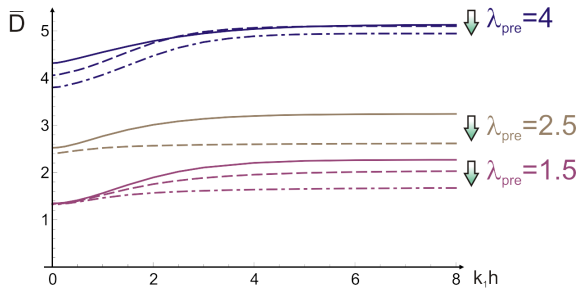

Figure 7.9: Comparison between antisymmetric modes (Gent material model with different electrostrictive parameters (3.52), (4.37), (5.1)) for the same initial $\lambda_{\rm pre}$: line for set #0, dashed line for set #1 and dot-dashed line for set #2.

In Fig. 7.10, diffuse-mode instability (i.e. antisymmetric modes of instability)is analysed for a prestretched specimen at different $\lambda_{\rm pre}$ and for different sets of electrostrictive parameters (see Table 5.1) for an extended Gent electroelastic free energy (3.52), (4.37).

In each of the three plots at the top of the figure, the horizontal axis refers to the dimensionless wavenumber k_1h, therefore high values of this parameter denote a surface-like modes (see Sect. 7.1.1, the asymptotic

values of critical $\bar{D}$ at $k_1 h \to \infty$ correspond to the findings previously obtained), while low $k_1 h$'s correspond to buckling-like modes.

The change of permittivity with deformation influences the critical electric displacement at bifurcation. This can be easily inferred comparing the top three plots for the same initial λ_{pre} and the comparison in Fig. 7.9. In general, a high degree of electrostriction will lower the critical electric actuation. The reason can be understood observing that the instability occurs when the axial stress T_{11} becomes compressive and this takes place, at equal conditions, at a slightly low $\bar{D}$ for high electrostriction, as shown in Fig. 6.4. As experimental results on electrostriction are available only for stretched membranes (see Sect. 5.2), the calculated values of parameters $\bar{\gamma}_i$ well interpolate the behaviour for $\lambda_{\text{pre}} > 1$, while for $\lambda_{\text{pre}} < 1$ we have verified that the resulting ϵ_r is far from reasonable values. Then, in Fig. 7.10, for $\lambda_{\text{pre}} = 0.8$ only the curve for constant ϵ_r has been sketched. For Set #2, the curve for $\lambda_{\text{pre}} = 2.5$ is not reported as at this value of the prestretch the specimen is in the range where band-localization takes place. The geometrical instability pattern for modes $k_1 h = 0.4, 1.3$ is reported at the bottom part of the figure, respectively marked with $*$ and $**$.

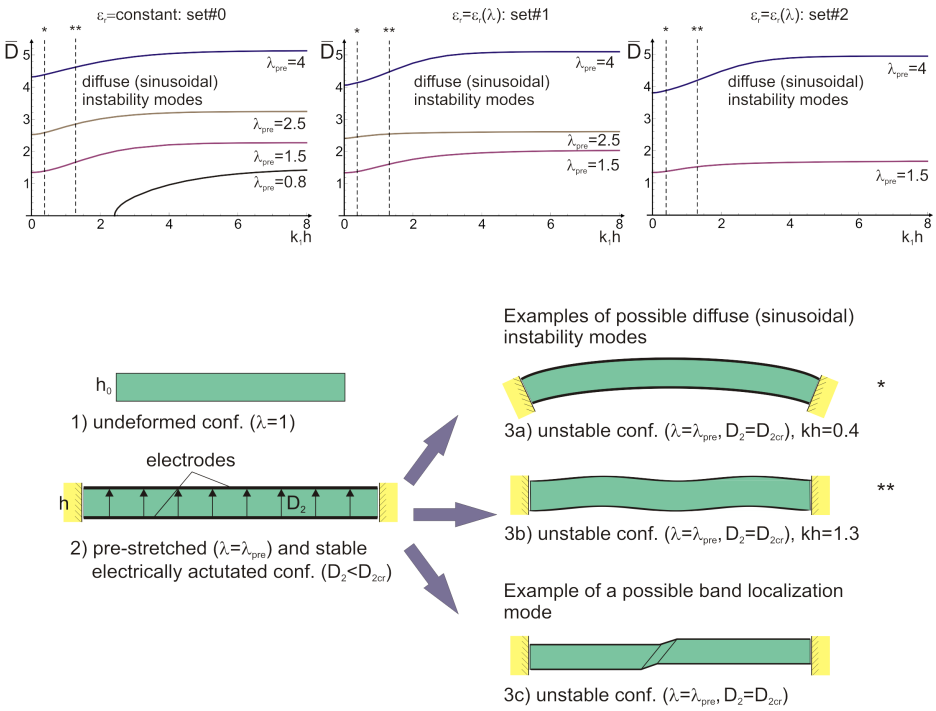

Figure 7.10: Diffuse instability modes for a prestretched actuator in plane strain (Gent material). Top line: Plots for different values of $\lambda_{\rm pre}$, in the $(k_1 h, \bar{D})$-plane, where $k_1 h$ is the current non-dimensional wavenumber, while $\bar{D}$ is the non-dimensional electric displacement. The three different graphs highlight the role of electrostriction: for the different set of electrostrictive parameters, diffuse modes occur for lower value of $\bar{D}$ and band-localization arises for different value of electric displacement. Bottom part: the figure shows possible visualizations of diffuse modes corresponding to two arbitrary values of $k_1 h$, denoted by $*$ and $**$, as well as a representation of band-localization instability.

7.4 Band Localization Instability

A local instability mode that could arise in large-strain solid mechanics is band localization where fields at bifurcation are discontinuous across a narrow band of unknown inclination. The condition of its onset along the homogeneous paths previously introduced can be determined investigat-

ing the admissible jumps between incremental quantities across the interface between band (superscript 'b') and the rest of the solid (superscript 'o'). Band-localization of electroelastic solids have been also considered by Bertoldi and Gei [2] and Rudykh and deBotton [41] by searching the conditions of existence of static discontinuities in the incremental electroelastic problem. Here, we consider jumps across the interface between homogeneous solid and band and we build the general solution of the problem. In this first formulation we consider electric displacement as independent field, then we use the electroelastic formulation developed in Sects. 4.5 and 4.7.

In the current configuration, let $\mathbf{n}$ be the normal to the band and $\mathbf{m}$ the orthogonal unit vector, aligned to the band, such that $\mathbf{m}\cdot\mathbf{n}=0$. At a certain point of the electro-mechanical loading process imagine that $\mathbf{L}^{\mathrm{o}}$ and $\hat{\mathbf{d}}^{\mathrm{o}}$ be the uniform response of the solid to an incremental change in the boundary conditions, except within the considered band where the incremental displacement $\mathbf{u}$ is assumed constant on planes $\mathbf{x}\cdot\mathbf{n}=$ const and $\hat{\mathbf{d}}^{\mathrm{b}}$ uniform. Compatibility relationships across the interface, namely $(\mathbf{L}^{\,\mathrm{b}}-\mathbf{L}^{\mathrm{o}})\mathbf{m}=\mathbf{0}$ and continuity of the normal component of $\hat{\mathbf{d}}$, require respectively that

$$\mathbf{L}^{\,\mathrm{b}}=\mathbf{L}^{\mathrm{o}}+\xi\mathbf{m}\otimes\mathbf{n},\quad \hat{\mathbf{d}}^{\,\mathrm{b}}=\hat{\mathbf{d}}^{\,\mathrm{o}}+\zeta\mathbf{m}, \tag{7.29}$$

where ξ and ζ are real scalars and represent mode amplitudes in the band. Note that fields $\mathbf{L}^{\,\mathrm{b}}$ and $\hat{\mathbf{d}}^{\,\mathrm{b}}$ satisfy field equations (7.17) and (7.19) in the band and the relative displacement field in $(7.29)_1$ associated with the dyadic term is an isochoric simple shear of amount ξ. On the other hand, continuity of the incremental traction and of the tangential component of the electric field require

$$(\mathbf{\Sigma}^{\,\mathrm{b}}-\mathbf{\Sigma}^{\,\mathrm{o}})\mathbf{n}=\mathbf{0},\quad \hat{\mathbf{e}}^{\,\mathrm{b}}-\hat{\mathbf{e}}^{\,\mathrm{o}}=\alpha\mathbf{n}, \tag{7.30}$$

where, again, α is real.

The use of (7.29) in the constitutive equations and in (7.30) provides, in component form, respectively (recalling eqs. (4.64), (4.65), (4.66))

$$Q_{ik}m_k-\frac{1}{\xi}(\dot{p}^{\,\mathrm{b}}-\dot{p}^{\,\mathrm{o}})n_i+\bar{\zeta}B_{iqa}m_an_q=0, \tag{7.31}$$

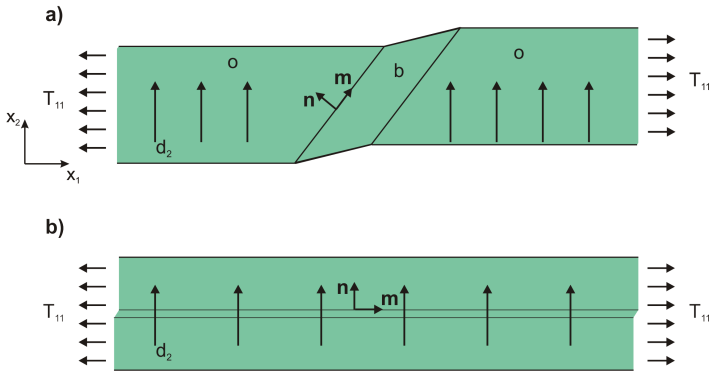

Figure 7.11: Band-localization instability. a) General sketch of the band. b) Orientation of the band occurring at the onset for extended Mooney-Rivlin and Gent material models. In the proposed linear analysis, the band thickness remains unknown.

$$B_{iqa}m_i n_q + \bar{\zeta}A_{ab}m_b = \bar{\alpha}n_a,$$

where $Q_{ik} = C_{iqkp}n_p n_q$ (called 'acoustic tensor'), $\bar{\zeta} = \zeta/\xi$ and $\bar{\alpha} = \alpha/\xi$. The manipulation of (7.31) yields the scaled amplitudes

$$\bar{\zeta} = -\frac{B_{iqa}m_i n_q m_a}{A_{ab}m_a m_b}, \qquad \bar{\alpha} = B_{iqa}m_i n_q n_a + \bar{\zeta}A_{ab}n_a m_b, \tag{7.32}$$

the incremental pressure difference across the interface

$$\frac{1}{\xi}(\dot{p}^{\,\mathrm{b}} - \dot{p}^{\,\mathrm{o}}) = Q_{ik}m_k n_i + \bar{\zeta}B_{iqa}n_i n_q m_a,$$

as well as the condition for band localization, namely ($A_{ab}m_a m_b \neq 0$)

$$A_{ab}m_a m_b Q_{ik}m_i m_k - (B_{iqa}m_i n_q m_a)^2 = 0. \tag{7.33}$$

Eq. (7.33) clearly depends on the current finite state and on the normal to the band $\mathbf{n}$ (the components of $\mathbf{m}$ can be easily substituted exploiting the

connection $m_r = e_{sr} n_s$, where $e_{12} = -e_{21} = 1,\ e_{11} = e_{22} = 0$). The final general form of the localization equation (7.33) is

$$\Gamma_6 \nu^6 + \Gamma_5 \nu^5 + \Gamma_4 \nu^4 + \Gamma_3 \nu^3 + \Gamma_2 \nu^2 + \Gamma_1 \nu + \Gamma_0 = 0, \tag{7.34}$$

which is a complete polynomial with:

$$\begin{aligned}
\Gamma_6 &= B_{121}^2 - A_{11} C_{1212}, \\
\Gamma_5 &= 2(B_{121}(B_{111} - B_{122} - B_{221}) + A_{12} C_{1212} + A_{11}(C_{1112} - C_{1222})), \\
\Gamma_4 &= (+B_{122} + B_{221} - B_{111})^2 - 2B_{121}(B_{112} + B_{211} - B_{222}) \\
&\quad - A_{22} C_{1212} + 4A_{12}(C_{1112} - C_{1222}) \\
&\quad - A_{11}(C_{1111} - 2C_{1122} - 2C_{1221} + C_{2222}), \\
\Gamma_3 &= 2(B_{121} B_{212} - (B_{111} - B_{122} - B_{221})(B_{112} + B_{211} - B_{222}) \\
&\quad + A_{22}(C_{1222} - C_{1112}) + A_{11}(C_{1121} - C_{2122}) \\
&\quad + A_{12}(C_{1111} - 2C_{1122} - 2C_{1221} + C_{2222})), \\
\Gamma_2 &= 2B_{212}(B_{111} - B_{122} - B_{221}) + (B_{112} + B_{211} - B_{222})^2 \\
&\quad - A_{11} C_{2121} - 4A_{12}(C_{1121} - C_{2122}) \\
&\quad + A_{22}(-C_{1111} + 2C_{1122} + 2C_{1221} - C_{2222}), \\
\Gamma_1 &= 2(B_{212}(B_{222} - B_{112} - B_{211}) + A_{12} C_{2121} + A_{22}(C_{1121} - C_{2122})), \\
\Gamma_0 &= B_{212}^2 - A_{22} C_{2121}.
\end{aligned}$$

In (7.34), $\nu = n_2/n_1$ ($n_1 \neq 0$). Localization occurs when (7.34) has a real solution. We can note that $\nu = \mathrm{i}s$ (where s is that considered in (7.6)), so if ν is complex we do not have loss of ellipticity and diffuse modes can be explored.

7.4.1 Band-localization of a Homogeneous Layer

We specialize now the general equation (7.34) to the problem of the pre-stretched layer. Now, as seen already, constitutive tensors A_{ab}, B_{iqa}, C_{iqkp} assume the form (4.64), (4.65), (4.66) and $\mathbf{d} = d_2 \mathbf{i}_2$. Therefore, eq. (7.33) becomes

$$\Gamma_6 \nu^6 + \Gamma_4 \nu^4 + \Gamma_2 \nu^2 + \Gamma_0 = 0, \tag{7.35}$$

and coefficients Γ_i $(i = 0, 2, 4, 6)$ depend on the incremental moduli as

$$\begin{aligned}
\Gamma_6 &= B_{121}^2 - A_{11}C_{1212},\\
\Gamma_4 &= -2B_{121}(B_{121} - B_{222})\\
&\quad - A_{22}C_{1212} - A_{11}(C_{1111} - 2C_{1122} - 2C_{1221} + C_{2222}),\\
\Gamma_2 &= (B_{121} - B_{222})^2 - A_{11}C_{1221}\\
&\quad - A_{22}(C_{1111} - 2C_{1122} - 2C_{1221} + C_{2222}),\\
\Gamma_0 &= -A_{22}C_{2121}.
\end{aligned}$$

Again, band localization takes place when a real solution ν^* of eq. (7.35) exists.

Eq. (7.35) is a sextic with no odd powers that can be reduced to a cubic in the unknown ν^2. Its real roots can be determined explicitly following Tartaglia-Cardano's theory (valid for $\Gamma_6 \neq 0$). Two cases arise depending on the value of discriminant

$$\Delta = \frac{a^2}{4} + \frac{b^3}{27}, \tag{7.36}$$

where

$$a = -\frac{1}{3}\left(\frac{\Gamma_4}{\Gamma_6}\right)^2 + \frac{\Gamma_2}{\Gamma_6}, \qquad b = \frac{2}{27}\left(\frac{\Gamma_4}{\Gamma_6}\right)^3 - \frac{1}{3}\frac{\Gamma_2\Gamma_4}{\Gamma_6^2} + \frac{\Gamma_0}{\Gamma_6}.$$

When $\Delta \geq 0$, eq. (7.35) has only one real root, i.e.

$$\nu^2 = \sqrt[3]{-\frac{b}{2} + \sqrt{\Delta}} + \sqrt[3]{-\frac{b}{2} - \sqrt{\Delta}} - \frac{\Gamma_4}{3\Gamma_6}. \tag{7.37}$$

In the case $\Delta < 0$, eq. (7.35) has three real roots, namely

$$\nu_1^2 = 2\sqrt{-\frac{a}{3}}\cos\theta - \frac{\Gamma_4}{3\Gamma_6},$$

$$\nu_2^2 = 2\sqrt{-\frac{a}{3}}\cos\left(\frac{\theta + 2\pi}{3}\right) - \frac{\Gamma_4}{3\Gamma_6}, \quad \nu_3^2 = 2\sqrt{-\frac{a}{3}}\cos\left(\frac{\theta + 4\pi}{3}\right) - \frac{\Gamma_4}{3\Gamma_6},$$

where $\theta = \arctan\left(-2\sqrt{-\Delta}/b\right)$ $[\theta = \pi + \arctan\left(-2\sqrt{-\Delta}/b\right)]$ if $b \leq 0$ $[b > 0]$.

When $\Gamma_6 = 0$, eq. (7.35) becomes a biquadratic and the roots can be easily obtained.

For the general form of the free-energy employed in this work and homogeneous paths considered for the homogeneous actuators, the expressions of coefficients Γ_i are

$$\Gamma_6 = \frac{1}{\epsilon_0^2\bar{\epsilon}_r^2\lambda^4}\Big[d_2^2(-\bar{\gamma}_2^2+\bar{\gamma}_0(\bar{\gamma}_1\lambda^2+\bar{\gamma}_2(2+\lambda^4)))+\epsilon_0\bar{\epsilon}_r(\bar{\gamma}_0+\bar{\gamma}_1\lambda^2+\bar{\gamma}_2\lambda^4)\mu(\bar{\alpha_1}-\bar{\alpha_{-1}})\Big],$$

$$\begin{aligned}\Gamma_4 = \frac{1}{\epsilon_0^2\bar{\epsilon}_r^2\lambda^6}\Bigg\{ & d_2^2\lambda^2\Big[\bar{\gamma}_2(\bar{\gamma}_1\lambda^2+\bar{\gamma}_2(-4+3\lambda^4))+\bar{\gamma}_0(\bar{\gamma}_1\lambda^2(1+\lambda^4) \\ & +\bar{\gamma}_2(6+\lambda^8))\Big]+\epsilon_0\bar{\epsilon}_r\mu\Bigg[(\bar{\alpha}_1-\bar{\alpha}_{-1})\lambda^2\big(\bar{\gamma}_0+2\bar{\gamma}_0\lambda^4+\bar{\gamma}_1\lambda^2(2+\lambda^4) \\ & +\bar{\gamma}_2(1+\lambda^4+\lambda^8)\big)-2(-1+\lambda^4)^2(\bar{\gamma}_0+\bar{\gamma}_1\lambda^2+\bar{\gamma}_2\lambda^4)\left(\frac{\partial\bar{\alpha}_{-1}}{\partial I_2}-\frac{\partial\bar{\alpha}_1}{\partial I_1}\right)\Bigg]\Bigg\},\end{aligned}$$

$$\begin{aligned}\Gamma_2 = \frac{1}{\epsilon_0^2\bar{\epsilon}_r^2}\Bigg\{ & \frac{d_2^2(-\bar{\gamma}_1\lambda^2+\bar{\gamma}_2(-3+\lambda^4))^2}{\lambda^4} \\ & +(\bar{\gamma}_0+\bar{\gamma}_1\lambda^2+\bar{\gamma}_2\lambda^4)(\bar{\gamma}_2 d_2^2+(\bar{\alpha}_1-\bar{\alpha}_{-1})\epsilon_0\bar{\epsilon}_r\mu) \\ & -\frac{1}{\lambda^6}\big(\bar{\gamma}_2+\bar{\gamma}_1\lambda^2+\bar{\gamma}_0\lambda^4\big)\Bigg[d_2^2\lambda^2(-\bar{\gamma}_1\lambda^2+2\bar{\gamma}_2(-3+\lambda^4)) \\ & +\epsilon_0\bar{\epsilon}_r\mu\left((\bar{\alpha}_{-1}-\bar{\alpha}_1)(\lambda^2+\lambda^6)+2(-1+\lambda^4)^2\left(\frac{\partial\bar{\alpha}_{-1}}{\partial I_2}-\frac{\partial\bar{\alpha}_1}{\partial I_1}\right)\right)\Bigg]\Bigg\},\end{aligned}$$

and

$$\Gamma_0 = \frac{1}{\epsilon_0^2\bar{\epsilon}_r^2}(\bar{\gamma}_2+\bar{\gamma}_1\lambda^2+\bar{\gamma}_0\lambda^4)(d_2^2\bar{\gamma}_2+\epsilon_0\bar{\epsilon}_r\mu(\bar{\alpha}_1-\bar{\alpha}_2)).$$

As far as instability is concerned, the onset of band localization arises when one of the following conditions is satisfied: i) $\Gamma_6 = 0$, ii) $\Gamma_0 = 0$, and

iii) $\Delta = 0$. In the first case, the following relation between λ and $\bar{D}$ can be found

$$\bar{D} = \sqrt{\frac{-(\bar{\gamma_0} + \bar{\gamma_1}\lambda^2 + \bar{\gamma}_2\lambda^4)(\bar{\alpha}_1 - \bar{\alpha}_{-1})}{\bar{\gamma}_2^2 + \bar{\gamma}_0(\bar{\gamma}_1\lambda^2 + \bar{\gamma}_2(2+\lambda^4))}},$$

in the second case

$$\bar{D} = \sqrt{-\frac{\bar{\alpha}_1 - \bar{\alpha}_{-1}}{\bar{\gamma}_2}},$$

while the third case the expression is too involved and it will be not reported explicitly.

Results

An example of band-localization instability analysis for homogeneously deformed actuators is reported in Fig. 7.12 for an extended Gent free-energy function with set of parameters #1. In a) and b) the actuator is prestressed with a given nominal traction $\tilde{S}$, following a nonlinear electroelastic deformation described in Sect. 6.1.2. In c) and d) the specimen is prestretched at $\lambda = \lambda_{\text{pre}}$ and then actuated, as considered in the analysis of diffuse modes. In a), b), and d) long dashed portions of the loading path curves (bounded by red circles) denote ranges where band localization occurs. Even though in our analysis we can predict the onset of such instability and nothing can be said about the evolution of the band, we note that in electroelasticity there are stable homogeneous nonlinear deformations also beyond the theoretical emergence of the band, suggesting that the range of instability can be crossed in some way to reach again the stable path (the same applies to electroelastic deformations where the actuator deforms biaxially, computations not reported). Comparison with experiments is difficult as we are not aware of papers dealing with electroelastic band-localization instability. The following additional comments must be added to clarify the issue:

i) this type of instability is strongly dependent on the way the incremental problem is set. Polynomial (7.35) is obtained taking $\hat{\mathbf{d}}$ as the independent electric incremental variable, which means that physically we perturb the surface charge. Alternatively, if $\hat{\mathbf{e}}$ is chosen, and then a perturbation in the voltage is induced, the onset of the band along the same finite

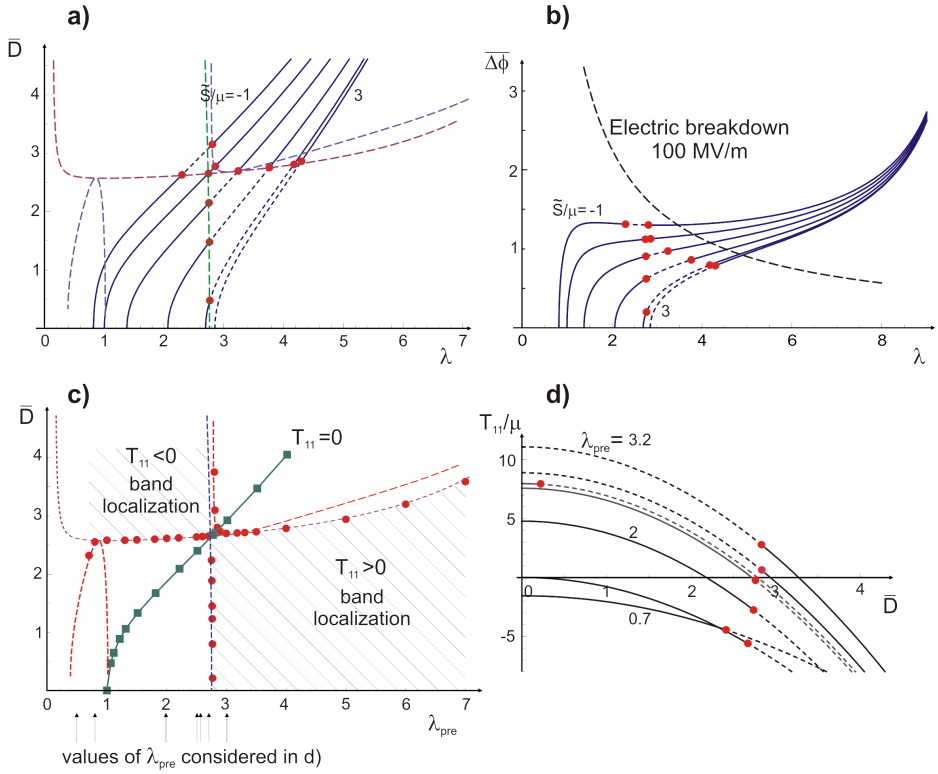

Figure 7.12: Band-localization instability analysis for an electrically actuated DE layer in plane strain (Gent material, set of parameter #1, see Table 5.1). a), b): plots for prestressed actuators with different $\tilde{S}/\mu$ (in ascending order $\tilde{S}/\mu = -1, 0, 1, 2, 2.8, 3$); dashed lines indicate ranges where instability occurs (bounded by red circles). c), d): results for actuators initially prestretched at $\lambda = \lambda_{\rm pre}$. In particular: c): instability region in the $\lambda_{\rm pre}$–$\bar{D}$ diagram; the line marked by green squares corresponds to $T_{11} = 0$ ('loss of tension' threshold: beyond this line the specimen is compressed; d) dimensionless longitudinal stress (T_{11}/μ) and localization ranges (indicated by dashed lines) in terms of electrical actuation $\bar{D}$. In a) and c) dashed coloured lines represent the analytical zones which delimit the boundary where instability occurs, i.e. $\Gamma_6 = 0$, $\Gamma_0 = 0$ and $\Delta = 0$.

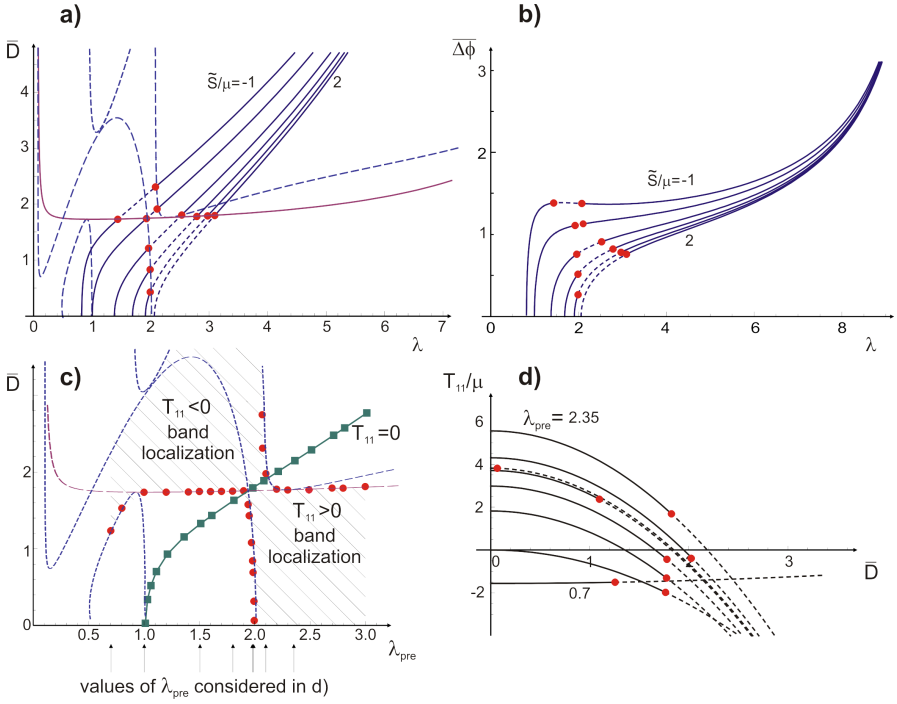

Figure 7.13: Band-localization instability analysis for an electrically actuated DE layer in plane strain (Gent material, set of parameter #2, see Table 5.1). a), b): plots for prestressed actuators with different $\tilde{S}/\mu$ (in ascending order $\tilde{S}/\mu = -1, 0, 1, 1.5, 1.8, 2$); dashed lines indicate ranges where instability occurs (bounded by red circles). c), d): results for actuators initially prestretched at $\lambda = \lambda_{\rm pre}$. In particular: c): instability region in the $\lambda_{\rm pre}$–$\bar{D}$ diagram; the line marked by green squares corresponds to $T_{11} = 0$ ('loss of tension' threshold: beyond this line the specimen is compressed; d) dimensionless longitudinal stress (T_{11}/μ) and localization ranges (indicated by dashed lines) in terms of electrical actuation $\bar{D}$. In a) and c) dashed coloured lines represent the analytical zones which delimit the boundary where instability occurs, i.e. $\Gamma_6 = 0$, $\Gamma_0 = 0$ and $\Delta = 0$.

deformation path, with the same free energy, is ruled out and the system remains stable at every stage of the electrical actuation (see the pertinent band-localization analysis in Appendix 10.4);

ii) the onset of localization is strongly dependent on the electrostriction. If it is absent, i.e. $\epsilon_r = \bar{\epsilon}_r$, any localization is predicted. Therefore, to detect the emergence of a band in an experiment, the electrostrictive properties of the specimen must be carefully measured and identified. We point out also that, as shown in Sect. 3.6, the Gent material model does not exhibit localization under pure mechanical loadings;

iii) a failure mode observed experimentally in DE actuators is electric breakdown, where the dielectric becomes conductive when the electric field inside the solid reaches a material-dependent threshold value, leading to a discharge between the electrodes. We argue that the electric breakdown can be induced by a band-localization instability. Indeed, at its onset, and for both fundamental paths, the band is always orthogonal to the direction of the electric field ($\nu \to \infty$, see Fig. 7.11b). Through relationships (7.32) we can estimate the incremental fields inside the band by fixing the amplitude ξ. Well, for $\tilde{S}/\mu = 0$ in Fig. 7.12 b) we have found that the increment of the electric field $\hat{\mathbf{e}}^{\mathrm{b}}$ inside the band is almost six times larger then that outside (i.e., $\hat{\mathbf{e}}^{\mathrm{o}}$) showing a strong localized behaviour of the incremental electric field. This can clearly cooperate with micromechanical issues to promote electric breakdown. In Fig. 7.12 b) the curve $\overline{\Delta\phi}(\lambda)$ for an electric breakdown of $\mathbf{e}_{EB} = 100$ MV/m (a typical value for acrylic elastomers) is sketched showing that localization may imply failure of the specimen.

Therefore, weather or not a band will develop in a real sample is something still uncertain that requires additional investigation, both experimentally and theoretically. For the latter aspect, it could be important to adopt a microelectromechanical model to follow the evolution of the band and check if the predicted shear bands are stable or unstable.

Coming back to the Fig. 7.12, for both fundamental paths it is clear that $\lambda \approx 2.76$ provides a theoretical critical threshold. As this limit depends strongly on the degree of electrostriction, for set #2 (Fig. 7.13) it can be appreciated that it falls to $\lambda \approx 1.97$. For prestretched actuators (parts c) and d)) similar considerations apply. In c), in addition to the re-

gions where localization is theoretically critical, the line where the electric actuation (represented by $\bar{D}$) induces a null longitudinal stress ($T_{11} = 0$, 'loss of tension' threshold) is also reported, as typical devices must operate under a tensile stress state to avoid the buckling instability. Therefore, only points at the right-hand side of the line $T_{11} = 0$ correspond to meaningful configurations for real actuators. The arrows below the abscissa axis in part c) (ranging from $\lambda_{\text{pre}} = 0.7$ to $\lambda_{\text{pre}} = 3.2$) indicate the loading path reported in part d) that is similar to Fig. 6.4 a), but with the data of the localization analysis for each λ_{pre} added.

As already reminded, Fig. 7.13 is very similar to Fig. 7.12 but calculated for set #2.

As a conclusion for this part, we point out that a first analysis of band-localization instability has been developed. We suppose that this instability may trigger electric breakdown and failure of actual prestretched/prestressed specimens. However, further investigations are needed both theoretically and experimentally to clarify how localization may develop within a DE actuator under various electromechanical loading conditions.

Chapter 8

Composite Dielectric Elastomers

Investigation of the behaviour of two-phase rank-one laminates is made. In particular, the performance improvement of DE composites in terms of actuaction with respect to the homogeneous case is analysed.

8.1 Modelling of Layered Composites

Composite materials represent a promising way to improve the electromechanical coupling in soft dielectric elastomers and then the actuation performance of DE actuators [55]. The ideal recipe consists in mixing a stiff and high conductive phase (for instance polyanilines) with a soft matrix (typically made up of silicone or acrylate elastomer). The microstructure of the composite can play a fundamental role, even though its control is not easy during the processing [51].

While for general composites the overall performance can only be estimated through the formulation of bounds [38], for a layered solid the solution can be expressed in closed form as a function of phase properties. For this reason, we focus on this class of composites; in particular, rank-one bi-layered soft dielectrics under plane-strain conditions are analysed. The two phases, a and b, have volume fractions $c^a = h^{0a}/\left(h^{0a} + h^{0b}\right)$ and $c^b = 1 - c^a$ respectively, where h^{0a} and h^{0b} represent the relevant thick-

nesses in the reference configuration $\mathcal{B}^0$ (see Fig. 8.1). The actuation can be achieved by either imposing the voltage or the charge. The latter method has been recently exploited by Keplinger et al. [27].

Actuation properties of samples made up of this class of simple composites have been also investigated (see deBotton et al. [11], Tian et al. [46]), however our goal is to study in detail the evolution of the microstructure under large deformations and to highlight instability mechanisms typical of the composite, possibly not observed in a homogeneous material. Although this approach can also be applied to higher-rank layered composites, here only results for rank-one solids will be provided.

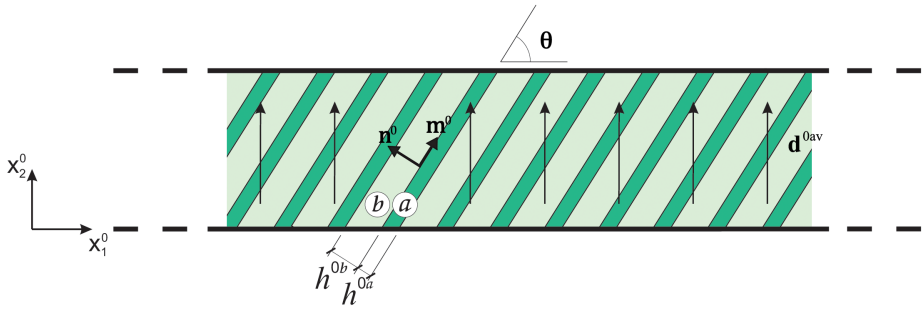

Figure 8.1: Biphasic layered dielectric actuator deformed under the effect of a constant nominal electric displacement field $\mathbf{d}^{0\mathrm{av}}$.

8.2 Modelling Layered DE Composites with $\mathbf{d}^{0\mathrm{av}}$ as Independent Variable

In this first formulation, we consider as independent quantity the macroscopic deformation gradient $\mathbf{F}^{\mathrm{av}}$ and the reference electric displacement $\mathbf{d}^{0\,\mathrm{av}}$, similarly to Sect. 4.5. Under the assumption of a homogeneous response in each phase, $\mathbf{F}^{\mathrm{av}}$ and $\mathbf{d}^{0\,\mathrm{av}}$ are the weighted sum of those in each

phase, namely ([47], [11], [2])

$$\mathbf{F}^{\mathrm{av}} = c^a\mathbf{F}^a + c^b\mathbf{F}^b, \qquad \mathbf{d}^{0\mathrm{av}} = c^a\mathbf{d}^{0a} + c^b\mathbf{d}^{0b}. \tag{8.1}$$

On the other hand, for a composite medium, the b.v.p. formulated in (4.17) and (4.18) is completed by the following boundary conditions across the interface $\partial\mathcal{B}^0_{int}$ between phases (see Fig. 8.1):

$$[\![\mathbf{v}^0]\!] = \mathbf{0}, \quad [\![\mathbf{S}]\!]\mathbf{n}^0 = \mathbf{0}, \quad [\![\mathbf{d}^0]\!]\cdot\mathbf{n}^0 = 0, \quad \mathbf{n}^0\times[\![\mathbf{e}^0]\!] = \mathbf{0} \ \ (\text{on } \partial\mathcal{B}^0_{int}). \tag{8.2}$$

Interface continuity $(8.2)_3$ requires

$$\mathbf{d}^{0a} - \mathbf{d}^{0b} = \beta\mathbf{m}^0, \tag{8.3}$$

where β is a real parameter and $\mathbf{m}^0$ is a unit vector aligned with the layers. It follows from eqns. $(8.1)_2$ and (8.3) that

$$\mathbf{d}^{0a} = \mathbf{d}^{0\mathrm{av}} + c^b\beta\mathbf{m}^0, \quad \mathbf{d}^{0b} = \mathbf{d}^{0\mathrm{av}} - c^a\beta\mathbf{m}^0.$$

Similarly, interface compatibility, $[\![\mathbf{F}]\!]\mathbf{m}^0 = \mathbf{0}$, provides

$$\mathbf{F}^a = \mathbf{F}^{\mathrm{av}}\left(\mathbf{I} + \alpha\, c^b\mathbf{m}^0\otimes\mathbf{n}^0\right), \quad \mathbf{F}^b = \mathbf{F}^{\mathrm{av}}\left(\mathbf{I} - \alpha\, c^a\mathbf{m}^0\otimes\mathbf{n}^0\right),$$

where α is a real parameter. Quantities α and β are obtained enforcing $(8.2)_{2,4}$. In the present context, the latter can be also written $[\![\mathbf{e}^0]\!]\cdot\mathbf{m}^0 = 0$. As both phases are described by an extended Mooney-Rivlin free energy (4.37)-(3.46) with no electrostriction ($\bar\gamma^i_0 = \bar\gamma^i_2 = 0$, $\bar\gamma^i_1 = 1$, $\epsilon^i = \epsilon_0\bar\epsilon^i_r$, $i = a, b$) their expressions are

$$\alpha = \frac{\mu^b - \mu^a}{c^a\mu^b + c^b\mu^a}\frac{\mathbf{F}^{\mathrm{av}}\mathbf{n}^0\cdot\mathbf{F}^{\mathrm{av}}\mathbf{m}^0}{\mathbf{F}^{\mathrm{av}}\mathbf{m}^0\cdot\mathbf{F}^{\mathrm{av}}\mathbf{m}^0}, \tag{8.4}$$

$$\beta = \frac{\epsilon^a - \epsilon^b}{c^a\epsilon^a + c^b\epsilon^b}\frac{\mathbf{F}^{\mathrm{av}}\mathbf{d}^{\,0\ \mathrm{av}}\cdot\mathbf{F}^{\mathrm{av}}\mathbf{m}^0}{\mathbf{F}^{\mathrm{av}}\mathbf{m}^0\cdot\mathbf{F}^{\mathrm{av}}\mathbf{m}^0} - \alpha\mathbf{d}^{\,0\ \mathrm{av}}\cdot\mathbf{n}^0.$$

While $(8.4)_1$ has been found in [2], $(8.4)_2$ is alternative to that obtained in the same paper and is new.

The jump in hydrostatic pressure across each interface is obtained by multiplying the traction continuity condition $(8.2)_2$ with vector $(\mathbf{F}^{\mathrm{av}})^{-T}$, yielding

$$p^b - p^a = \left[\frac{\epsilon^a - \epsilon^b}{\epsilon^a \epsilon^b}\left(\mathbf{d}^{0\mathrm{av}} \cdot \mathbf{n}^0\right)^2 + \mu^b - \mu^a\right] \frac{1}{(\mathbf{F}^{\mathrm{av}})^{-T}\mathbf{n}^0 \cdot (\mathbf{F}^{\mathrm{av}})^{-T}\mathbf{n}^0}. \quad (8.5)$$

The macroscopic free energy of the composite is given by

$$W^{\mathrm{av}} = c^a W^a(\mathbf{F}^a, \mathbf{d}^{0a}) + c^b W^b(\mathbf{F}^b, \mathbf{d}^{0b}) \quad (8.6)$$

and the macroscopic total stress and electric field can be obtained from W^{av} via the constitutive equations as

$$\mathbf{S}^{\mathrm{av}} = \frac{\partial W^{\mathrm{av}}}{\partial \mathbf{F}^{\mathrm{av}}} - p^{\mathrm{av}}\,(\mathbf{F}^{\mathrm{av}})^{-T}, \quad \mathbf{e}^{0\mathrm{av}} = \frac{\partial W^{\mathrm{av}}}{\partial \mathbf{d}^{0\mathrm{av}}}. \quad (8.7)$$

The response of a planar dielectric elastomer actuator made up of a bilayered composite is analysed: the specimen is subjected to a transverse lagrangian electric displacement field $\mathbf{d}^{0\mathrm{av}} = d^{0\mathrm{av}}\mathbf{i}_2$; we assume a homogeneous overall deformation of plain strain and $S_{22}^{\mathrm{av}} = S_{11}^{\mathrm{av}} = 0$. The solution depends on properties of phases and on the geometry (lamination angle θ).

8.2.1 Incremental Problem

Assuming that the constitutive equations (8.7) can be linearized, the incremental total first Piola-Kirchhoff is

$$\dot{\mathbf{S}}^{\mathrm{av}} = -\dot{p}(\mathbf{F}^{\mathrm{av}})^{-T} + p(\mathbf{F}^{\mathrm{av}})^{-T}(\dot{\mathbf{F}}^{\mathrm{av}})^T(\mathbf{F}^{\mathrm{av}})^{-T} + \mathbb{C}^{0\mathrm{av}}\dot{\mathbf{F}}^{\mathrm{av}} + \mathbb{B}^{0\mathrm{av}}\dot{\mathbf{d}}^{0\mathrm{av}}$$

and the electric field

$$\dot{\mathbf{e}}^{0\mathrm{av}} = \mathbb{B}^{0\mathrm{av}T^*}\dot{\mathbf{F}}^{\mathrm{av}} + \mathbb{A}^{0\mathrm{av}}\dot{\mathbf{d}}^{0\mathrm{av}},$$

where $(B^{0\mathrm{av}T^*})_{MiJ} = B^{0\mathrm{av}}_{iJM}$ (see eq. (4.53))and the electroelastic moduli tensors $\mathbb{C}^{0\mathrm{av}}$, $\mathbb{B}^{0\mathrm{av}}$ and $\mathbb{A}^{0\mathrm{av}}$ are given in components by

$$C^{0\mathrm{av}}_{iJkL} = \frac{\partial^2 W^{\mathrm{av}}}{\partial F^{\mathrm{av}}_{iJ}\partial F^{\mathrm{av}}_{kL}}, \quad B^{0\mathrm{av}}_{iJM} = \frac{\partial^2 W^{\mathrm{av}}}{\partial F^{\mathrm{av}}_{iJ}\partial d^{0\mathrm{av}}_{M}}, \quad A^{0\mathrm{av}}_{MN} = \frac{\partial^2 W^{\mathrm{av}}}{\partial d^{0\mathrm{av}}_{M}\partial d^{0\mathrm{av}}_{N}},$$

which imply the following symmetries

$$C^{0\mathrm{av}}_{iJkL} = C^{0\mathrm{av}}_{kLiJ}, \quad A^{0\mathrm{av}}_{MN} = A^{0\mathrm{av}}_{NM}.$$

The components of the updated constitutive tensors are given (specialized keeping in mind the incompressibility constraint) by (see eq. (4.63))

$$\begin{aligned} C^{\mathrm{av}}_{iqkp} &= C^{0\mathrm{av}}_{iJkL} F^{\mathrm{av}}_{pL} F^{\mathrm{av}}_{qJ}, \\ B^{\mathrm{av}}_{iqa} &= B^{0\mathrm{av}}_{iJM} F^{\mathrm{av}}_{qJ} (F^{\mathrm{av}})^{-1}_{Ma}, \\ A^{\mathrm{av}}_{ab} &= A^{0\mathrm{av}}_{MN} (F^{\mathrm{av}})^{-1}_{Ma} (F^{\mathrm{av}})^{-1}_{Nb}. \end{aligned} \tag{8.8}$$

8.2.2 Performance Evaluation

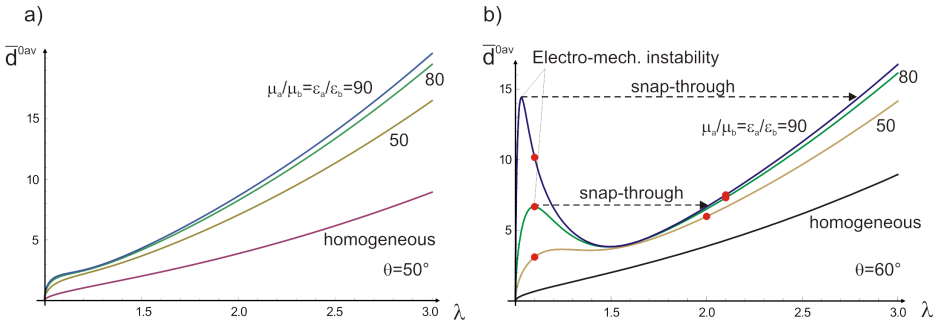

Figure 8.2: Different loading paths for a bilayer actuator ($\mu^a/\mu^b = \epsilon^a/\epsilon^b = 1, 50, 80, 90$, $c_b = 0.9$) deformed under the action of an electric displacement field along x_2 (extended Mooney-Rivlin free energy). a) $\theta = 50°$; b) $\theta = 60°$.

In Fig. 8.2 some typical loading paths are reported in the λ–$\bar{d}^{0\mathrm{av}}$ space (where $\bar{d}^{0\mathrm{av}} = d^{0\mathrm{av}}/\sqrt{\epsilon_0 \epsilon_r^b \mu^b}$) for $c_b = 0.9$ and $\mu^a/\mu^b = \epsilon^a/\epsilon^b = 1, 50, 80, 90$. The value of the angle inclination is $\theta = 50°$ in part a), while $\theta = 60°$ in part b). We note, comparing a) and b), that the overall response is very sensitive to the layering angle. In part b), for high values of the contrast parameter $\mu^a/\mu^b = \epsilon^a/\epsilon^b$ a peak at low stretch in the curve occurs, indicating the possibility of a snap-through instability for the actuator.

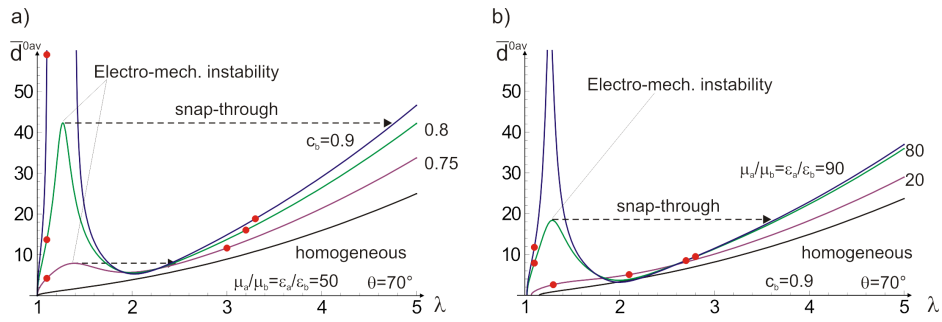

Figure 8.3: Different loading paths for a bilayer actuator deformed under the action of an electric displacement field along x_2, in a) ($\mu^a/\mu^b = \epsilon^a/\epsilon^b = 50$, $c_b = 0.75, 0.8, 0.9$, $\theta = 70°$), with null prestress ($\tilde{S} = 0$), in b) ($\mu^a/\mu^b = \epsilon^a/\epsilon^b = 20, 80, 90$, $c_b = 0.9$, $\theta = 70°$), with prestress $\tilde{S} = 0.5$ (extended Mooney-Rivlin free energy).

In Fig. 8.3 (a), loading paths, with the same electromechanical parameters ($\mu^a/\mu^b = \epsilon^a/\epsilon^b = 50$) and the same angle $\theta = 50°$, are presented in the λ–$\bar{d}^{0\mathrm{av}}$ space, varying the volume fraction c_b: it can be noted that for higher value of c_b, there is the chance of snap-trough instability. Fig. 8.3 (b), loading path with a low prestress $\tilde{S} = 0.5$ are reported, showing modified behaviour, changing the electromechanical parameters: for high permettivity and stiffness, snap-throught instability and stiffening effect are admissible. Points are pointed out in Figs. 8.2 and 8.3 in some loading paths marking the occurrence of band-localization instability. For a layered composite, this threshold is associated with large-wavelength bifurcations (see Bertoldi and Gei [2] and Rudykh and deBotton [41]) and can be analysed using the procedure outlined in Sect. 7.4 employing the incremental moduli (8.8). In this case the polynomial is complete.

It is important to remark that the composite configurations considered in Figs. 8.2 and 8.3 are not 'optimal', in fact the overall response is worse than that of a homogeneous actuator composed uniquely of phase b (the matrix). The goal was to show that for some configurations a snap-through instability becomes available (to conceive release-actuated system) and localization may occur at quite low stretching, leading to a possible early

failure of the specimen.

The choice of the electric displacement field $\mathbf{d}^{0\mathrm{av}}$ as the independent variable for the modelling poses some questions regarding the effective application of the results to real actuators. It may help to recall that $\mathbf{d}$ is controlled by charges, while $\mathbf{e}$ is controlled by voltage. Therefore, it seems more meaningful to adopt the electric field as an independent descriptor as actual devices are driven by an external voltage applied through electrodes. However, some recent works (see for instance Keplinger et al. [27]) have shown how to activate a DE actuator in charge-controlled mode, adapting a procedure pioneered by Roentgen, who considered a layer-shaped specimen on which charges were sprayed on the surface through needle combs at high voltage. The advantage is that, for 3d actuators, electromechanical (pull-in) instability is prevented and therefore the severe limitations imposed to typical actuators controlled by voltage are ruled out.

In Fig. 8.4, the microstructure of a multilayered rank-one composite is highlighted: the stiffening effect can be explained regarding the evolution of the true electric field $\mathbf{e}^{\mathrm{av}}$, for different growing values of stretch ($\lambda = 1.1, 1.8, 3$). In addition, it is observed that increasing λ, true electric field $\mathbf{e}^{\mathrm{av}}$ aligns to the reference electric displacement $\mathbf{d}^{0\mathrm{av}}$.

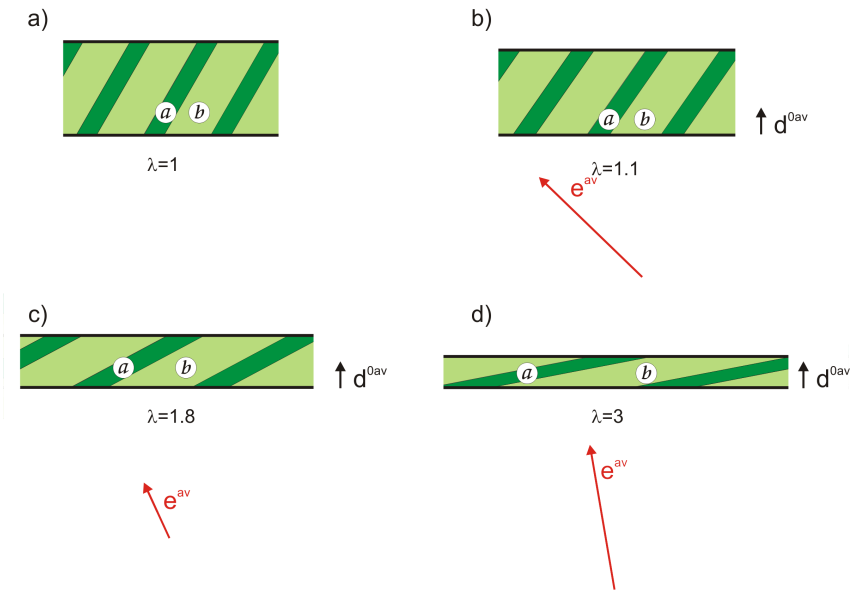

Figure 8.4: Microstructure evolution ($\mu^a/\mu^b = \epsilon^a/\epsilon^b = 90$, $\theta = 60°$, $c_b = 0.9$) and intensity of electric fields. Starting from the undeformed configuration a), Fig. b-c-d) show the configuration development increasing λ, clarifying the stiffening effect outcome.

8.3 Modelling Layered DE Composites with $\mathbf{e}^{0\mathbf{av}}$ as Independent Variable

In this formulation, we consider as independent quantity the deformation gradient $\mathbf{F}^{\mathrm{av}}$ and the reference electric field $\mathbf{e}^{0\,\mathrm{av}}$, as seen in Sect. 4.6. The macroscopic deformation gradient has the form seen before, in $(8.1)_1$, and the average lagrangian electric field is:

$$\mathbf{e}^{0\,\mathrm{av}} = c^a \mathbf{e}^{0\,a} + c^b \mathbf{e}^{0\,b}. \tag{8.9}$$

The boundary conditions are the same presented in (8.2). Interface continuity $(8.2)_4$ requires

$$\mathbf{e}^{0a} - \mathbf{e}^{0b} = \tilde{\beta}\mathbf{n}^0, \tag{8.10}$$

where $\tilde{\beta}$ is a real parameter and $\mathbf{n}^0$ is a unit vector orthogonal to the layers. It follows from eqs. $(8.9)_2$ and (8.10) that

$$\mathbf{e}^{0a} = \mathbf{e}^{0\mathrm{av}} + c^b\tilde{\beta}\mathbf{m}^0, \;\; \mathbf{e}^{0b} = \mathbf{e}^{0\mathrm{av}} - c^a\tilde{\beta}\mathbf{m}^0.$$

The parameter $\tilde{\beta}$ is obtained enforcing $(8.2)_{2,3}$ and its expression is

$$\tilde{\beta} = \frac{\epsilon^b - \epsilon^a}{c^b\epsilon^a + c^a\epsilon^b}\frac{\mathbf{F}^{\mathrm{av}-T}\mathbf{e}^{0\ \mathrm{av}}\cdot\mathbf{F}^{\mathrm{av}-T}\mathbf{n}^0}{\mathbf{F}^{\mathrm{av}-T}\mathbf{n}^0\cdot\mathbf{F}^{\mathrm{av}-T}\mathbf{n}^0} + \alpha\mathbf{e}^{0\ \mathrm{av}}\cdot\mathbf{m}^0,$$

while α is given again by $(8.4)_1$.
The jump in hydrostatic pressure across each interface is obtained, as above (8.5), by multiplying the traction continuity condition $(8.2)_2$ with vector $(\mathbf{F}^{\mathrm{av}})^{-T}$, yielding

$$\begin{aligned} p^b - p^a = \Bigg\{ & \epsilon^b\left[(\mathbf{F}^{\mathrm{av}})^{-T}\left(\mathbf{e}^{0\mathrm{av}} + c^a(\alpha\mathbf{e}^{0\mathrm{av}}\cdot\mathbf{m}^0 - \tilde{\beta})\mathbf{n}^0\right)\cdot(\mathbf{F}^{\mathrm{av}})^{-T}\mathbf{n}^0\right]^2 \\ & - \epsilon^a\left[(\mathbf{F}^{\mathrm{av}})^{-T}\left(\mathbf{e}^{0\mathrm{av}} - c^b(\alpha\mathbf{e}^{0\mathrm{av}}\cdot\mathbf{m}^0 - \tilde{\beta})\mathbf{n}^0\right)\cdot(\mathbf{F}^{\mathrm{av}})^{-T}\mathbf{n}^0\right]^2 \\ & + \mu^b - \mu^a\Bigg\}\frac{1}{(\mathbf{F}^{\mathrm{av}})^{-T}\mathbf{n}^0\cdot(\mathbf{F}^{\mathrm{av}})^{-T}\mathbf{n}^0}. \end{aligned} \tag{8.11}$$

The macroscopic free energy of the composite is given by

$$H^{\mathrm{av}} = c^a H^a(\mathbf{F}^a, \mathbf{e}^{0a}) + c^b H^b(\mathbf{F}^b, \mathbf{e}^{0b})$$

and the macroscopic total stress and electric field can be obtained from H^{av} via the constitutive equations as

$$\mathbf{S}^{\mathrm{av}} = \frac{\partial H^{\mathrm{av}}}{\partial\mathbf{F}^{\mathrm{av}}} - p^{\mathrm{av}}\,(\mathbf{F}^{\mathrm{av}})^{-T}, \quad \mathbf{d}^{0\mathrm{av}} = -\frac{\partial H^{\mathrm{av}}}{\partial\mathbf{e}^{0\mathrm{av}}}. \tag{8.12}$$

The response of a planar dielectric elastomer actuator made up of a bi-layered composite is analysed: the specimen is subjected to a transverse lagrangian electric field field $\mathbf{e}^{0\mathrm{av}} = e^{0\mathrm{av}}\mathbf{i}_2$; we assume a homogeneous overall deformation of plain strain and $S_{22}^{\mathrm{av}} = S_{11}^{\mathrm{av}} = 0$. The solution again depends on properties of phases and on the geometry (lamination angle θ).

8.3.1 Incremental Problem

Assuming that the constitutive equation (8.12) can be linearized, it turns out that the incremental Piola-Kirchhoff is

$$\dot{\mathbf{S}}^{\mathrm{av}} = -\dot{p}(\mathbf{F}^{\mathrm{av}})^{-T} + p((\mathbf{F}^{\mathrm{av}})^{-T}(\dot{\mathbf{F}}^{\mathrm{av}})^{T}(\mathbf{F}^{\mathrm{av}})^{-T}) + \mathbb{C}^{0,H\mathrm{av}}\dot{\mathbf{F}}^{\mathrm{av}} + \mathbb{B}^{0,H\mathrm{av}}\dot{\mathbf{e}}^{0\mathrm{av}}$$

and the electric displacement field

$$\dot{\mathbf{d}}^{0\mathrm{av}} = \mathbb{B}^{0,H\mathrm{av}T^*}\dot{\mathbf{F}}^{\mathrm{av}} + \mathbb{A}^{0,H\mathrm{av}}\dot{\mathbf{e}}^{0\mathrm{av}},$$

where $(B^{0,H\mathrm{av}T^*})_{MiJ} = B_{iJM}^{0,H\mathrm{av}}$ (see eq. (4.68)) and the electroelastic moduli tensors $\mathbb{C}^{0,H\mathrm{av}}$, $\mathbb{B}^{0,H\mathrm{av}}$ and $\mathbb{A}^{0,H\mathrm{av}}$ are given (eq. (4.72)) in components by

$$C_{iJkL}^{0,H\mathrm{av}} = \frac{\partial^2 H^{\mathrm{av}}}{\partial F_{iJ}^{\mathrm{av}}\partial F_{kL}^{\mathrm{av}}}, \quad B_{iJM}^{0,H\mathrm{av}} = -\frac{\partial^2 H^{\mathrm{av}}}{\partial F_{iJ}^{\mathrm{av}}\partial e_M^{0\mathrm{av}}}, \quad A_{MN}^{0,H\mathrm{av}} = -\frac{\partial^2 H^{\mathrm{av}}}{\partial e_M^{0\mathrm{av}}\partial e_N^{0\mathrm{av}}},$$

which imply the following symmetries

$$C_{iJkL}^{0,H\mathrm{av}} = C_{kLiJ}^{0,H\mathrm{av}}, \quad A_{MN}^{0,H\mathrm{av}} = A_{NM}^{0,H\mathrm{av}}.$$

The component of the updated constitutive tensors are

$$\begin{aligned} C_{iqkp}^{H\mathrm{av}} &= C_{iJkL}^{0,H\mathrm{av}}F_{pL}^{\mathrm{av}}F_{qJ}^{\mathrm{av}}, \\ B_{iqa}^{H\mathrm{av}} &= B_{iJM}^{0,H\mathrm{av}}F_{qJ}^{\mathrm{av}}F_{aM}^{\mathrm{av}}, \\ A_{ab}^{H\mathrm{av}} &= A_{MN}^{0,H\mathrm{av}}F_{aM}^{\mathrm{av}}F_{bN}^{\mathrm{av}}. \end{aligned} \tag{8.13}$$

8.3.2 Performance Evolution

Results calculated assuming $\mathbf{e}^{0av}$ as the independent electrical quantity for the composite are reported in this section. As previously anticipated, the advantage of this formulation is that the electric field derives directly from the voltage $\Delta\phi$ applied to the flexible electrodes, as $\mathbf{e}^{0av} = \Delta\phi/h^0$.

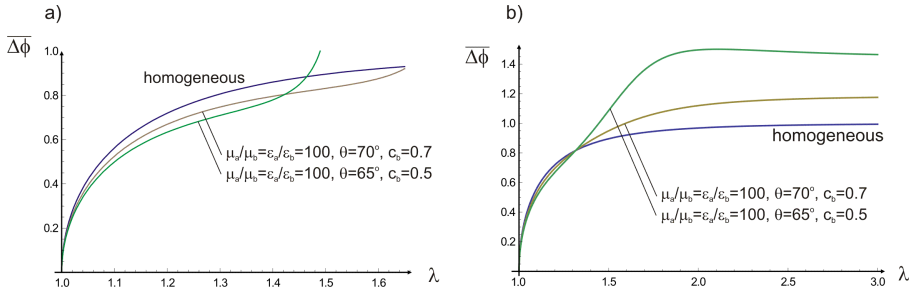

Figure 8.5: Comparison between the actuation performance of two types of layered composites and that of a homogeneous specimen as a function of the voltage applied to electrodes (extended Mooney-Rivlin free energy). a) low deformation range ($1 < \lambda < 1.7$); b) $1 < \lambda < 3$.

In Fig. 8.5, the overall behaviour of a composite with imposed voltage $\Delta\phi$ (in the plane λ–$\overline{\Delta\phi}$, where $\overline{\Delta\phi} = \Delta\phi\sqrt{\epsilon^b/\mu^b}/h^0$) is reported for $S_{11}^{\text{av}} = S_{22}^{\text{av}} = 0$. The geometrical/mechanical parameters (see the figure) are in the range where the performance of heterogeneous actuators is improved compared to the homogeneous case, at least for $\lambda < 1.5$ (part a of the figure). At higher stretches the composite behaves worse, i.e., a higher voltage is needed to reach the same deformation (part b). In the range $1 < \lambda < 1.5$, the actuation enhancement of the rank-one layered device is remarkable, as shown in plots displayed in Fig. 8.6. The improvement is studied in terms of stiffness and permittivity ratio (part a), layer inclination (part b), and matrix volume fraction (part c). In all cases, the dimensionless index

$$M = \frac{\log \lambda_{comp} - \log \lambda_{hom}}{\log \lambda_{hom}}$$

is considered, where λ_{comp} and λ_{hom} identify longitudinal stretches for the composite and for the homogeneous specimen, respectively.

It is found that the higher the stiffness/permittivity ratio, the higher is the enhancement of the performance, even though the advantage becomes quite localized around $\overline{\Delta\phi} \approx 0.8$; the optimal layering angle lies within the range $50° < \theta < 75°$, while, still for $1 < \lambda < 1.5$, a higher volume fraction of the stiff phase will improve the actuation strain of the composite.

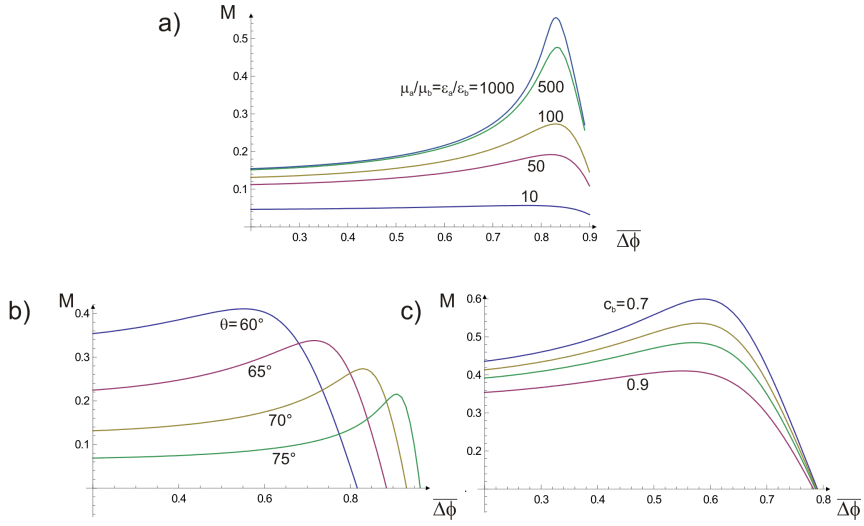

Figure 8.6: Performance improvement of a rank-one layered composite actuator compared to that of homogeneous specimen (extended Mooney-Rivlin free energy) under plane strain deformation in the range $1 < \lambda < 1.5$. a) stiffness and permittivity ratio ($c_b = 0.9$, $\theta = 70°$, and $\mu_a/\mu_b = \epsilon_a/\epsilon_b = 10, 50, 100, 500, 100$); b) layer inclination ($\mu_a/\mu_b = 100$, $c_b = 0.9$, $\theta = 60°, 65°, 70°, 75°$); c) matrix volume fraction ($\mu_a/\mu_b = 100$, $\theta = 60°$ and $c_b = 0.7, 0.8, 0.85, 0.9$).

In Fig. 8.7 and 8.8, the ratios $\mu_a/\mu_b = \epsilon_a/\epsilon_b$ are taken to be the same (this choice is consistent with real materials) and we can observe that the improvement is higher for higher $\mu_a/\mu_b = \epsilon_a/\epsilon_b$ ratios and for angles greater than 50° (the best is around $60° - 70°$). In particular for

$\mu_a/\mu_b = \epsilon_a/\epsilon_b = 100$ there is a strong stiffening effect and the enhanced behaviour lies in the range $(1 < \lambda < 1.6)$.

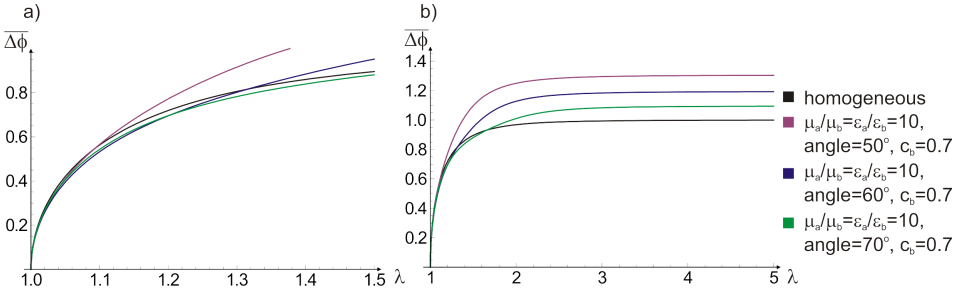

Figure 8.7: Comparison between the actuation performance of three types of layered composites whit the same electromechanical properties ($\mu_a/\mu_b = \epsilon_a/\epsilon_b = 10$), equal volume fraction $c_b = 0.7$, but having different inclination angles, and that of a homogeneous specimen as a function of the voltage applied to electrodes (extended Mooney-Rivlin free energy).

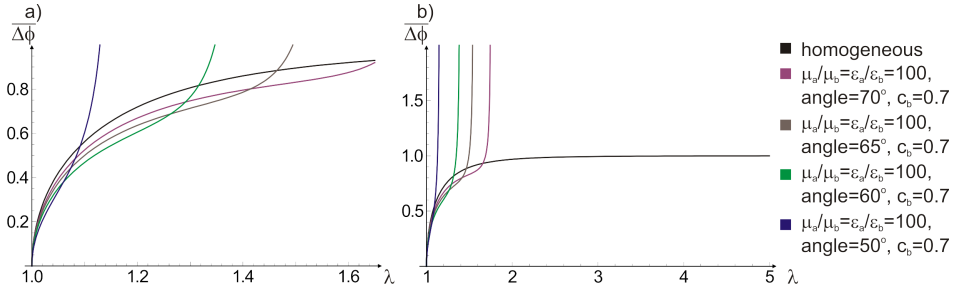

Figure 8.8: Comparison between the actuation performance of four types of layered composites whit the same electromechanical properties ($\mu_a/\mu_b = \epsilon_a/\epsilon_b = 100$), equal volume fraction $c_b = 0.7$, but having different inclination angles, and that of a homogeneous specimen as a function of the voltage applied to electrodes (extended Mooney-Rivlin free energy). The greater the angle, the greater the range of improvement.

In Fig. 8.9, it can be noted that peaks in the curves are present, corre-

sponding to points of electromechanical instability. Then, also for applied $\mathbf{e}^{0\mathrm{av}}$, it is possible to conceive actuators with new instabilities compared to the behaviour of homogeneous specimen.

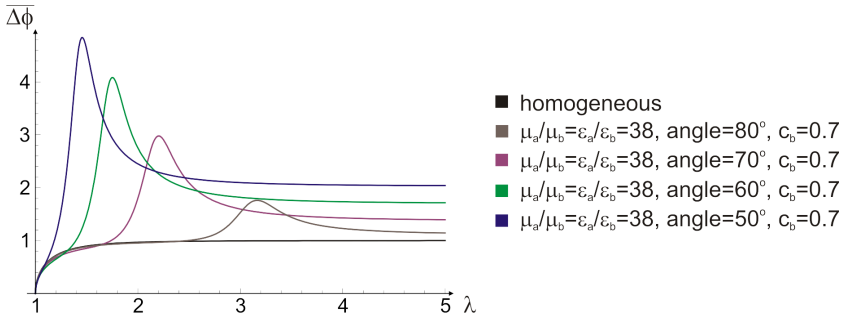

Figure 8.9: Comparison between the actuation performance of four types of layered composites which the same electromechanical properties ($\mu_a/\mu_b = \epsilon_a/\epsilon_b = 38$), equal volume fraction $c_b = 0.7$, but having different inclination angles, and that of a homogeneous specimen as a function of the voltage applied to electrodes (extended Mooney-Rivlin free energy).

In Fig. 8.10 some optimal configurations are considered, putting in evidence that band localization (see Sect. 10.4) may occur for some particular choices of the mechanical/geometrical parameters.

Finally, in Fig. 8.11 (as above 8.4) the microstructure of a multilayered rank-one composite is considered, noting that, increasing λ, the true electric displacement $\mathbf{d}^{\mathrm{av}}$ aligns to the reference electric field $\mathbf{e}^{0\mathrm{av}}$.

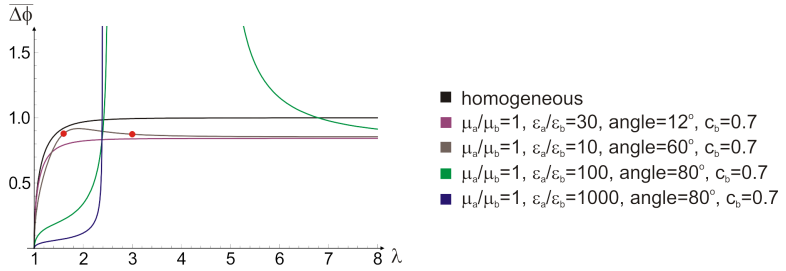

Figure 8.10: Some optimal configurations, in terms of actuation, are reported. At the same stiffness ratio ($\mu_a/\mu_b = 1$) and volume fraction ($c_b = 0.7$), for low permittivity ratio and little angle ($\epsilon_a/\epsilon_b = 10, 30$, $\theta = 12, 60°$), an amelioration is noted, even if in one case ($\epsilon_a/\epsilon_b = 10$, $\theta = 60°$) band-localization occurs at low stretch. In the other cases ($\epsilon_a/\epsilon_b = 100, 1000$, $\theta = 80°$), a remarkable stiffening effect is deduced at approximately $\lambda \approx 2.4$.

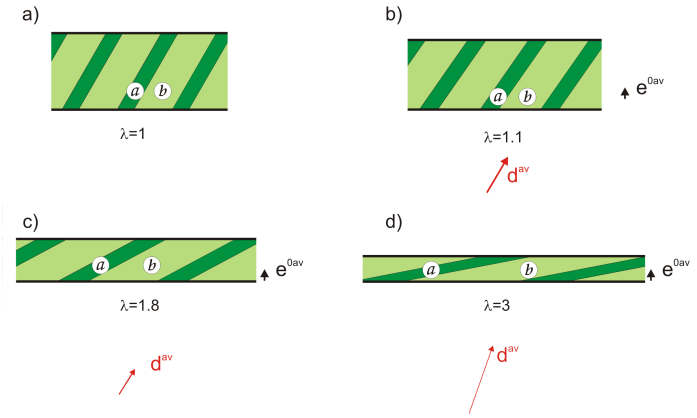

Figure 8.11: Microstructure evolution ($\mu^a/\mu^b = \epsilon^a/\epsilon^b = 90$, $\theta = 60°$, $c_b = 0.9$) and intensity of electric displacement fields. Starting from the undeformed configuration a), Fig. b-c-d) show the configuration development increasing λ, clarifying the stiffening effect outcome.

Chapter 9

Conclusions

In this work, instabilities in prestressed/prestretched dielectric elastomer actuators (DEAs) have been investigated for specimens deforming under plane-strain conditions.

In particular, after having recalled the fundamentals of the theory of elastic dielectrics at finite strain and defined in detail the incremental electroelastic boundary-value problem, the phenomenon of electrostriction (namely, the dependency of the permittivity on the deformation) has been modelled using the theory of invariants for isotropic electroelastic solids. The resulting unknown constants were obtained interpolating experimental data available for a typical acrylic elastomer.

We have shown that electrostriction strongly affects diffuse-sinusoidal mode instabilities in DEAs (such modes comprise both surface instabilities and Euler-like modes, the latter being extensively exploited in buckling-like actuators). Moreover, electrostriction may trigger band-localization instability, that has been thoroughly investigated. In plane strain, the critical condition corresponds to the emergence of real solutions of a bicubic equation, whose roots can be obtained by analytically following Tartaglia-Cardano's theory.

In the second part of the work, rank-one layered dielectric composite actuators, whose phases have constant permittivity, are studied in detail,

with particular attention to layouts that are able to display a better performance with respect to homogeneous devices. The behaviour of layered composites has been presented in terms of the two possible independent average electric quantities: electric displacement $\mathbf{d}^{0\mathrm{av}}$ and electric field $\mathbf{e}^{0\mathrm{av}}$, that can be selected by acting on the charge and the voltage, respectively.

We have also observed that a layered composite may display an electromechanical instability, which can be exploited to induce snap-through mechanisms useful in conceiving and realizing release-actuated transducers. On the other hand, the analyses of band localization show that this instability may limit the range of applicability of such systems in terms of maximum longitudinal stretch. Possible improvements of the actuation performance of layered dielectric composite actuators may be obtained by employing rank-two materials.

Chapter 10

Appendix

10.1 Appendix for the Cubic

We treat the polynomial of the third order

$$x^3 + ax^2 + bx + c = 0,$$

remembering that without loss of generality we can consider the polynomial to be monic. Acting the change of variable $x = y - \frac{a}{3}$ we have

$$x^3 + ax^2 + bx + c = 0 \Leftrightarrow y^3 + py + q = 0,$$

where $y = x + \frac{a}{3}$ and

$$\begin{cases} p &= -\frac{a^2}{3} + b, \\ q &= \frac{2}{27}a^3 - \frac{ab}{3} + c. \end{cases}$$

Formula $x = y - \frac{a}{3}$ is less misterious than it can seem. Given a monic polynomial equation of n degree, $x^n + ax^{n-1} + \ldots = 0$, the coefficient a is the opposite of the roots sum. Since in this case, roots are three, $\frac{a}{3}$ is the barycentre of the roots. The change of variables $x = y - \frac{a}{3}$ is a translation which brings the origin to be coincident with this barycentre. The new coefficient will be the new sum of roots, which has to be zero, because

the new barycentre is the origin. So we have a new polynomial equation, without the quadratic term:

$$y^3 + py + q = 0.$$

For "unfathomable" reasons, we search for solution y as the sum of two numbers u and v:

$$y = u + v.$$

Substituting, we obtain

$$\begin{aligned} 0 = y^3 + py + q &= (u+v)^3 + p(u+v) + q \\ &= u^3 + 3u^2v + 3uv^2 + v^3 + p(u+v) + q \\ &= \underbrace{(u^3 + v^3 + q)} + (u+v)\underbrace{(3uv + p)}. \end{aligned}$$

This is an equation in two variables. Fixing, for example u, the equation is in the third order in v, and the difficulty is equivalent to that of the initial problem. But there is a particular combination in u and v which is very easy to calculate: it's necessary to impose

$$\begin{cases} u^3 + v^3 = -q, \\ uv = -\frac{p}{3}. \end{cases}$$

Now we want to prove the equivalence between the equation and the system:

$$y^3 + py + q = 0 \Leftrightarrow \exists u, v \text{ such that } \begin{cases} u + v = y, \\ u^3 + v^3 = -q, \\ uv = -\frac{p}{3}. \end{cases}$$

The left arrow $\Leftarrow$ is immediately proved due to the identity $y^3 + py + q = (u^3 + v^3 + q) + (u + v)(3uv + p)$. Viceversa, given a solution y such that $y^3 + py + q = 0$, then we can find u and v such that $u + v = y$, $uv = -\frac{p}{3}$ and from $0 = y^3 + py + q = (u^3 + v^3 + q) + (u + v)(3uv + p)$ we have that

$u^3 + v^3 + q = 0$, as it was required. Now, we proceed to the resolution of the system in u, v. Passing to the cube of the second equation, we have

$$\begin{cases} u^3 + v^3 = -q, \\ uv = -\frac{p}{3}. \end{cases} \Rightarrow \begin{cases} u^3 + v^3 = -q, \\ u^3 v^3 = -\frac{p^3}{27}, \end{cases}$$

(note the fact that the arrow is only in the right side). So for u^3 and v^3 we know their sum and product. So that we find that

$$\left\{u^3, v^3\right\} = \left\{z : z^2 + qz - \frac{p^3}{27} = 0\right\}.$$

The equation in z-variable is soon resolved:

$$z = -\frac{q}{2} \pm \sqrt{\frac{q^2}{4} + \frac{p^3}{27}},$$

so we can write

$$u^3 = -\frac{q}{2} + \sqrt{\frac{q^2}{4} + \frac{p^3}{27}}, \quad v^3 = -\frac{q}{2} - \sqrt{\frac{q^2}{4} + \frac{p^3}{27}},$$

and it follows that

$$y = \sqrt[3]{-\frac{q}{2} + \sqrt{\frac{q^2}{4} + \frac{p^3}{27}}} + \sqrt[3]{-\frac{q}{2} - \sqrt{\frac{q^2}{4} + \frac{p^3}{27}}},$$

which is the known solving formula for the cubic equation, discovered by Gerolamo Cardano [7].

It should be noted that the solutions for $\begin{cases} u^3 + v^3 = -q, \\ uv = -\frac{p}{3}. \end{cases}$ are the solutions of $\begin{cases} u^3 + v^3 = -q, \\ u^3 v^3 = -\frac{p^3}{27} \end{cases}$ such that $uv = -\frac{p}{3}$. If the polynomial equation is with real coefficients, then it's crucial the sign of the discriminant $\Delta = \frac{q^2}{4} + \frac{p^3}{27}$.

First case: $\Delta > 0$. In this case, the solving formula gives only one real solution of the equation, if all the radicals are interpreted as real in the strict sense. In order to have the other two roots, we have to recall the non–real cubic roots of the unity, that are $\cos 2\pi/3 \pm i \sin 2\pi/3 = -(1/2) \pm i\sqrt{3}/2$. So the three roots for each u and v are written respectively as:

$$u_1 := \sqrt[3]{-\frac{q}{2} + \sqrt{\Delta}}, \quad u_2 := u_1\left(-\frac{1}{2} + i\frac{\sqrt{3}}{2}\right), \quad u_2 := u_1\left(-\frac{1}{2} - i\frac{\sqrt{3}}{2}\right)$$
$$v_1 := \sqrt[3]{-\frac{q}{2} - \sqrt{\Delta}}, \quad v_2 := v_1\left(-\frac{1}{2} + i\frac{\sqrt{3}}{2}\right), \quad v_2 := v_1\left(-\frac{1}{2} - i\frac{\sqrt{3}}{2}\right).$$

In order to select the roots above the nine possibilities, it's sufficient to verify that $uv = -p/3$, or better that $uv \in \mathbb{R}$. Then the three roots are given by:

$$\begin{aligned} y_1 &= u_1 + v_1, \\ y_2 &= -\frac{1}{2}y_1 + i\frac{\sqrt{3}}{2}(u_1 - v_1), \\ y_3 &= -\frac{1}{2}y_1 - i\frac{\sqrt{3}}{2}(u_1 - v_1), \end{aligned}$$

where we note that y_2 and y_3 are complex conjugated roots.
Second case: $\Delta = 0$. In this case, since the coefficients are real, $q = \pm\frac{2\sqrt{3}}{9}\sqrt{-p^3}$ and necessarily $p < 0$ In this case we have that $u_1 = v_1$. Then the three roots are given by

$$\begin{aligned} y_1 &= \mp 2\sqrt{-\frac{p}{3}}, \\ y_2 &= \pm\sqrt{-\frac{p}{3}}, \\ y_3 &= \pm\sqrt{-\frac{p}{3}}, \end{aligned}$$

where we note that $y_2 = y_3$.
Third case: $\Delta < 0$. The cubic radicals are given by

$$-\frac{q}{2} \pm i\sqrt{\Delta}$$

and they are complex conjugated, with modulus R corresponding to

$$R := \left|-\frac{q}{2} \pm i\sqrt{\Delta}\right| = \sqrt{\left(-\frac{q}{2}\right)^2 - \Delta} = \sqrt{-\frac{p^3}{27}},$$

(note that if $\Delta < 0$ then necessarily $p < 0$, so that the last radical is real) and with argument an angle $\pm\theta$ whose tangent is

$$\tan\theta = \frac{\sqrt{-\Delta}}{-\frac{q}{2}} \text{ if } q \neq 0.$$

To be precise:

$$\text{if } -q/2 > 0 \text{ then } \theta = \arctan\left(-\frac{2\sqrt{-\Delta}}{q}\right);$$
$$\text{if } -q/2 < 0 \text{ then } \theta = \pi + \arctan\left(-\frac{2\sqrt{-\Delta}}{q}\right).$$

So, indicating the complex number as a couple of modulus and argument, the value for u^3 and v^3 are given by

$$u^3 = (R, \theta), \quad v^3 = (R, -\theta),$$

so that the cubic roots are

$$u_1 := \left(\sqrt[3]{R}, \frac{\theta}{3}\right), \quad u_2 := \left(\sqrt[3]{R}, \frac{\theta + 2\pi}{3}\right), \quad u_3 := \left(\sqrt[3]{R}, \frac{\theta + 4\pi}{3}\right),$$
$$v_1 := \left(\sqrt[3]{R}, -\frac{\theta}{3}\right), \quad v_2 := \left(\sqrt[3]{R}, \frac{-\theta + 2\pi}{3}\right), \quad v_3 := \left(\sqrt[3]{R}, \frac{-\theta + 4\pi}{3}\right).$$

As before, it has to be chosen the combination (u, v) such that $uv = -p/3$ and the right couples are the same: $\{u_1, v_1\}, \{u_2, v_3\}, \{u_3, v_2\}$, where we

note that u and v are conjugated to each other. The three couples give three real solutions $y = u + v$, because the sum of complex conjugated roots is real. So the three roots for the cubic equation are given by:

$$y_1 = 2\sqrt{-\frac{p}{3}}\cos\frac{\theta}{3},$$
$$y_2 = 2\sqrt{-\frac{p}{3}}\cos\frac{\theta + 2\pi}{3},$$
$$y_3 = 2\sqrt{-\frac{p}{3}}\cos\frac{\theta + 4\pi}{3}.$$

Since Δ is strictly negative, then θ is not a multiple of π, so the three roots are distinct.

10.2 Updated Incremental Electric Displacement and Electric Field

Tensor $\mathbf{\Sigma}$ arises, using Nanson's formula (3.11), as

$$\int_{\partial\mathcal{B}^0} [\![\dot{\mathbf{S}}]\!]\mathbf{n}^0 dA^0 = \int_{\partial\mathcal{B}} \frac{1}{J}[\![\dot{\mathbf{S}}]\!]\mathbf{F}^T\mathbf{n}dA = \int_{\partial\mathcal{B}} [\![\mathbf{\Sigma}]\!]\mathbf{n}dA.$$

Then

$$\int_{\partial\mathcal{B}^0} [\![\dot{\mathbf{d}}^0]\!]\mathbf{n}^0 dA^0 = \int_{\partial\mathcal{B}} \frac{1}{J}[\![\dot{\mathbf{d}}^0]\!]\mathbf{F}^T\mathbf{n}dA = \int_{\partial\mathcal{B}} [\![\hat{\mathbf{d}}]\!]\mathbf{n}dA. \tag{10.1}$$

The updated Lagrangian formulation for the electric field is obtained considering an arbitrary integration path Γ^0 in the reference configuration and an infinitesimal fibre $d\mathbf{l}^0$ tangent to Γ^0. In the current configuration $\Gamma = \boldsymbol{\chi}(\Gamma^0)$ and $d\mathbf{l} = \mathbf{F}d\mathbf{l}^0$, so that

$$\int_{\partial\Gamma^0} \dot{\mathbf{e}^0} \cdot d\mathbf{l}^0 = \int_{\partial\Gamma} \dot{\mathbf{e}^0} \cdot \mathbf{F}^{-1} d\mathbf{l} = \int_{\partial\Gamma} \hat{\mathbf{e}} \cdot d\mathbf{l}. \tag{10.2}$$

10.3 Some Derivatives of Invariants

Here, we record for reference the expressions for the first derivatives of the six invariants with respect to $\mathbf{F}$ and $\mathbf{d}^0$

$$\begin{aligned}
&\frac{\partial I_1}{\partial F_{iJ}} = 2F_{iJ}, \qquad \frac{\partial I_2}{\partial F_{iJ}} = 2(I_1 F_{iJ} - C_{JL}F_{iL}),\\
&\frac{\partial I_3}{\partial F_{iJ}} = 2I_3 F^{-1}_{Ji}, \quad \frac{\partial I_4}{\partial F_{iJ}} = 0, \quad \frac{\partial I_5}{\partial F_{iJ}} = 2d^0_L F_{iJ} d^0_J,\\
&\frac{\partial I_6}{\partial F_{iJ}} = 2(C_{JP}d^0_P F_{iL} d^0_L + d^0_J F_{iL} C_{LP} d^0_P),\\
&\frac{\partial I_4}{\partial d^0_J} = 2d^0_J, \qquad \frac{\partial I_5}{\partial d^0_J} = 2C_{JP}d^0_P, \quad \frac{\partial I_6}{\partial d^0_J} = 2C^2_{JP}d^0_P.
\end{aligned}$$

Note that I_1, I_2, I_3 do not depend on $\mathbf{d}^0$. The second derivatives with respect to $\mathbf{F}$ are

$$\begin{aligned}
&\frac{\partial^2 I_1}{\partial F_{iJ}F_{kL}} = 2\delta_{ik}\delta_{JL}, \quad \frac{\partial^2 I_3}{\partial F_{iJ}F_{kL}} = 2I_3(2F^{-1}_{Ji}F^{-1}_{Lk} - F^{-1}_{Jk}F^{-1}_{Li}),\\
&\frac{\partial^2 I_2}{\partial F_{iJ}F_{kL}} = 2(\delta_{ik}C_{JL} + F_{iL}F_{kJ} + \delta_{JL}B_{ik} - I_1\delta_{ik}\delta_{JL} - F_{iJ}F_{kL}),\\
&\frac{\partial^2 I_4}{\partial F_{iJ}F_{kL}} = 0, \qquad \frac{\partial^2 I_5}{\partial F_{iJ}F_{kL}} = \delta_{ik}d^0_J d^0_L,\\
&\frac{\partial^2 I_6}{\partial F_{iJ}F_{kL}} = \delta_{ik}d^0_S(C_{JS}d^0_L + C_{LS}d^0_J) + F_{iR}d^0_R(\delta_{JL}F_{kS}d^0_S + F_{kJ}d^0_L)\\
&\qquad\qquad + F_{iL}F_{kS}d^0_S d^0_J + B_{ik}d^0_J d^0_L.
\end{aligned}$$

The mixed derivatives of I_1, I_2, I_3 and I_4 with respect to $\mathbf{F}$ and $\mathbf{d}^0$ vanish, and

$$\begin{aligned}
&\frac{\partial^2 I_5}{\partial F_{iJ}d^0_M} = F_{iM}d^0_J + F_{iS}d^0_S\delta_{JM},\\
&\frac{\partial^2 I_6}{\partial F_{iJ}d^0_M} = F_{iM}C_{JS}d^0_S + F_{iS}C_{JM}d^0_S + F_{iS}C_{SM}d^0_J + F_{iR}C_{RS}d^0_S\delta_{JM}.
\end{aligned}$$

The second derivatives of I_4, I_5, I_6 with respect to $\mathbf{d}^0$ are

$$\frac{\partial^2 I_4}{\partial d^0_M d^0_N} = \delta_{MN}, \quad \frac{\partial^2 I_5}{\partial d^0_M d^0_N} = C_{MN}, \quad \frac{\partial^2 I_6}{\partial d^0_M d^0_N} = C^2_{MN}.$$

10.4 Band Localization: Formulation in Terms of Electric Field

In this second formulation we consider electric field in place of electric displacement seen in Sect. 7.4.
Compatibility relationships across the interface for $\mathbf{L}$ require $(7.29)_1$, while continuity of the normal component of $\hat{\mathbf{e}}$, requires that

$$\hat{\mathbf{e}}^{\,\mathrm{b}} = \hat{\mathbf{e}}^{\,\mathrm{o}} + \tilde{\alpha}\mathbf{n}, \tag{10.3}$$

where $\tilde{\alpha}$ is a real scalar and represent mode amplitudes in the band. Note that fields $\mathbf{L}^{\,\mathrm{b}}$ and $\hat{\mathbf{e}}^{\,\mathrm{b}}$ satisfy field equations (7.17) and (7.19) in the band and the relative displacement field in $(10.3)_1$ associated with the dyadic term is an isochoric simple shear of amount ξ. On the other hand, continuity of the incremental traction and of the tangential component of the electric field require $(7.30)_1$ for $\mathbf{\Sigma}$ and for the electric displacement

$$\hat{\mathbf{d}}^{\,\mathrm{b}} - \hat{\mathbf{d}}^{\,\mathrm{o}} = \tilde{\zeta}\mathbf{m}, \tag{10.4}$$

where, again, $\tilde{\zeta}$ is real.

The use of (10.3) in the constitutive equations and in (10.4) provides, in component form, respectively (recalling eqs. (4.73), (4.74), (4.75))

$$Q^H_{ik} m_k - \frac{1}{\xi}(\dot{p}^{\,\mathrm{b}} - \dot{p}^{\,\mathrm{o}}) n_i - \bar{\alpha} B^H_{iqa} n_a n_q = 0, \tag{10.5}$$

$$\xi B^H_{iqa} m_i n_q + \tilde{\alpha} A^H_{ab} n_b = \tilde{\zeta} m_a,$$

where $Q^H_{ik} = C^H_{iqkp} n_p n_q$ and we recall that ξ is referred to $(7.29)_1$. The manipulation of (10.5) yields

$$\frac{\tilde{\alpha}}{\xi} = -\frac{B^H_{iqa} m_i n_q n_a}{A^H_{ab} n_a n_b}, \tag{10.6}$$

as well as the condition for band localization, namely ($A^H_{ab} n_a n_b \neq 0$)

$$A^H_{ab} n_a n_b Q^H_{ik} m_i m_k + (B^H_{iqa} m_i n_q n_a)^2 = 0. \tag{10.7}$$

Eq. (10.7) clearly depends on the current finite state and on the normal to the band **n** (the components of **m** can be easily substituted exploiting the connection $m_r = e_{sr} n_s$, where $e_{12} = -e_{21} = 1,\ e_{11} = e_{22} = 0$). The final form of the localization equation (10.7) is

$$\Omega_6 \upsilon^6 + \Omega_5 \upsilon^5 + \Omega_4 \upsilon^4 + \Omega_3 \upsilon^3 + \Omega_2 \upsilon^2 + \Omega_1 \upsilon + \Omega_0 = 0, \tag{10.8}$$

which is a complete polynomial with:

$$\begin{aligned}
\Omega_6 &= B^2_{122} + A_{22} C_{1212}, \\
\Omega_5 &= 2(B_{122}(B_{112} + B_{121} - B_{222}) + A_{12} C_{1212} + A_{22}(C_{1112} - C_{1222})), \\
\Omega_4 &= (B_{112} + B_{121} - B_{222})^2 + 2B_{122}(B_{111} - B_{212} - B_{221}) \\
&\quad + A_{11} C_{1212} + 4A_{12}(C_{1112} - C_{1222}) \\
&\quad + A_{22}(C_{1111} - 2C_{1122} - 2C_{1221} + C_{2222}), \\
\Omega_3 &= 2(-B_{122} B_{211} + (B_{111} - B_{212} - B_{221})(B_{112} + B_{121} - B_{222}) \\
&\quad + A_{11}(C_{1112} - C_{1222}) + A_{22}(C_{2221} - C_{1121}) \\
&\quad + A_{12}(C_{1111} - 2C_{1122} - 2C_{1221} + C_{2222})), \\
\Omega_2 &= -2B_{211}(B_{112} + B_{121} - B_{222}) + (B_{212} + B_{221} - B_{111})^2 \\
&\quad + A_{22} C_{2121} - 4A_{12}(C_{1121} - C_{2122}) \\
&\quad + A_{11}(C_{1111} - 2C_{1122} - 2C_{1221} + C_{2222}), \\
\Omega_1 &= 2(B_{211}(B_{212} + B_{221} - B_{111}) + A_{12} C_{2121} + A_{11}(C_{2221} - C_{1121})), \\
\Omega_0 &= B^2_{211} + A_{11} C_{2121}.
\end{aligned}$$

Bibliography

[1] Arruda, E.M. and Boyce, M.C., "A three-dimensional constitutive model for the large stretch behaviour of rubber elastic materials", *J. Mech. Phys. Solids*, **41**, 389–412 (1993).

[2] Bertoldi, K. and Gei, M., "Instability in multilayered soft dielectrics", *J. Mech. Phys. Solids*, **59**, 18–42 (2011).

[3] Beatty, M.F., "Direct comparison of the Gent and ArrudaBoyce constitutive models of rubber elasticity", *J. Elasticity*, **70**, 65–86 (2003).

[4] Biot, M.A., *Mechanics of Incremental Deformations*, Wiley, New York (1965).

[5] Boyce, M.C., "Direct Comparison of the Gent and the Arruda-Boyce Constitutive Models of Rubber Elasticity", *Rubber Chemistry Technol.*, **69**, 781–785 (1996).

[6] Bustamante, R., Dorfmann, A. and Ogden, R.W., "Nonlinear electroelastostatics: a variational framework", *ZAMP*, **60**, 154–177 (2009).

[7] Cardano, G., *Artis magnae sive de regulis algebraicis liber unus* , Nuremberg (1545).

[8] Carpi, F., De Rossi, D., Kornbluh, R., Pelrine, R . and Sommer-Larsen, P. (Eds.) *Dielectric Elastomers as Electromechanical Transducers*, Elsevier, Oxford, UK (2008).

[9] Carpi, F., Gallone, G., Galantini, F. and De Rossi, D., "Silicone-poly(hexylthiophene) blends as elastomers with enhanced electromechanical transduction properties", *Adv. Funct. Mater.*, **18**, 235–241 (2008).

[10] Cohen, A., "A Padé approximant to the inverse Langevin function", *Rheol. Acta*, **30**, 270–273 (1991).

[11] deBotton, G., Tevet-Deree, L. and Socolsky, E.A., "Electroactive heterogeneous polymers: analysis and applications to laminated composites", *Mech. Adv. Mate. Struct.*, **14**, 13–22 (2007).

[12] Dorfmann, A. and Ogden, R.W., "Nonlinear electroelasticity", *Acta Mech.*, **174**, 167–183 (2005).

[13] Dorfmann, A. and Ogden, R.W., "Nonlinear electroelastostatics: Incremental equations and stability", *Int. J. Eng. Sciences*, **48**, 1–14 (2010).

[14] Dowaikh, M.A. and Ogden, R.W., "Interfacial waves and deformations in pre-stressed elastic media", *Proc. R. Soc. Lond.*, A**433**, 313–328 (1991).

[15] Eringen, A.C., "On the Foundations of Elastostatics", *Int. J. Eng. Sciences*, **1**, 127–153 (1963).

[16] Gei, M., Colonnelli, S. and Springhetti, R., "The role of electrostriction on the stability of dielectric elastomer actuators", submitted.

[17] Gei, M., Colonnelli, S. and Springhetti, R., "A framework to investigate instabilities of homogeneous composite dielectric elastomer actuators", *Proc. Smart Structures/NDE, 2012*, paper No. **8340-34**, San Diego (USA) March 11-15, 2012,

[18] Gent, A.N., "A New Constitutive Relation for Rubber", *Rubber Chem. Technol.*, **69**, 59–61 (1996).

[19] Guillot, M. F., Jarynski, J. and Balizer, E., "Measurement of electrostrictive coefficients of polymer films", *J. Acoust. Soc. Am*, **110**, 2980–2990 (2001).

[20] Gurtin, M.E., *An Introduction of Continuum Mechanics*, Academic Press, San Diego (1981).

[21] Hill, R., "On uniqueness and stability in the theory of finite elastic strain", *J. Mech. Phys. Solids*, **5**, 229–241 (1957).

[22] Hill, R., "On constitutive inequalities for simple materials-I", *J. Mech. Phys. Solids*, **16**, 229–242 (1968).

[23] Hill, R. and Hutchinson, J.W., "Bifurcation phenomena in the plane tension test", *J. Mech. Phys. Solids*, **23**, 239–264 (1975).

[24] Horgan, C.O. and Saccomandi, G., "A Molecular-Statistical Basis for the Gent Constitutive Model of Rubber Elasticity", *J. of Elast.*, **68**, 167–176 (2002).

[25] Horgan, C.O. and Saccomandi, G., "Phenomenological hyperelastic strain-stiffening constitutive models for rubber", *Rubber Chemistry and Technology*, **79**, 152–169 (2006).

[26] Huang, C., Zhang, Q.M., deBotton, G. and Bhattacharya, K., "All-organic dielectric-percolative three-component composite materials with high electromechanical response", *Appl. Phys. Lett.*, **84**, 4391–4393 (2004).

[27] Keplinger, C., Kaltenbrunner, M., Arnold, N. and Bauer, S., "Rontgen's electrode–free elastomer actuators without electromechanical pull–in instability", *PNAS*, **107**, 4505–4510 (2010).

[28] Li, B., Chen, H., Qiang, J., Hu, S., Zhu, Z. and Wang., Y., "Effect of mechanical pre-stretch on the stabilization of dielectric elastomer actuaction", *J. Phys. D: Appl. Phys.*, **44**, 155301, 1–8, (2011).

[29] Mark, J.E. and Erman, B., *Rubberlike Elasticity A Molecular Primer*, John Wiley, New York, (1988).

[30] Maugin, G.A and Eringen, A. C., *Electrodynamics of Continua I, Foundations and Solid Media*, Springer-Verlag (1989).

[31] McMeeking, R.M. and Landis, C.M., "Electrostatic forces and stored energy for deformable dielectric materials", *J. Appl. Mech., Trans. ASME*, **72**, 581–590 (2005).

[32] Mooney, M, " A theory of large elastic deformation", *J. Appl. Phys.*, **11**(9), 582–592 (1940).

[33] Oden, J.T., *Finite Elemetns of Nonlinear Continua*, Mc Graw-Hill, New York (1972).

[34] Ogden, R.W., " A theory of large elastic deformation", *Proc. R. Soc. Lond. A*, **326**, 565–584 (1972).

[35] Ogden, R.W., *Non linear elastic deformation*, Dover, New York (1997).

[36] Pelrine, R., Kornbluh, R., Pei, Q. and Joseph, J. "High–speed electrically actuated elasotmers with strain greater than 100%", *Science*, **287**, 836–839 (2000).

[37] Peng, S.T.J. and Landel, R.F. "Stored energy function and compressibility of compressible rubber like materials under large strain", *J. Appl. Phys.*, **46**, 2599 (1975).

[38] Ponte Castañeda, P. and Siboni, M.H. "A finite-strain constitutive theory for electro-active polymer composites via homogenization", *Int. J. Nonlinear Mech.*, in press (2011).

[39] Rinaldi, C. and Brenner, H., "Body versus surface forces in continuum mechanics: Is the Maxwell stress tensor a physically objective Cauchy stress?", *ZAMP*, **65**, 036615, 1–14 (2002).

[40] Rivlin, R.S., "Large elastic deformations of isotropic materials. IV. Further developments of the general theory", *Philosophical Transactions of the Royal Society of London. Series A, Mathematical and Physical Sciences*, **241**(835), 379–397 (1948).

[41] Rudykh, S. and deBotton, G., "Stability of anisotropic electroactive polymers with application to layered media", *ZAMP*, in press (2011).

[42] Sernesi, E., *Geometria 1*, Bollati-Boringhieri, (1989).

[43] Simo, J. and Hughes, T.J.R., *Computational Inelasticity*, Springer-Verlag, New York (1998).

[44] Stark, K,H. and Garton, C.G., "Electric strength of irradiated polythene", *Nature*, **176**, 1225–1226 (1955).

[45] Suo, Z., Zhao, X. and Green, W.H., "A nonlinear field theory of deformable dielectrics", *J. Mech. Phys. Solids*, **56**, 467–486 (2008).

[46] Tian, L., Tevet–Deree, L., deBotton, G. and Bhattacharya, K., "Dielectric elastomer composites", *J. Mech. Phys. Solids*, in press (2011).

[47] Toupin, R.A., "The elastic dielectric", *Arch. Ration. Mech. Anal.* , **5**, 849–915 (1956).

[48] Treloar, L.R.G, "Stress-strain data for vulcanised rubber under various types of deformation", *Trans. Faraday Soc.* , **40**, 59–70 (1944).

[49] Treloar, L.R.G, *The Physics of Rubber Elasticity*, Oxford University Press, Oxford (1975).

[50] Truesdell, C. and Noll, W., *The Non-Linear Field Theories of Mechanics*, Encyclopedia pf Physics, III/3, Springer-Verlag (1965).

[51] Verdejo, R., Bernal, M.M., Romasanta, L.J. and Lopez-Manchado, M.A., "Graphene filled polymer nanocomposites", *J. Mater. Chem.*, **21**, 3301–3310 (2011).

[52] Wang, M.C., Guth, E. "Statistical Theory of Networks of Non-Gaussian Flexible Chains", *J. Chem. Phys*, **20**, 1144 (1952).

[53] Wissler, M. and Mazza, E., "Electromechanical coupling in dielectric elastomer actuators", *Sens. Actuators A*, **138**, 384–393 (2007).

[54] Yeoh, O.H., "Some forms of the strain energy function for rubber", *Rubber Chemistry Technol.*, **66**, 754–771 (1993).

[55] Zhang, Q.M., Li, H., Poh, M., Xia, F., Cheng, Z.-Y., Xu, H. and Huang, C., "An all-organic composite actuator material with a high dielectric constant", *Nature*, **419**, 284–289 (2002).

[56] Zhenyi, M., Scheinbeim, J.I., Lee, J.W. and Newman, B.A. "High Field Electrostrictive Response of Polymers", *J. Polym. Sci. Part B: Polym. Phys.*, **32**, 2721–2731 (1994).

[57] Dang, Z.M., Peng, B., Xie, D., Yao, S.H., Jiang, M.J. and Bai, J., "High dielectric permittivity silver/polyimide composite films with excellent thermal stability", *Appl. Phys. Lett.* **92**,1063/1.2894571 (3 pages) (2008).